

PRACTICAL STRUCTURAL DESIGN AND CONTROL FOR DIGITAL CLAY

Haihong Zhu



Woodruff School of Mechanical Engineering
Georgia Institute of Technology

**PRACTICAL STRUCTURAL DESIGN AND CONTROL FOR
DIGITAL CLAY**

A Dissertation
Presented to
The Academic Faculty

By

Haihong Zhu

In Partial Fulfillment
of the Requirements for the Degree
Doctor of Philosophy in the
Woodruff School of Mechanical Engineering

Georgia Institute of Technology
August 2005

Copyright © 2005 by Haihong Zhu

PRACTICAL STRUCTURAL DESIGN AND CONTROL FOR DIGITAL CLAY

Approved by:

Dr. Wayne J. Book, Advisor
School of Mechanical Engineering
Georgia Institute of Technology

Dr. Imme Ebert-uphoff
School of Mechanical Engineering
Georgia Institute of Technology

Dr. Mark Allen
School of ECE
Georgia Institute of Technology

Dr. David Rosen
School of Mechanical Engineering
Georgia Institute of Technology

Dr. Jarek Rossignac
School of COC
Georgia Institute of Technology

Date Approved: July 15, 2005

ACKNOWLEDGEMENTS

After four years work on the project Digital Clay, I proudly present this Ph.D. thesis. It is performed in the Intelligent Machine and Dynamics Laboratory, at the Georgia Institute of Technology. During this research, I received the support of many people to whom I am very grateful. Here, I would like to express my appreciation to

- My Advisor, Dr. Wayne Book, for advising and inspiring me during the research;
- Dr. Imme Ebert-uphoff, Dr. David Rosen, Dr. Jarek Rossignac, and Dr. Mark Allen, for giving me a lot of advice and being my graduate committee members;
- Dr. Ari Glezer for giving me a lot of advice;
- Mr. James D. Huggins, for great help on the fabrication and design of mechanical structures;
- Terri Keita, for her prompt administrative assistance;
- Yanzhu Zhao, for cooperation on structure design;
- Sharon Wu, for cooperation on structure design and fabrication;
- The members of the Intelligent Machine and Dynamics Laboratory, as a whole, for creating such a pleasant working environment;
- Dalong Gao, for creating a pleasant office environment;

I would like to thank all my family members, for their permanent support and encouragements. I am especially grateful to my father, Yunming, who had an important contribution in my formation as a scientist and to my mother, Yunfang, for the care and love she put in raising me.

TABLE OF CONTENTS

ACKNOWLEDGEMENTS.....	III
LIST OF TABLES	VIII
LIST OF FIGURES	IX
SUMMARY	XIV
CHAPTER 1 INTRODUCTION	1
1.1 BASIC IDEA: 3D TANGIBLE HAPTIC SURFACE	1
1.2 ADVANTAGES AND POTENTIAL APPLICATIONS OF DIGITAL CLAY	4
1.2.1 3D Dynamic Mapping.....	5
1.2.2 Medical Diagnostics.....	6
1.2.3 Engineering Design.....	6
1.2.4 Scientific Research.....	7
1.2.5 Vision Impaired Assistance	7
1.2.6 Entertainment.....	7
1.3 DIGITAL CLAY’S FEATURES	8
1.3.1 Actuation Type.....	9
1.3.2 Control of Digital Clay	10
1.4 SCOPE OF THE RESEARCH.....	12
1.5 OUTLINE OF THE THESIS.....	12
CHAPTER 2 BACKGROUND AND CONTEXT	15
2.1 VIRTUAL REALITY (VR)	16
2.1.1 Visual Virtual Reality (VVR)	17
2.1.2 Haptic Interfaces	18
2.2 COMBINATION OF HAPTIC INTERFACE AND VISUAL INTERFACES.....	21
2.2.1 Project FEELEX	22
2.2.2 Project Popup!.....	23
2.3 CONTROL ISSUES.....	24

CHAPTER 3 CELL OF DIGITAL CLAY	28
3.1 OVERVIEW	28
3.2 CELL LEVEL CONTROL FOR THE SINGLE CELL SYSTEM	33
3.2.1 Experimental System	35
3.2.2 Processing the Pressure Signal Affected by the On/off Valve	36
3.2.3 Pressure Control vs. Position Control	37
3.2.4 Cell Level Control Structure	38
3.2.5 User Gesture Interpretation	41
3.2.6 Experimental Results	43
3.3 DISPLACEMENT SENSING METHODS.....	45
3.3.1 PWM Displacement Estimation.....	46
3.3.2 Capacitive Sensor.....	64
3.3.3 Concept of Non-contacting Resistive Displacement Sensor	65
3.4 DESIGN OF MICRO ACTUATOR	66
3.4.1 Displacement Sensor Embedded Micro Actuator	67
3.5 CONCLUSION	71
CHAPTER 4 MULTI-CELL ARRAY OF DIGITAL CLAY	73
4.1 OVERVIEW	73
4.2 HYDRAULIC “N2 BY 2N” MATRIX DRIVE	76
4.3 SURFACE REFRESH METHODS FOR THE FLUIDIC MATRIX DRIVE	80
4.3.1 Model of the Fluidic Matrix Drive Node	80
4.3.2 Matrix Representation of the Basic Control.....	81
4.3.3 One-time Refresh Method.....	84
4.3.4 Gradual Refresh Method.....	86
4.3.5 Gradual Approximation Refresh Method.....	88
4.4 CONTROL OF THE FLUIDIC MATRIX DRIVE.....	90
4.4.1 User API	92
4.4.2 Surface Level Control	94

4.4.3	Surface Refresh Coordinator.....	96
4.4.4	Hot area Processor	97
4.4.5	Valve Controller.....	98
4.5	CONCLUSIONS	98
CHAPTER 5 IMPLEMENTATION OF THE CELL ARRAY SYSTEM		100
5.1	OVERVIEW	100
5.2	MECHANICAL STRUCTURE DESIGN FOR LARGE SCALE CELL ARRAY	102
5.2.1	Functional Modules of The Mechanical System.....	103
5.2.2	Design of the Control Adapter	104
5.2.3	Time Sequence for “N2 by 2N” Matrix Drive	107
5.2.4	Displacement Sensor Embedded Actuator Array Assembly.....	108
5.2.5	Pressure Sensor Array Mounting Base	110
5.3	ELECTRONIC SYSTEM FOR CELL ARRAY	111
5.3.1	Pressure Sensor Signal Filtering and Multiplexing.....	113
5.3.2	Displacement Sensor Signal Conditioning and Multiplexing	114
5.4	CONCLUSION	122
CHAPTER 6 5 X 5 CELL ARRAY PROTOTYPE OF DIGITAL CLAY		124
6.1	OVERVIEW	124
6.2	STEREOLITHOGRAPHY TECHNOLOGY (SLA).....	125
6.3	MECHANICAL SYSTEM OF THE 5X5 PROTOTYPE	127
6.3.1	Row Channel Hydraulic Board and Column Channel Hydraulic Board.....	128
6.3.2	Pressure Sensor Array Mounting Base	130
6.3.3	Hydraulic Channel Concentrating Block	131
6.3.4	Displacement Sensor Embedded Actuator Array Assembly.....	132
6.4	CONTROL HARDWARE.....	134
6.4.1	“Spike and Hold” Over-driver	134
6.4.2	Displacement Sensor Signal Conditioner.....	136
6.4.3	Displacement Sensor Multiplexer	136

6.4.4	Low-pass Filter for the Pressure Signal	137
6.4.5	Pressure Sensor Multiplexer	137
6.4.6	Reducing Control Signals for Multiplexers	138
6.5	TEST OBJECTIVES, CONTROL STRUCTURE AND TEST RESULTS	139
6.5.1	5x5 Cell Array Prototype	140
6.5.2	Surface Generation Testing.....	141
6.5.3	Speed Control on a Single Cell	143
6.5.4	Pressure Sensor Testing	144
6.6	CONCLUSIONS	144
CHAPTER 7 CONCLUSIONS AND RECOMMENDATIONS		146
7.1	SUMMARY AND CONCLUSIONS	146
7.2	CONTRIBUTIONS	150
7.3	RECOMMENDATIONS FOR FUTURE RESEARCH.....	151
APPENDIX A DEVELOPED PROTOTYPES		154
APPENDIX B PSEUDO PROGRAMS.....		155
APPENDIX C LIST OF KEY MATERIAL/COMPONENTS		160
APPENDIX D SCHEMATIC CIRCUITS FOR BASIC ELECTRONICS		162
REFERENCES		164

LIST OF TABLES

Table 1-1 Comparison of Three Main Actuation Methods.....	9
Table 3-1 Features of Key Components	36
Table 3-2 Parameters Used in Testing	61
Table 4-1 Table of Definitions of Terms and Symbols	91
Table 5-1 Comparison of Solutions for Control Adapter	106

LIST OF FIGURES

Figure 1-1 Concept of Digital Clay	2
Figure 1-2 Potential Applications of Digital Clay	8
Figure 1-3 General Control Structure	10
Figure 2-1 Project FEELEX.....	23
Figure 2-2 Project Popup!.....	24
Figure 3-1 Kinematical Structures for Digital Clay.....	29
Figure 3-2 Single Dimensional and Three Dimensional Cell.....	29
Figure 3-3 Model of a Point on Material	32
Figure 3-4 Cell Level Control for the Signal Cell System.....	34
Figure 3-5 Experimental Setup of the Single Cell System	35
Figure 3-6 Efficacy of the Second Order Filter	37
Figure 3-7 Inlet Circuit for Control using PWM	38
Figure 3-8 Working Modes vs. Control States	39
Figure 3-9 Elastic and Plastic States.....	40
Figure 3-10 Shaping State.....	41
Figure 3-11 User Gesture Interpretation	42
Figure 3-12 Experimental Results	44
Figure 3-13 Experimental System	47
Figure 3-14 PWM Method Testing Results.....	49
Figure 3-15 Variance for $\Delta P_v = 11$ PSI.....	49
Figure 3-16 Free Body Diagram of the Solenoid Valve.....	50
Figure 3-17 Valve Plunger Trajectory Simulation.....	51

Figure 3-18 Solenoid Valve Working Phases under PWM Method.....	52
Figure 3-19 Simulation and Analysis for Phase II.....	53
Figure 3-20 Approximated Plunger Trajectory for Phase III.....	55
Figure 3-21 Approximated Plunger Trajectory.....	56
Figure 3-22 Curve Fitting Results.....	57
Figure 3-23 Flow Rate Curves Divided by $\sqrt{\Delta P_v}$	58
Figure 3-24 Look-up Table of Flow Rate to Duty	59
Figure 3-25 Structure of Velocity and Position Control using PWM.....	60
Figure 3-26 Testing System for Control using PWM.....	60
Figure 3-27 Displacement under Zero Disturbance Pressure	61
Figure 3-28 Absolute Error vs. Desired Displacement.....	62
Figure 3-29 Displacement under Varying Disturbance Pressure.....	63
Figure 3-30 Absolute Error vs. Desired Displacement.....	63
Figure 3-31 Capacitive Sensor Concept	64
Figure 3-32 Proposed Capacitive Sensor Dimensions.....	64
Figure 3-33 Capacitance Variation Due to the Eccentrics.....	65
Figure 3-34 Non-contacting Resistive Displacement Sensor	65
Figure 3-35 Solutions for Actuators of Digital Clay	66
Figure 3-36 Micro Cylinder With Displacement Sensor Embedded	68
Figure 3-37 Test Setup on the Non-contacting Resistive Sensor	69
Figure 3-38 Test Results for the Non-contacting Resistive Sensor	70
Figure 3-39 Curve Fitting Results for the Non-contacting Resistive Sensor.....	70
Figure 4-1 Planar Pin-rod Array Concept.....	74

Figure 4-2 Matrix Drive for LED array	77
Figure 4-3 “ N^2 by $2N$ ” Fluidic Matrix Drive Concept	78
Figure 4-4 Working Principle of “ N^2 by $2N$ ” Fluidic Matrix Drive.....	79
Figure 4-5 “ $N^2 - 2N$ ” Fluidic Matrix Drive for Double Acting Actuator	80
Figure 4-6 Simplified Node Model.....	81
Figure 4-7 Control Architecture for the Fluidic Matrix Drive.....	92
Figure 4-8 Low Level Control Architecture	93
Figure 4-9 Surface Level Control Functional Block Diagram.....	94
Figure 4-10 Valve Control Functional Block Diagram	98
Figure 5-1 Functional Modules of Digital Clay.....	103
Figure 5-2 Solutions for Control Adapter Structure	104
Figure 5-3 Residue Volume in the Control Adapter.....	107
Figure 5-4 Timing Table for Row, Column and Pressure Selection Valves	108
Figure 5-5 Structures of Actuator Arrays for Digital Clay	109
Figure 5-6 Mounting Base per Solution 1.....	110
Figure 5-7 Mounting Base per Solution 2.....	111
Figure 5-8 Functional Block Diagram of the Electronic System.....	112
Figure 5-9 Pressure Sensor Signal Filtering and Multiplexing.....	113
Figure 5-10 Multiplexing Scheme for the Pressure Sensor Array	114
Figure 5-11 Functional Block Diagram of Signal Conditioner for Displacement Sensor.....	115
Figure 5-12 Simple Multiplexing Scheme.....	116
Figure 5-13 Matlab Simulation Result.....	118

Figure 5-14 Multiplexing Scheme Solution 1	119
Figure 5-15 Results of the Multiplexer	121
Figure 5-16 Multiplexing using STDP Switch	122
Figure 6-1 The Stereo Lithography Machine.....	126
Figure 6-2 Row Channel Hydraulic Board	128
Figure 6-3 Column Channel Hydraulic Board.....	128
Figure 6-4 Assembly of the Row-Column Channel Hydraulic Boards	129
Figure 6-5 Row and Column Channel Hydraulic Boards.....	130
Figure 6-6 Pressure Sensor Array Block	131
Figure 6-7 Channel Concentrating Block	132
Figure 6-8 Displacement Sensor and Actuator Block.....	133
Figure 6-9 Dip-coating Method for Massive Production.....	133
Figure 6-10 Control Hardware for Multi-cell Array.....	135
Figure 6-11 Solenoid Valve Over-driver	135
Figure 6-12 Schematic Circuit for Multiplexer	136
Figure 6-13 Functional Block Diagram for the Low-pass Filter	137
Figure 6-14 Pressure Sensor Array Multiplexing Circuit.....	138
Figure 6-15 Schematic Circuit for Sharing Control Signals.....	139
Figure 6-16 5x5 Cell Array Prototype	141
Figure 6-17 Result of the Surface Generation	142
Figure 6-18 Displacement Verification using Machine Vision	142
Figure 6-19 Displacement Verification for Speed Control using Machine Vision	143
Figure 6-20 Testing Result for Single Cell Speed Control.....	143

Figure 6-21 Test of the Pressure Sensor Array 144

SUMMARY

Digital Clay is proposed as a next generation human-machine communication interface based on a tangible haptic surface. This thesis embraces this revolutionary concept and seeks to give it a physical embodiment that will confirm its feasibility and enable experimentation relating to its utility and possible improvements. At the current stage, the pin-rod planar array approach seems to be the most promising technology to implement Digital Clay and, therefore, is investigated in this work. Per this approach, Digital Clay could be described as a “3D monitor” whose pixels can move perpendicularly to the screen to form a morphing surface. Users can view, touch and modify the shape of the working surface formed by these “pixels”. In reality, the “pixels” are the tips of micro hydraulic actuators or “Hapcels”[†].

Digital Clay’s name comes from the similarity to modeling clay (a mud used to sculpt or mold). The user can touch, reshape and inspect the working surface of Digital Clay. Beyond ordinary clay, Digital Clay also provides parameters to the computer that represent the shape of the working surface to the computer for further actions such as recording, analysis and editing, etc. Furthermore, the user computer can also command Digital Clay to form the desired shape. Since the Digital Clay supports the haptic interface, the user can get a feel of the desired material properties when he/she touches the working surface. The potential applications of Digital Clay cover a wide range from computer aided engineering design to scientific research to medical diagnoses, 3D

[†] Hapcel stands for the haptic cell. It is the basic haptic unit of the working surface. A hapcel consists of an actuator and related control hardware.

dynamic mapping and entertainment. One could predict a future in which, by using Digital Clay, not only could the user watch an actor in a movie, but also touch the face of the actor!

Digital Clay comprises a working surface that plays the key role of the tangible haptic interface. The surface is formed by a large scale array of fluidic cells which are under control and act together to convey the surface topography of desired 3D objects. **Please note that, in this thesis, “large scale array” means an array consists of a large number of units.** Each cell comprises a fluidic actuator that is connected to two pressure sources through dedicated micro-miniature valves. Sensors are embedded in each cell. Ultimately, the hardware of Digital Clay will be manufactured by the MEMS and lithography technology that is under development at Georgia Tech.

This research starts from the review of the background of virtual reality. Though there is no directly similar concept / idea reported before, related technologies and projects are reviewed and discussed. Then the concept and features of the proposed Digital Clay is provided.

Research stages and a 5x5 cell array prototype are presented in this thesis on the structural design and control of Digital Clay. The first stage of the research focuses on the design and control of a single cell system of Digital Clay. Control issues (such as signal processing, control state switch, and user gesture interpretation) of a single cell system constructed using conventional and off-the-shelf components are discussed first in detail followed by experimental results. Then practical designs of micro actuators and sensors are presented.

The second stage of the research deals with the cell array system of Digital Clay. Practical structural design and control methods are discussed which are suitable for a 100x 100 (even 1000X 1000) cell array. Conceptual design and detailed implementations and technologies are presented including the Fluidic Matrix Drive, signal multiplexing and control architecture for the Fluidic Matrix Drive.

Through the research and design of Digital Clay, key parameters considered include: spatial resolution, accuracy and extension, amplitude of displacement, spatial differential of amplitude, force levels and speed of response.

Finally, a 5 x 5 cell array prototype with following features for testing is constructed using the discussed design solutions:

Resolution: 5x5 with 5mm center to center distance in 2D linear pattern,

Hapcel's linear speed: 0~50mm/second

Bandwidth: 40 Hz

Hapcel's stroke: > 48 mm (no upper limit theoretically)

Force and applied force measurement: pressure sensor array;

Accuracy of position control: <0.3 mm

Hardware and control methods are presented and experimental results of the 5x5 prototype are shown. This requirement for economical scalability is as important to the eventual deployment of Digital Clay as are requirements for performance.

A very important issue that needs to point out is the structural designs discussed in this research make it possible to manufacture the cell array in hours and even minutes.

CHAPTER 1

INTRODUCTION

In this chapter, research on a 3D tangible haptic surface / shape based human-computer communication interface device, the Digital Clay, is introduced. The state-of-the-art of the 3D tangible haptic surface communication technology is introduced first. The advantages and applications of the Digital Clay are then introduced. Features of Digital Clay and objectives of this research are proposed. Finally the outline of the thesis is given.

1.1 BASIC IDEA: 3D TANGIBLE HAPTIC SURFACE

With the benefit of the rapid development of computer technology, computing power has been expanding dramatically. Human-kind depends more and more on computers to carry out scientific research, engineering design, commercial activity, education, entertainment, etc. Human-computer communication methods, which provide one of the most effective avenues to maximize the function of computers, are facing major revolutions. Nowadays, however, human-computer communication is still dominated by the keyboard, mouse, monitor and speaker. These traditional methods stimulate only two senses: sight and hearing. To make human-computer communication more effective, research is being carried out on enhancements of human-computer interfaces by providing comparable modalities between input, display and task.

Shape is a key element in successful communication, interpretation, and understanding of complex data and the geometrical features in virtually every area of

engineering, art, science, medical diagnosis and entertainment, etc. Touch, as another important sense, has been introduced to the human-computer interface for quite some time. Applications for which touch may be the preferred modality include:

1. Design of shape,
2. Feel resistance (mechanical impedance), texture, spatial relationship;
3. Exploration of models and experimental data for understanding;
4. Training of both rare and common skills, retraining/rehabilitation, conditioning;
5. Enhancement of motion capabilities in surgery, manufacturing, construction in normal and hazardous environments;
6. Entertainment and communication of emotion;
7. Assistance to those visually impaired people.



Figure 1-1 Concept of Digital Clay

Digital Clay is a novel tangible haptic (i.e. the sense of touch) 3D surface based interface whose working surface can be shaped by a user and immediately acquired by a computer or shaped by the computer for the user to examine. Its name comes from the similarity to the modeling clay, a material for shaping and sculpture. Like ordinary clay, Digital Clay will allow an area of moderate size to be touched, reshaped with pressure/force, and inspected by the user in a 3D form as illustrated in figure 1-1.

Beyond ordinary clay, Digital Clay provides parameters to the computer that represent the shape of its working surface for further analysis, storage, replication, communication and modification. Digital Clay will also allow the computer to command its shape as portrayed in figure 1-1. Notice that though the concept shown in figure 1-1 is more likely a 2.5D device, the ultimate device could be a true 3D device given the proper actuators.

Digital Clay comprises a working surface that plays the key role of the tangible haptic interface. This surface is formed by a large scale array of fluidic cells which are under control and act together to convey the surface topography of desired 3D objects. **Please note that, in this thesis, “large scale array” means an array consists of a large number of units.** Sensors are embedded in each cell. Ultimately, the hardware of Digital Clay will be manufactured by the MEMS and lithography technology that is under development at Georgia Tech.

During the research and design of Digital Clay, key parameters considered include: spatial resolution, accuracy and extension, amplitude of displacement, spatial differential of amplitude, force levels and speed of response.

Digital Clay’s control will be organized into three levels. The top application level is represented by application programming interface (User API) software that communicates with other computer applications, decides high level human-computer interaction strategies, and generates commands for the surface control level to process. The API will be designed to simplify validation and development of a target set of applications.

The middle control level, surface control, considers cell-cell interaction and coordinates the cell level controls. The surface control is responsible for achieving the

best fit to the ideal surface defined by the CAD model and translated by the API into certain parameters which the surface level controller can understand. The surface control is dependent on the implementation of Digital Clay under control but that will be hidden from both the higher and lower level of control software.

The bottom control level, cell level, commands individual valves based on the received commands and feedbacks.

Note: This research is not related to a manipulator based haptic device that has been given a similar name in a recent article [1]. In this research, Digital Clay's ideal success would be indistinguishable from real clay to the eye and to the touch.

1.2 ADVANTAGES AND POTENTIAL APPLICATIONS OF DIGITAL CLAY

When performing analysis, design or communication with computer, the user may occasionally refocus into the real world around and the sensorial richness it offers relative to the world of the computer. Digital Clay seeks to lessen the disparity between these two environments.

Before the 3D CAD technology was available, engineers had to look at 2D engineering drawings and translate those complicated 2D drawings into 3D models before they could work. This process usually took a long time and often generated mistakes. The situation is greatly changed due to the 3D CAD technology, by which engineers can directly work on the 3D model "inside" the monitor. It benefits not only the engineering design but virtually all graphic based areas such as scientific analysis. However, inconveniences are still found even given the best commercialized 3D technologies. Working on the virtual models with mouse and keyboards, finding the proper commands in the huge command pool, and modeling parts according to the

preprogrammed steps often take a long time to learn and practice. Even for an expert or guru, a large amount of time is spent operating the interface rather than focusing on the design work. Therefore, a more natural, simple and efficient human machine communication interface is desired. Moreover, visually impaired people are not able to use any of these virtual technologies.

Digital Clay concept becomes a new solution to compensate for the shortage of a natural simple and efficient human machine interface by providing a tangible and haptic surface for the user to view and touch as well. The user can work on the CAD model with both vision and hand (just like shaping the clay) through the very simple and straightforward human-computer interface provided by Digital Clay. As a result, the user can fully focus on the design/research task. Therefore, the mental powers of intuition, perception and creation are greatly improved.

In general, the potential applications of Digital Clay cover a wide range from engineering design to entertainment (Figure 1-2). Some of the applications are listed below and examples are given for reference.

1.2.1 3D Dynamic Mapping

By using certain color rendering technology, the working surface can display color images. Therefore Digital Clay can be used to display 3D terrain topographies as depicted in the left picture in figure 1-2. Furthermore, by using GPS technology, the displayed map can change its shape dynamically when carried around by the user. Such mapping technology provides great advantages when dealing with the tasks need fast response to the surroundings. For instance, when in the battle field, the soldier can quickly respond to the surroundings, reducing the time and error attendant to looking at

and understanding the contours on a paper map. When performing a civil rescue task, for example, 3D map of the building or mountain area can be quickly and dynamically addressed, which can reduce the time and eliminate the error.

1.2.2 Medical Diagnostics

As depicted in the middle picture of figure 1-2, equipped with the CT technology (which is now able to get the elastic property of each point scanned), Digital Clay can display a 3D model of the patient's organ which cannot be palpated directly by the doctor. Therefore the doctor can touch the modeled "organ" without opening the patient's body. This could drastically speed up the diagnosis of certain severe diseases such as tumor, cancer and ulcer. Merits can also be found when dealing with certain diagnosis involving privacy and moral principles such as breast cancer examination, obstetric and gynecology examinations.

1.2.3 Engineering Design

Digital Clay can help the designer to design using very natural and straightforward means. The design task will be as simple as modeling ordinary clay. More importantly, the design work is under the supervision provided by the computer which makes it extremely easy and error-free proof. For instance, when creating a sphere (ball) feature on a mechanical part, the user only needs to use his/her finger to prescribe the diameter / radius of the sphere, Digital Clay can automatically generate a perfect sphere under the control of the computer. This is extremely difficult when modeling on the ordinary clay. Another example one can imagine is in the design a golf course. Digital Clay can prevent errors such as slopes too steep and ditches too deep by preventing the user from shaping beyond the limits virtually set in the computer expert system.

1.2.4 Scientific Research

Similar to the applications for the engineering design, Digital Clay can help the user during the scientific research. For instance, it can help the user to feel the relation and force interaction between atomic level structures.

1.2.5 Vision Impaired Assistance

Quite beyond just providing Braille symbols to vision impaired people like the tactile arrays under development, Digital Clay can provide shapes of objects for those people to feel and learn. This is extremely important when helping them “see” big objects around them, such as shapes of buildings, mountains, etc. It is also very important to help them understanding the geometric relationship between objects.

1.2.6 Entertainment

This application could be a very important use of Digital Clay. For example, the user could touch the face or body of an actor or actress when watching a movie or TV, which would be very attractive to most users. Remember that Digital Clay is a haptic surface, which means the user can get the tactile sense of the material that forms the object when touching it. Moreover, the 3D touchable images are not limited to an actor or actress. They can be of beloved relatives such as a husband, wife, father or mother and even of a deceased grandfather or grandmother or of a friend.

Potential applications are also found in the video game industry. Players can have a 3D shape, and even “punch” the objects displayed by Digital Clay (force needs to be limited of course).

Advertisement usage is another potential big application. Instead of big flat color board, Digital Clay can provide a colored, refreshable 3D advertisement board which will be more attractive to users.

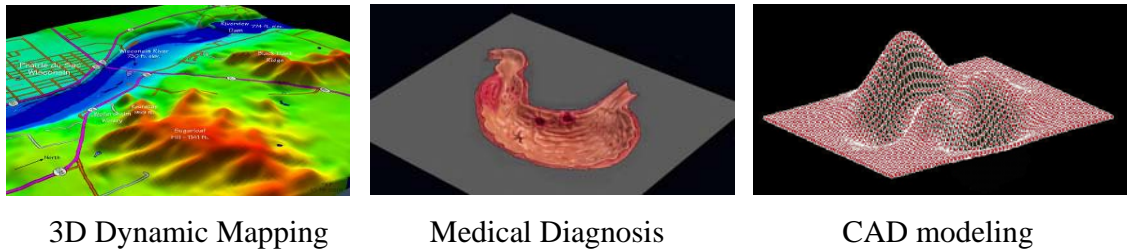


Figure 1-2 Potential Applications of Digital Clay

1.3 DIGITAL CLAY'S FEATURES

Digital Clay comprises an instrumented, actuated, computer-supervised tangible and haptic surface that acts as the human-computer interface. This surface is formed by an array of cells, which act together to convey the surface topography of 3D objects to the volume of the clay by means of manipulation of an internal scaffolding (in the present “bed of nails” implementation this scaffolding is not needed). Currently, in this work, the distance between Digital Clay’s cells (i.e. the spatial resolution) is 5 mm. (In the original proposal approved by NSF, the distance between cells is < 3 mm, which will be achieved in the future.) A prototype is provided in this research that is composed of a 5x5 cell array. All the design and control features are aimed and can be easily adapted to a much large scale cell array system (100 x 100, even 1000 x1000 cell array). Ultimately Digital Clay will be manufactured using combined technologies including MEMS and lithography that are under development at Georgia Tech.

Digital Clay can display shape features in a 3D form. Both kinematics and tactile sensations are provided by Digital Clay. The citations above repeatedly stress the need for a more appropriate actuator that can provide the density and forces required. The proposed fluidic actuators will meet these needs and the manufacturing feasibility as well.

1.3.1 Actuation Type

Digital Clay's actuation system is based on hydraulics. Compared with electrical actuators and pneumatic actuators, hydraulic actuators are better in terms of compactness, light weight, efficiency, and controllability as can be found from Table 1-1. (Comparison between actuators with the same output power)

Table 1-1 Comparison of Three Main Actuation Methods

FACTOR	AIR	ELECTRICITY	HYDRAULICS
Reliability	Poor	Good	Good
Weight	Light	Heavy	Light
Installation	Simple	Simple	Simple
Control Mechanism	Valves	Switches and solenoids	Valves
Maintenance	Constant attention necessary	Difficult, requiring skilled personnel	Simple
Vulnerability	High pressure bottle dangerous; broken lines cause failure and danger to personnel and equipment	Good	Safe; broken lines cause failure
Response	Slow for both starting and stopping	Rapid starting, slow stopping	Instant starting and stopping
Controllability	Poor	Good	Good
Quietness of Operation	Poor	Poor	Good

At the current stage, a hydraulic actuator of 1.6 mm (in diameter) is achievable. It is believed that the actuator can be made even more compact. A shape Memory Alloy (SMA) actuator is another potential actuator for Digital Clay. But since SMA essentially works through temperature change, and heat transfer is not as prompt as electricity or fluid power, the response will be relatively slow. Furthermore, force control is difficult with SMA.

1.3.2 Control of Digital Clay

Due to the structural features of Digital Clay, the control method will be different from classic control. Digital Clay's control is organized into three levels: cell control level, surface control level and the user API. The general control structure is shown in Figure 1-3.

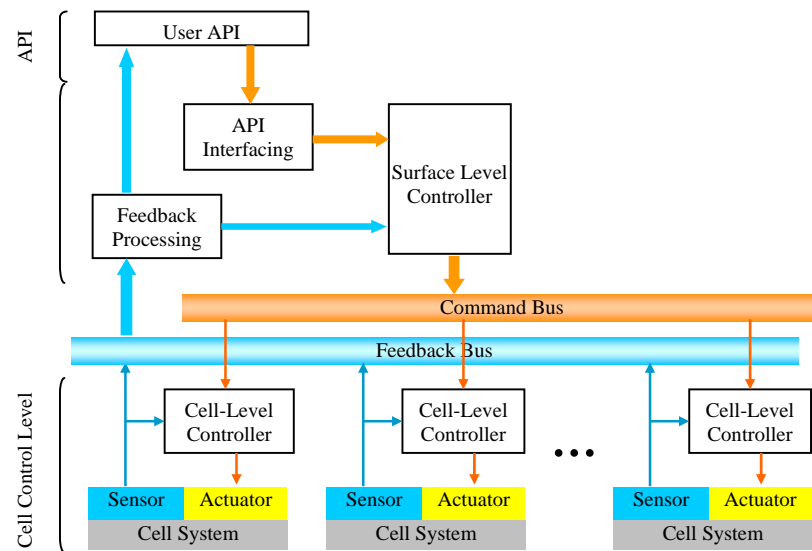


Figure 1-3 General Control Structure

The cell level control and surface level control are investigated in this research while the user API will be fulfilled with the cooperation of the computer science group of the Digital Clay project. For the cell level control, research focuses on: 1) the on-off valve control, 2) the control states switching, and 3) the user gesture interpretation. For the Surface Level Control, the control of the large scale sensor/actuator arrays system is the most difficult aspect. Some previous research is valuable in studying these particular aspects of the control of Digital Clay.

1.4 SCOPE OF THE RESEARCH

This research aims at the practical structural design and fundamental control of a novel human-computer communication device – Digital Clay. The suggested device is essentially a hydraulic actuator array that forms and actuates the working surface to provide required shape and haptic sensation. The practical structural design covers:

1. Overall structure (actuation type and general structure),
2. Hydraulic control system hardware, (hydraulic routes and valves)
3. Actuators (actuator type, structure of one actuator and actuator array),
4. Sensing system hardware (sensor design and integration)
5. Electronic system (multiplexer, valve drivers, filters, etc.)

The control of Digital Clay covers:

1. Single cell of Digital Clay (Shape Display and Haptic Interface)
2. Cell array of Digital Clay (Shape Display and Simple Haptic Interface)

The objective of this thesis is to present the research on practical mechanical structures and control methods for Digital Clay. The research and prototypes delivered can be used as guidelines and tests on the feasibility to realize the concept of Digital Clay. Furthermore, the mechanical system configurations, sensor technologies, novel actuators, and control methods delivered can be applied to other applications.

1.5 OUTLINE OF THE THESIS

In this thesis, the elementary unit of Digital Clay, the cell, is investigated first. This topic covers the practical mechanical structure design, feedback signal processing and control issues. The goal of the investigation is to show it is possible to construct and control a scalable elementary unit of Digital Clay. Design solutions and control methods

are shown, and some best solutions are recommended and implemented. Results are discussed and presented in the forms of diagrams and pictures.

After that, research on conceptual structural design and control for the cell array of Digital Clay is presented. The cell array forms the working surface of Digital Clay. A novel Fluidic Matrix Drive structure is introduced which can greatly simplify the mechanical system and the control. Based on the Fluidic Matrix Drive, the surface level control and user API are studied.

Based on the conceptual mechanical system and control system design, practical realization of Digital Clay is investigated. Digital Clay is essentially composed of an array of intelligent fluidic subsystems and peripherals. Modular subsystems of Digital Clay are introduced; the deployment of an array of displacement sensor/actuators is discussed; the practical realization for the hydraulic “matrix drive” structure is investigated; the structural design of a large scale pressure sensor array is introduced and the multiplexing circuits that reduce the number of data acquisition channels are investigated.

Finally, designs and approaches are introduced to realize the Digital Clay in the form of a small but scalable array system (the 5x5 cell array prototype).

Finally, conclusions and recommendations for future research are given at the end of the thesis.

In chapter 2, background and context of the research are presented.

In chapter 3, the single cell system of Digital Clay is investigated.

In chapter 4, the general structure design and control architecture for the multi-cell array system are provided.

In chapter 5, detailed implementations of the cell array system of Digital Clay are studied.

Based on design and research introduced in previous chapters, a 5x5 cell array prototype is introduced in chapter 6.

In chapter 7, conclusions and recommendations are given.

.

CHAPTER 2

BACKGROUND AND CONTEXT

The human body has five major senses which operate to gather information from the world: sight, hearing, smell, taste, and touch. Any stimulus to one of these sense areas is detected by sensory nerves and then sent to the brain for interpretation. Currently, human-computer communication methods are dominated by the keyboard, mouse, monitor and speaker. These traditional methods only stimulate two senses: sight and hearing. To make the human-computer communication more effective, research is being carried out on enhancements of human machine interfaces by providing input display modalities comparable to the task. Touch, as one of the most important senses has been introduced to the human-computer interface for some time. Sometime, tasks are preferentially interfaced through touch. Visual impairment of some potential users makes touch the sense of choice even for many tasks for which sighted users choose vision. Applications for which touch may be the preferred modality include: design of shape, feel, resistance (mechanical impedance), texture, spatial relationship; exploration of models and experimental data for understanding; training of both rare and common skills, retraining/rehabilitation, conditioning; enhancement of motion capabilities in surgery, manufacturing, construction in normal and hazardous environments; entertainment; and communication of emotion.

2.1 VIRTUAL REALITY (VR)

Virtual Reality (VR) is defined as “A Computer-Generated, 3D Spatial Environment in Which Users Can Participate in Real-time.”[2] A VR system stimulates most senses (Sight, sound and touch) to create an “environment that is indistinguishable from reality” or user to experience a environment, event or situation. Born in the mid-1960s, VR technology is developing very quickly nowadays.

The term "Virtual Reality" is broadly used and widely interpreted. (Isdale 1993) Relating to this research, VR is a human-computer interface that allows users to experience computer generated environment in three dimensions and haptics using interactive systems include visual devices, sound devices and haptic devices (to sense movement in the hands or on the body).

VR can be divided into three stages -- passive, exploratory, and immersive. Passive VR refers to activities like watching TV, seeing movies, reading books, or visiting amusement parks. Exploratory VR is interactively exploring a 3D environment solely through the monitor of a computer. With immersive VR, the user can fully interact with the computer generated environment with stimulation provided by the computer and have their actions directly affect the computer.

VR is not able to provide fully real world experience mainly because it cannot provide all necessary information of a real world (e.g. smells)

Dominating devices to realize VR technology can be divided into three categories: graphics system, sound system, and haptic system. The graphics system and the haptic system are discussed in the following paragraph while the sound system is omitted due to the loose relation to this research.

2.1.1 Visual Virtual Reality (VVR)

Surrounding environment information is mainly obtained through human visual system (eyes). There are two different processing methods for human visual system to process the visual information: 1) conscious and 2) preconscious processing [3].

Several key factors that can affect the sensation in VVR are: 1) field of view, 2) frame refresh rate, and 3) eye tracking. Field of view must be broad enough to prevent a tunnel vision feeling. Frame refresh rates must be high enough to provide a continuous motion and to limit the sense of latency. Eye tracking can help to reduce computational load when rendering frames, since the human can render in high resolution only where the eyes are looking.

The sense of virtual immersion is usually achieved via some means of position and orientation tracking. The most common means of tracking include optic, ultrasonic, electromagnetic, and mechanical. All of these means have been used on various head mounted display (HMD) devices. HMDs come in three basic varieties including stereoscopic, monocular, and head coupled.

Problems

VVR systems both hold much promise and have many problems. These problems include poor display resolution, limited field of view, visual latency, and position tracking latency. Furthermore, the VVR systems only provide the visual sense to human. To stimulate the modality of touch, research has been put on the technique that displays shape attributes through the sense of touch. This technology is also known as haptic.

2.1.2 Haptic Interfaces

There is some significant prior research in the area of haptic interfaces [4] [5]. Early haptic interface devices provided the user with a tactile perception of molecular forces and torques [6]. Its mechanical structure is essentially a robot arm. Some alternative force-feedback devices with multiple degrees of freedom have been proposed in later research [7] [8]. These approaches provide an intuitive interface for the manipulation of rigid bodies that are subject to inertial, contact, or other forces. However, they are significantly less convenient for sensing and altering the shape of curves and surfaces [9]. There are several other attempts to use haptics in the design of surfaces [10]. For instance, the “Virtual Clay” system enables the user to attach a so-called 'Phantom stick' to any point on a virtual surface and then move the stick to pull, push, twist, or bend the surface, while the rigidity and inertia can be controlled. These techniques focus on force feedback, which assists the user in gauging the effort required to exert on surface in order to achieve the desired shape alteration. This approach may also be used to provide information about the stiffness or density of the surface [10]. In addition, such haptic approaches have been applied to the exploration of a field in a volume [11] or even of fluid dynamics [12] [13]. However, these approaches do not provide any direct tactile feedback regarding the shape of the surface. Running the tip of a computer cursor over the virtual surface has been suggested as a means for “haptic surface rendering” [10] [14] and has been extended to real-time detection of contacts when manipulating an object with six degrees of freedom [15]. Such approaches, based on exploration of a surface with the tip or side of a stylus, produce forces that would result from contact, palpation, or stroking actions. These forces may reveal surface anomalies or attract the attention of

the designer to small, high-spatial-frequency features that may be more difficult to detect visually. However, stylus-based approaches are far from exploiting the natural ability of a designer to touch and feel a surface with the hand.

Gloves, arrays of actuators and manipulators controlling a stylus held by the hand are some normal mechanical structures of haptic interfaces, which depict a surface. They attempt to supply sensations to our various touch and kinesthetic receptors, which are often broken into several regimes [16]: Vector macro forces are at the gross end of that scale and are readily displayed by manipulator-like haptic devices. Vibrations are by nature a scalar field and may be distributed widely over the surface of the skin. The amplitude and frequency are noticeable but not the direction. The most difficult to display are small shapes, for which arrays of stimulators are necessary. To achieve both kinesthetic and tactile sensations simultaneously, the combination of a haptic manipulator and a tactile array is currently required. Several concrete haptic interface devices are discussed below as related devices to Digital Clay:

A Tactile Array is a device typically constructed by a planar arrangement of linear actuators and/or sensors acting perpendicular to that plane. Fearing's "ideal stimulator"[17] has 50N/cm^2 peak pressure, 4 mm stroke, 25 Hz bandwidth and the density of one stimulator per mm^2 . Bliss [18] tried to use stimulators to display Braille to sightless readers. Current interest is greater in the combination of sensor and display (stimulator) to be used in tele-operation, with a particular interest in tele-surgery [19]. Electromagnetic [20], pneumatic [21] and shape memory alloy [22] actuators have been tried in building the tactile arrays. The sizes of these arrays are quite small, about the pad of a finger. The recent device by Kammermeier [20], for example, covers 16×16 mm with

36 sensors and tried to follow Fearing's target specifications for an ideal stimulator. Fearing also pointed out that stimulator-pins must be covered with rubber to low pass filter the pin force transmission to avoid aliasing. From his analysis, he concluded that the rubber thickness should be about 1.5 times the spacing of the pins. In some aspects, Digital Clay is like tactile sensors plus tactile stimulators [17] [19] [23] [24] [25] [26], except that Digital Clay's cells have a large stroke more than 60 mm.

Data Gloves [27] are hand-worn devices, which provide an alternative way to generate spatially related input, but the display of output is typically visual. Researchers are seeking to remedy this by modifying the glove concept to allow forces to shape the hand or resist its motion [28].

Haptic Manipulators provide a way to explore a haptic environment in a point wise fashion is by using the Haptic Stylus. If the stylus is attached to a manipulator, interaction forces can be generated which represent interaction of the stylus with a virtual world. Available point wise haptic displays including some commercial products such as the Phantom [29] allow forces and moments to be fed back to the user in 2 to 6 degrees of freedom. They are well suited to provide the kinesthetic portion of a haptic experience. The Haptic Mouse is another kind of device. It enables the user to feel the transition of the cursor between different regions of the screen [30]. These haptic manipulators open new possibilities of interfacing, but are comparable to displaying a picture to a viewer one pixel at a time. Haptic manipulators must provide spatial relationships only through temporal sequencing, greatly compromising their efficiency. Sample rates of 1000 Hz are typical with forces controlled at 30 Hz or more for adequate display of features such as a breast tumor. It is necessary to provide a totally synthetic view of the hand in the

environment if haptics are coordinated with vision. Viewing the stylus and its device provides no supporting optical illusion. Another disadvantage of the Phantom and numerous similar devices is that the ratio of the smallest to the largest displayable force is difficult to expand. When the hand should be moving unimpeded, it must at the same time exert a force to move the device forward. Yoshikawa [31] and others have removed this problem by utilizing a servomechanism based on the position of the hand to avoid contact (i.e., achieve 0 force) unless the contact should be displayed. (For Digital Clay the same effect can be achieved without a servomechanism, by simply avoiding contact when none should be displayed.)

Problems

Simple haptic interfaces have following problems: 1) the senses of touch and sight are not simultaneously stimulated in a natural way. Natural human senses of touch and sight are stimulated by the same object. Above haptic interfaces, however, separate these two senses. The user views the object in the display device while getting a feel of touch through another device. This will sometime confuse the user and distract the user from the task, 2) images displayed are essentially two dimensional, and 3) they only provide touch stimulation in a small area (usually one point or one finger-sized area) with very limited stroke..

There is some other research on the combination of the haptic interface with visual interfaces. FEELEX [32] and Pop Up! [33] represent the main trends of these research.

2.2 COMBINATION OF HAPTIC INTERFACE AND VISUAL INTERFACES

Haptic Display Interfaces (currently are still in their prototype stage) are devices built to displace shape with haptic interface using mechanisms. These mechanisms usually

utilize a planar pin-rod matrix array of vertically actuated linear actuators or pin-rods that can be raised in order to form the desired surface with their top ends. Two of the most relevant projects are introduced in the following sections.

In 1970, Bliss et al. [34] developed one of the first tactile sense device, --- the OPTACON, which converts character information into tactile information. However, its stroke is limited by its actuation type (PZT actuator).

Compared to the OPTACON, FEELEX[32] using pin-rods and servomotors. It achieved the interaction with computer graphics through haptic sensation.

The idea of "Tangible Bits", proposed by Ishii et al. at the MIT Media Laboratory, suggests using a physical object as an input interface between cyberspace and the physical environment. "Super Cillia Skin,"[35] "Pins"[36] and "SandScape"[37] are examples of Tangible User Interface (TUI).

Pop Up! [33] realizes a pin-rod matrix display with both a high density and a long range of movement.

2.2.1 Project FEELEX

In 1998, Hiroo Iwata reported project FEELEX [32]. It develops a new technology that combines the haptic sensation with computer graphics. As shown in Figure 2-1, the prototype comprises an array of electrical motors working as the actuators. It achieved the interaction with computer graphics through haptic sensation, and is one realization of WYSWYT (What You See Is What You Touch).

The force density seems to be a main problem for any device using electrical motors. Here, the actuator's force density means the ratio of the output force / torque over the size of the actuator. In FEELEX, the actuators (motors) occupy a big portion of the size of

the whole system. Currently it is still difficult to minimize the size while keep the output force / torque high enough, which directly affects the scalability and resolution of the haptic – visual displacement. In other words, the motor size is difficult to make small to reduce the spacing between actuators.



Figure 2-1 Project FEELEX

Therefore, although FEELEX was successful in displaying a relatively bumpy shape, due to the relatively large volume of the actuator, it is difficult to construct a large scale pin-rod matrix array with high resolution.

2.2.2 Project Popup!

Project POPUP! [33] is a project carried out in The University of Tokyo. It provides an innovative approach to display 3D objects by orchestrating the vertical motion of a dense array of pin-rods, as shown in figure 2-2. The effect is similar to the toy "Pop up book", where a flat surface transforms into a 3D form. Each pixel is composed of a simple component, and the driving method is scalable so that displays of any size can be constructed in the same way.

Pop Up! is a collective system of long stroke vertical pin-rods, using a coil-form Shape Memory Alloy (SMA) as an actuator. This material can be stretched or deformed from its original shape but would spontaneously return to its original shape when heated.

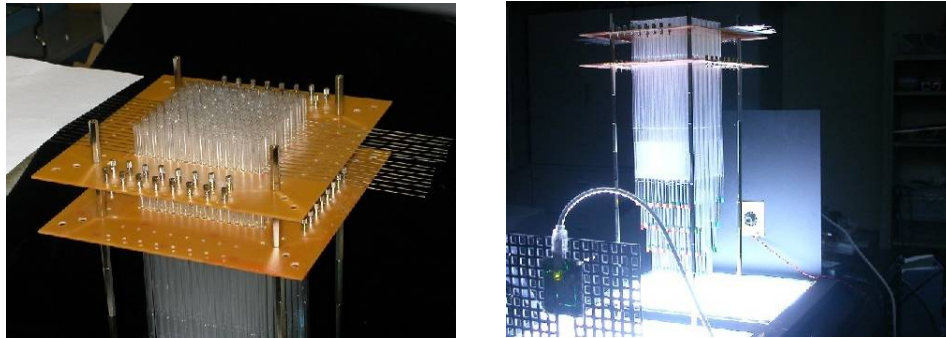


Figure 2-2 Project Popup!

Problem with Pop up! may lie in the control of the SMA actuator. Using SMA as an actuator is the most important aspect of this project. There have been a great variety of studies about the characteristics of SMA's. The main problem lies on the fact that SMA essentially works through the temperature change. Heat transfer is not quick compared with electricity and fluid power. Therefore, even though the SMA can be heated up quickly given high current passing through, the cool down process takes large amount of time. Thus the response will be relatively slow, and the force control is also difficult.

2.3 CONTROL ISSUES

Digital Clay is essentially an electro-fluidic system. The control valve is one of the fundamental control elements of the system. Compared to a servo valve, an on-off valve is easier to miniaturize using MEMS technology and is more reliable at small size around 1 mm². Hence on/off valve is targeted as the control valve. At the current stage,

solenoid valve is used instead of the final PZT on-off valve. The latter is still under development by the MEMS group [24].

The biggest drawback of on-off valves is the big pressure surge caused by their open/close operation. This big pressure surge can dramatically affect the pressure signal that represents the external force being applied on the cell. A low pass filter is used to suppress the noise. The feasibility is based on the fact that the solenoid valve noise usually has a frequency higher than 60 Hz while the frequency of the external force (usually exerted by the human hand) is normally lower than 6-7 Hz. Another challenge is to control the flow rate passing the on-off valve. It is difficult to control the on-off valves to precisely achieve desired flow rate using conventional methods. Research shows that it is possible to combine several on/off valves to achieve the flow rate control [38]. It is also reported that given the position of the valve's plunger, the PWM (Pulse Width Modulation) method can get a good flow and pressure control [39]. Other researches showed that the PWM method can achieve a rough flow rate control with limited flow rate control range [40] [41] [42]. These solutions are not suitable for Digital Clay since they either need multiple valves[38] or position feedback of the plunger[36], otherwise a significant change of controlled pressure due to switching action of valve will destroy the accuracy of the system[40] [41] [42]. Moreover, most of the above research deals with pneumatic systems.

Larger Scale Sensor-Actuator System Control

Digital Clay comprises a large number of cells. Each cell (or cell cluster) is an intelligent sensor/actuator system with a micro processor embedded. Thus the Surface

Level Control aims at the control of large scale systems with controlled units distributed over some spatial domain and operating asynchronously [25] [43].

There is a lot of research found in this area. Examples of technologies which have helped define the central issues in the theory of coordinated control of such systems can be found in Intelligent Vehicle Highway Systems and Air Traffic Management Systems [45]. However, with the scale of the systems expanding quickly to millions and even tens of millions of units, centralized control becomes unviable due to the limited centralized information and computing capability. (One million cells for Digital Clay represent a resolution of 1000×1000 in 2D or $100 \times 100 \times 100$ in 3D.) Decentralized control, on the other hand, using only local information while guaranteeing stability of the entire system is more suitable for this kind of large scale system. There are three types of decentralized control structures: Fully, Partially and hierarchically decentralized control [46]. D. Gavel, and P. Ioannou gave examples addressing the problem of decentralized control of large-scale systems in the framework of direct model reference adaptive control [47]. However, for tiny devices, because measurements will be subject to considerable noise, precise state information will be difficult and costly to obtain for a local closed loop control. Moreover, the operational time constants trend to be very short, which leads to a need for increased channel capacity in feedback links. J. Baillieul presented a paper with emphasis on general communications and information processing problems [48]. Though it is basically a modified centralized control solution, it touches the constraints of information carrying capacity in the feedback links connecting the sensors, controller, and actuators for some large scale systems.

Another related technology is the large scale LED array control structure, which controls each LED in a row and column matching manner. The biggest advantage is that it can greatly reduce the number of required control units (valves, sensor signal conditioners and low level microcontrollers). However, since pneumatic/hydraulic actuator of the Digital Clay is not a simple “pass through” device, this method needs to be modified before being applied.

Separately applying the preceding technologies to Digital Clay will face problems as mentioned above. Combination of those technologies, however, may provide a potential solution for the surface level control for Digital Clay.

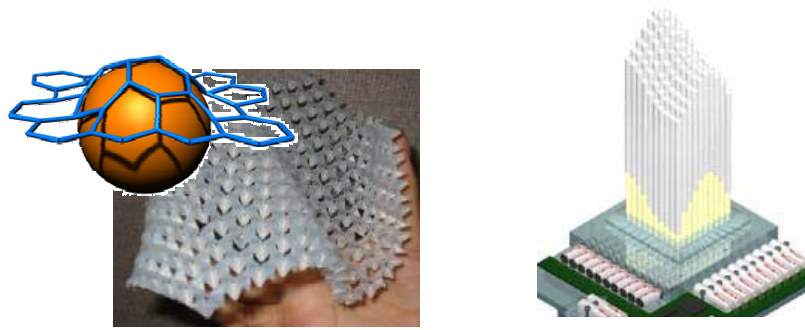
CHAPTER 3

CELL OF DIGITAL CLAY

In this chapter, the elementary unit of Digital Clay --- cell is investigated. A cell forms and actuates a point of the working surface. This topic covers the cell level control architecture, feedback acquisitions, and the practical mechanical structure design. Challenges to control are found on the on-off valve flow control, the processing of the pressure signal affected by the on-off valve, control states switching control, the user gesture interpretation and the motion planning of the shaping state (a control state that allow user to change the volume of the cell with only compressive force). Challenges on the mechanical structure design are mainly the actuator's structure, size, and deployment of sensors. The goal of the research on the single cell is to show the possibility to construct and control a scalable elementary unit of Digital Clay. Several design solutions and control methods are shown, and some of the best solutions are recommended and implemented. The results are presented with diagrams and pictures.

3.1 OVERVIEW

Basic structure of the Digital Clay has two solutions as proposed by Paul Bosscher and Austina Nguyen [49] [50] [51]: formable crust (Figure 3-1a) and formable body. At the current stage, formable crust and 3D formable body structure are far from practical. Therefore, the 2.5D formable body concept that can be realized by a planar x-y array of linear actuators acting in the z direction is studied here.



(a) Formable Crust Concept (b) Planar Pin-rod Array Concept

Figure 3-1 Kinematical Structures for Digital Clay

Cell is the elementary unit of Digital Clay. An array of cells forms and actuates the working surface of Digital Clay. The cell of Digital Clay, categorized by its actuation directions and degrees of freedom, has two possible types: one dimensional and three dimensional, as shown in Figure 3-2.

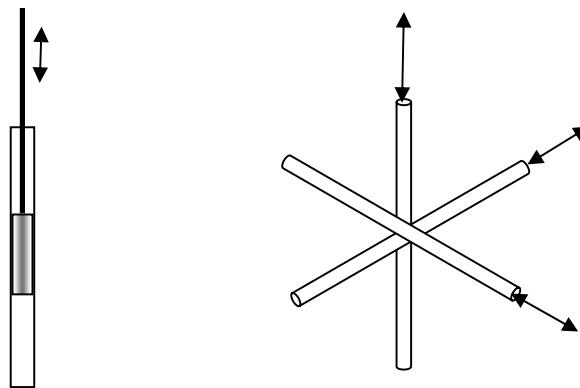


Figure 3-2 Single Dimensional and Three Dimensional Cell

Obviously, the one dimensional cell has the simplest structure, but can only form a 2.5D surface, i.e. the working surface cannot display shapes with side concaved features. The 3D type cell has more complex structure but can form a 3D model. This research

focuses on a one dimensional style cell since the 3D type cell presents conceptual difficulties beyond the scope of this thesis. To provide high resolution and good haptic sensation, the actuator is required to have high ratios of both force-over-volume and displacement-over-volume, and small size. After the comparison of several actuation types (table 1-1), hydraulic actuator is chosen to construct the actuation system for Digital Clay.

Since the actuation system consists of thousands even millions of cells, simplicity is highly critical for each cell. Hydraulic control valves are key components for the hydraulic actuation system. Therefore, the simple on-off valve is chosen because of its simple structure and bi-state working principle. Furthermore, on-off valves are very suitable to manufacture using MEMS technology. (Control valves and actuators may ultimately be manufactured using MEMS [52].)

The cell level control is responsible for inflating and deflating individual cells with certain pressure to achieve a specified dimension as well as to provide a haptic interface. Pressure differential, valve actuation and time are the parameters in the integral relationship that determines the extension of the cell. Initially this logic will be placed in a central computer, but it is desirable to embed as much of this capability in a cell or group of cells as possible.

Pressure and displacement are two feedbacks required to displace a haptic-visual shape. The forces applied by the user are not under our control and hence the pressure must be monitored frequently. Displacement sensing has some alternative methods. Displacement estimation using pressure difference under PWM method and micro miniature displacement sensor design are also discussed in this chapter [53].

Requirements for a Single Cell System

Digital Clay is essentially a hydraulic system with large amount of micro hydraulic actuators, micro sensors, and the control structure and algorithms with large scale control capability. Per the ultimate goal, the single cell of the Digital Clay should have the functions of visual display and haptic interaction. Display function requires that a single cell is able to change its dimension (to the required equilibrium position) with required speed under control. The haptic interaction requires that the cell is able to respond to the user input force by adjusting its dimension around the equilibrium position. Therefore, the single cell system is subjected to the requirements below:

Compact Size: In this thesis, actuators used are linear hydraulic cylinders with outside diameter $< \varnothing 4$ mm. Ultimately, the OD of the actuator will go under $\varnothing 3$ mm. Compact size helps to improve the display resolution and haptic effect.

Long Working Range: As proposed here, the working range of the cell should be around 50 mm. Big working stroke improves the shape display capability.

Actuation Type: One dimensional. Three-dimension actuation can display true 3D objects, but it is still far from practical. One dimensional actuator is proposed with the consideration of the current technology stage.

Structural Simplicity: Structural simplicity is critical to achieve a large scale, high resolution and low cost realization of the Digital Clay.

Position and Velocity Controllability: As shown in figure 3-3, A point on a material surface has three major parameters: elastic modulus E , damping ratio b , and equilibrium position X_0 . Therefore, to control the single cell to realize or simulate a point on a material, the speed and the position of the actuator are two basic control parameters.

Under this requirement, the cell level controller should be able to control the cell to reach desired displacement with certain speed.

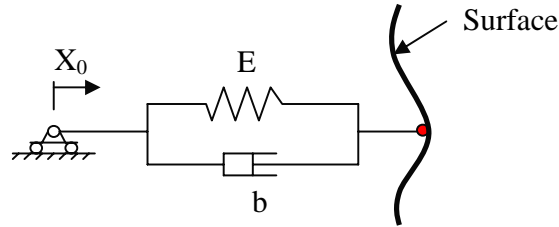


Figure 3-3 Model of a Point on Material

Logic Controllability: Logic control is provided by the cell level controller. The cell level controller takes the position and pressure feedbacks of the actuator and the commands from the surface level controller; determines the required position and velocity of the actuator in the next step; and then controls the actuator to realize the required speed and velocity. More specifically, the logic control includes the following topics:

Simulation of the mechanic behaviors of materials: To simulate the mechanic behaviors of materials is to control the actuator to mimic the visco-elastic and plastic state of the material. The key issue is to control the displacement and velocity regarding to the external force applied on the actuator, based on the desired relationship.

Realization of the volume change: Modifications applied to ordinary clay usually involves adding or subtraction volume from the clay. For Digital Clay, this can be realized through change the equilibrium position of the cell.

Switch between the control states: A single cell of Digital Clay has three control states: Elastic State, Plastic State, and Shaping State (a state that can realize the cell

volume change, i.e. adding or subtraction of volume). The control laws of these control states are different from each other. Therefore, the cell level control system should be able to switch between these control states stably.

This chapter is organized as follows:

In this chapter, cell level control for the single cell system is presented first. An experimental system is introduced. Processing on pressure signal that is affected by the solenoid valve is discussed. After that, control problems and solutions are presented, and experimental results are provided and discussed.

Then, the displacement sensing methods are discussed. Compared to the pressure sensor, whose size can be easily miniaturized, the displacement sensor is relatively difficult to get its size miniaturized. In this chapter, to dealing with this problem, three methods are discussed and a solution is chosen.

In this chapter, concepts for the micro actuator design and embedded displacement sensor design is also provided.

Conclusions are given as the final part.

3.2 CELL LEVEL CONTROL FOR THE SINGLE CELL SYSTEM

A cell of Digital Clay forms and mimics a point on a material surface. The cell's displacement and velocity is dependent on the external user force applied on it. The cell level controller responds for the haptic behaviors of the single cell and is composed of the cell level controller plus the communication mechanism. Cell level control is a kind of intelligent control. The general control mechanism for the cell level controller is shown in Figure 3-4.

By adjusting the displacements and velocities of the cells' deformation, Digital Clay can mimic the desired mechanics of a material, i.e. elastic and plastic. Hence, the cell level control is essentially to enforce the relationship of the cell's displacement and its inner pressure. At this control level, the displacement and the pressure are two measurements, and flow rate into/out of the cell is the parameter to be controlled. In this section, focus will be put on the pressure signal processing, the position and speed control method and control state switching method.

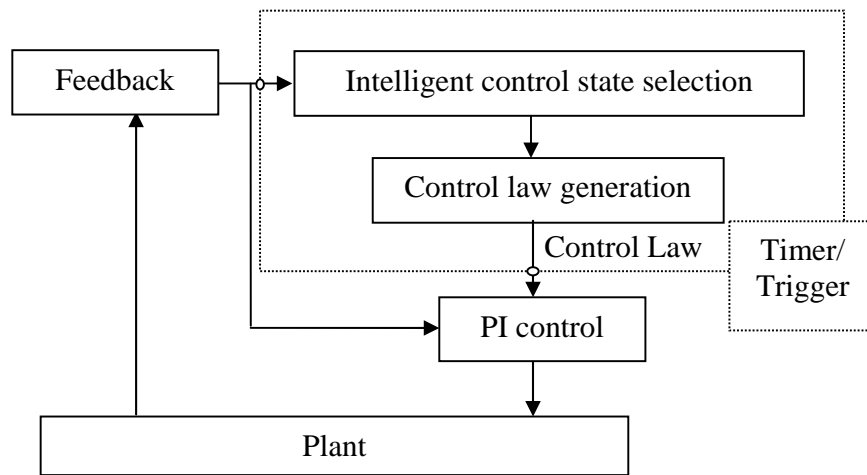


Figure 3-4 Cell Level Control for the Signal Cell System

In this section, cell level control algorithm for the single cell system is discussed and experimental results are provided. Common off-the-shelf hydraulic components are used to set up the experimental system since the research focuses on the control at this stage. Specially designed actuators, sensors and valves for Digital Clay will be discussed in later sections.

3.2.1 Experimental System

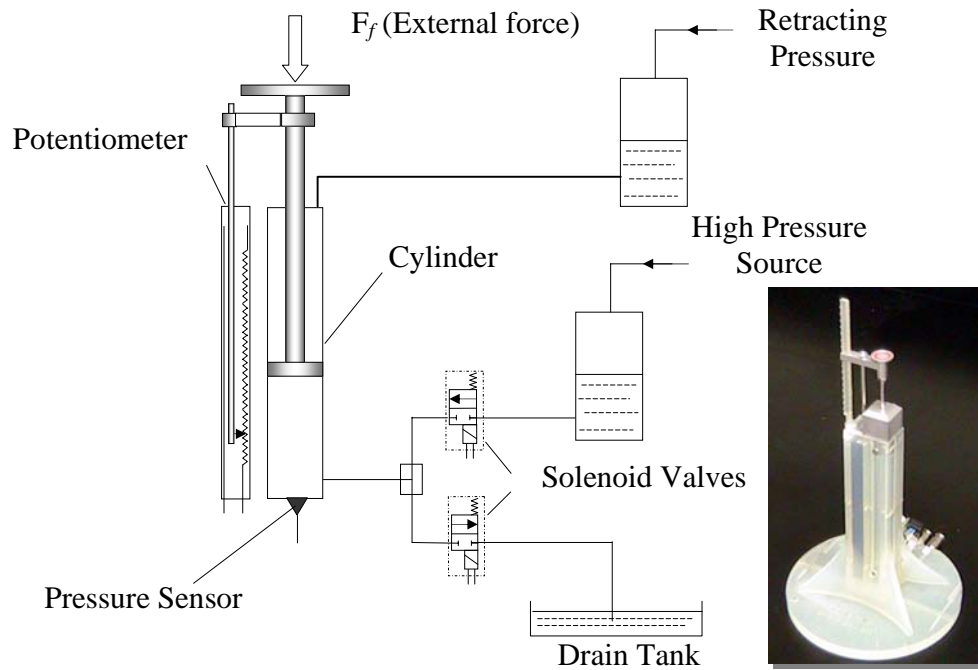


Figure 3-5 Experimental Setup of the Single Cell System

The experimental system schematic diagram is given in Figure 3-5. An ultra-low friction cylinder is chosen as the cell's actuator. Two miniature fast response solenoid valves are chosen as the control valves. The working fluid is pressurized by regulated compressed air. A pressure sensor is attached to the cylinder chamber to measure the pressure. A linear potentiometer is attached to the actuator to measure the displacement of the actuator. An Intel P4 computer works as the cell level controller system. A digital I/O card and an A/D card provide the interface between the computer and the experimental system. To improve the performance, Real-time Linux is adopted as the operating system. Features of the key components (control valves, cylinder, and sensor) are listed in table 3-1.

Table 3-1 Features of Key Components

ITEM	FEATURES	NOTES
Control Valve	30 PSI, Open time: 1ms, close time: 1ms	www.theleeco.com, HDI12111
Actuator	Ultra-low friction, 50mm stroke	www.Airpot.com, E09.40U
Pressure Sensor	15 PSI, 1ms response time	Honeywell, 40PC015A

3.2.2 Processing the Pressure Signal Affected by the On/off Valve

As mentioned before, pressure and displacement are two measurements used to control the system. The displacement signal contains relatively low noise, while the pressure signal taken from the actuator is subjected to very big undesired noise. Investigation showed that the pressure signal noise is caused by the on/off hydraulic control valves.

The big pressure surge is actually generated by the suddenly opening and closing of the on/off valve (as shown in Figure 3-6). This big pressure surge can dramatically affect the pressure sensor when trying to detect the external force acting on the actuator. To solve this problem, filters are considered to suppress the noise. This is possible because the on-off valve noise usually has a frequency higher than 60 Hz and can be made higher, while the external force generated by human user hand is normally lower than 7 Hz.

Two types of filters are investigated. One is the mechanical hydraulic filter. Another is the electrical filter composed of passive or active components.

The mechanical hydraulic filter is composed of a small orifice and an accumulator. The experimental result of this filter is not satisfactory, because the filter is first order. Therefore second and higher order electronic filters are tested. The efficacy of the second order electrical filter is shown in the Figure 3-6.

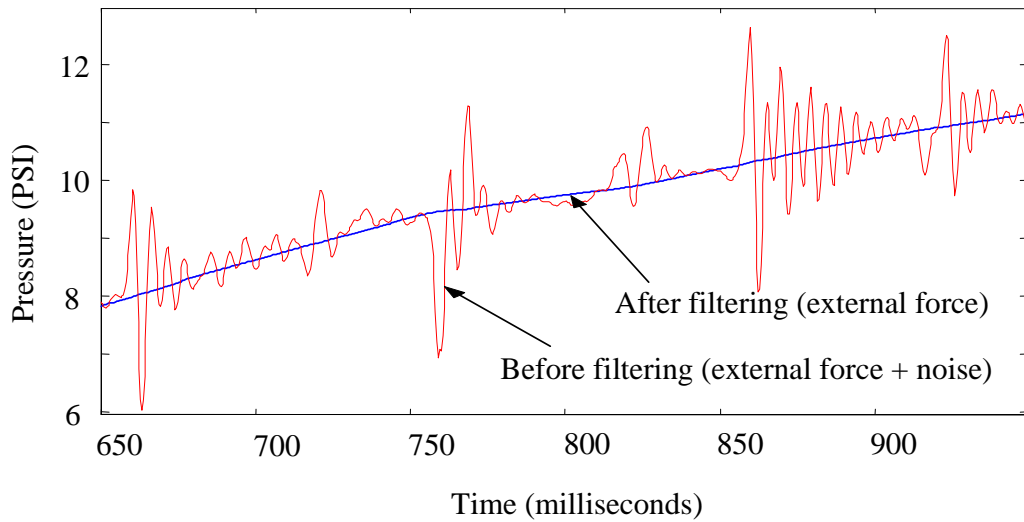


Figure 3-6 Efficacy of the Second Order Filter

3.2.3 Pressure Control vs. Position Control

To provide haptic effects, the cell's displacement should be controlled according to the external force acting on it. There are two methods to control the cell's displacement: the pressure control method and the position control method.

Under the pressure control method, the cylinder's pressure is regulated (by adjusting the orifice size of the control valve) according to the actuator's displacement feedback. This method cannot be directly applied when the control valve is an on/off valve. Therefore, Pulse Width Modulation (PWM) was investigated for controlling the on-off valve to mimic a proportional valve as shown in Figure 3-7. The problem found is the structural complexity caused by the accumulator and small orifice.

Position control method here means to adjust the actuator's displacement according to the actuator's pressure feedback that caused by the external force. Since the pressure

feedback contains a high frequency solenoid valve noise, so a low-pass electronic filter is placed between the pressure sensor and the computer to filter the pressure signal. Given that the second order filter can give a -40dB/decade effect on the pressure signal, it is quite effective in filtering the solenoid valve noise in the pressure signal leaving the part caused by the external force. (Figure 3-6).

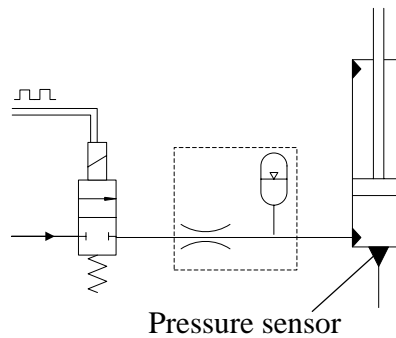


Figure 3-7 Inlet Circuit for Control using PWM

3.2.4 Cell Level Control Structure

As shown in Figure 3-4, cell level control for the single cell system is composed of intelligent control state selection algorithm, control law generation, and PI control algorithm. PI control algorithm is conventional, so it will not be discussed here. The focuses will be put on the intelligent control.

To simulate / mimic a solid material, each cell of Digital Clay should be able to mimic a point on a material. A point model of a material has been provided in Figure 3-3. According to the mechanics of materials, when one pushes the point with force F_f lower than the yielding limit F_y , the material is under the elastic state. If F_f exceeds F_y , the point will keep moving backwards, and the displacement of the point is no longer proportional to F_f . Furthermore, when pushing the point with different speeds, one can

feel the damping effect. This research focuses on the simulation of elastic and plastic states; the damping simulation will not be touched

Based on the above analysis, the cell level control structure for the experimental system is organized into two working modes: 1) the display mode consisting of three possible control states: elastic state and plastic state, and 2) the edit mode consisting of three control states: elastic state, plastic state and shaping state. The shaping state allows the user to virtually add or subtract volume from the displayed 3D surface.

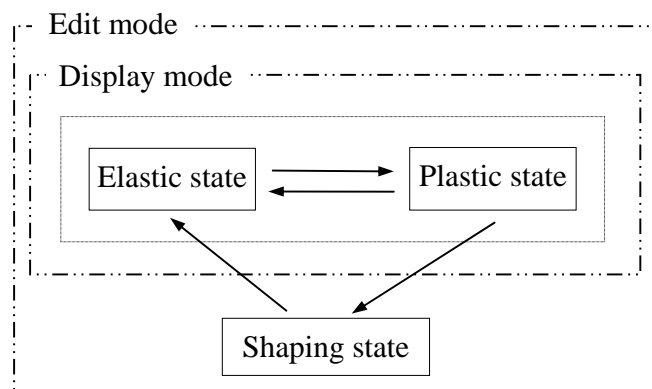


Figure 3-8 Working Modes vs. Control States

Under both the display mode and the edit mode, the user is allowed to view the shape, feel the properties of the displayed material. But only under the edit mode, the user can “add” or “subtract” volume from the displayed 3D surface and the interactions between Digital Clay and the user can be selectively digitally recorded for further editing needs such as “undo” and “redo”.

The relationship between working modes and working / control states is shown in Figure 3-8.

Elastic State

In the elastic state, the single cell system is controlled to perform like a spring, i.e. the displacement of the actuator is proportional to the external force F_f acting on the actuator.

Plastic State and Elastic-Plastic Switching

In the plastic state, the actuator keeps retracting until the plastic state is terminated (i.e. external force $F_f < \text{yielding limit } F_y$).

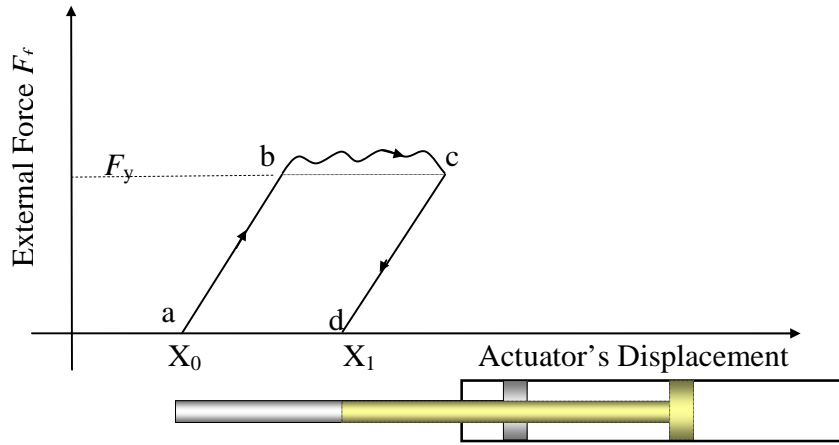


Figure 3-9 Elastic and Plastic States

Suppose the system starts in the elastic state, when the external force F_f is smaller than the yielding limit F_y , the cell system works in the elastic state (Line ab in Figure 3-9) with the equilibrium position X_0 . Then if the external force F_f exceeds the yielding limit F_y , the cell system turns into the plastic state, and the actuator keeps retracting until the external force F_f is smaller than F_y again. (Curve bc) At the same time, the new equilibrium position X_1 is calculated, the elastic modulus is restored and the system switches to the elastic state (Line cd).

Shaping state

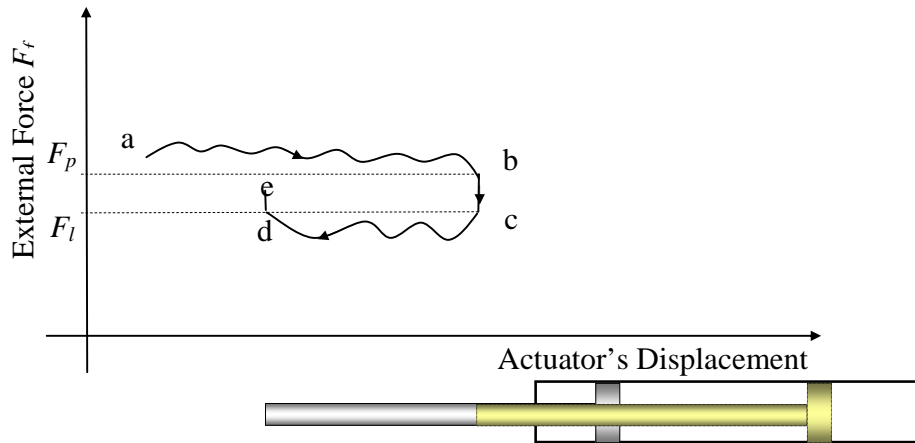


Figure 3-10 Shaping State

Shaping state allows the user to “add” or “subtract” volume from the system by the means of “lifting” or “pressing” the surface. In this control state, when the external force F_f is larger than the upper limit force F_p (set by the user), the actuator will retract (Curve ab in Figure 3-10). When the external force F_f is smaller than the lower limit force F_l , the actuator will extend (Curve cd). If the external force F_f is between the F_p and F_l , the actuator will stay stationary. (Curve de and bc) This control state is similar to the plastic state except that: 1) the force limits (F_y , F_p and F_l) are different, and 2) the user can command the actuator to extend by pressing the actuator in the shaping state. (In other control states, pressing only cause retraction)

3.2.5 User Gesture Interpretation

Digital Clay is an input/output device, so an effective, simple and friendly communication method between user and Digital Clay is critical.

The control system uses the three control states (described above) to deliver the information from the computer to the user. And the user can use preset gestures to express his or her intention.

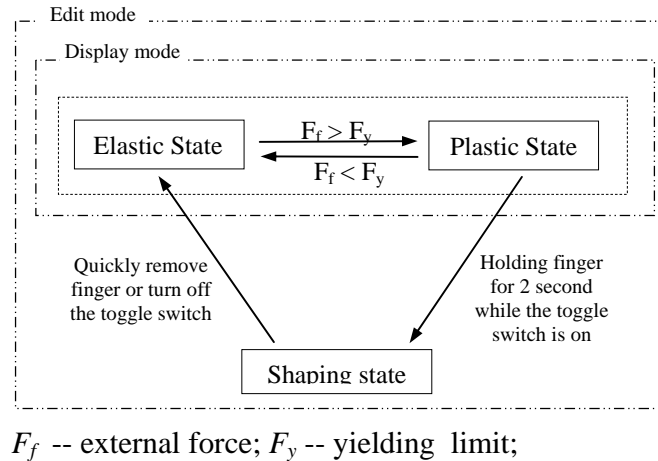


Figure 3-11 User Gesture Interpretation

The final solution is subjected to the following requirements: 1) Simple, i.e. both the hardware and the software should be as simple as possible; 2) Reliable, i.e. the computer must correctly detect the user's intention; 3) Easy to operate, i.e. the preset user gestures should be easy for the user to perform; and 4) Easy for user to remember. Based on above requirements several methods were investigated and the one selected is described below and its general block diagram is provided. (Figure 3-11)

Switch between Display Mode and Edit Mode

A toggle switch is used to toggle between the edit mode and the display mode. The switch could be a software switch controlled by the computer. Only when the switch is on, is it possible for the user to edit the model, i.e. the user can use the shaping state.

Switch between Elastic State and Plastic State

To switch the system from the elastic state to the plastic state is very simple: exert a force larger than the yield limit F_y . If under the display mode, when the external force is less than F_y again, the system goes back to elastic state.

When under edit mode, to shape the model, the user firstly has to reach the plastic state, i.e. exert a force bigger than F_y on the cylinder rod, and then keep the finger stationary for a short while, for example, 2 seconds. Then the system will go into the shaping state. In the shaping state, the cylinder rod tip will follow the finger until the finger is quickly removed (or turn off the toggle switch). This set of user gestures is quite easy to remember: Pushing hard (until it yields), waiting for the rod tip to “stick” to the finger, shaping the surface (currently only one point) with the finger and, if finish, quickly removing the finger to “get rid of” the rod tip.

The above user gestures are realized using the following method. When the toggle switch is on (i.e. in edit mode) and the system is in the plastic state, a software thread will start to monitor the movement of the cylinder rod. If the rod keeps stationary for a certain time, the system will switch to the shaping mode. In the shaping mode, if $(-dF_f/dt)$ is detected to be bigger than a certain value, the system will record the rod position and go back to the elastic state. Here, F_f is the finger force. The recorded rod position will be the new equilibrium position for the elastic state.

3.2.6 Experimental Results

This method is tested on the experimental device described above. The result is shown in Figure 3-12. The data were recorded under edit mode and the experiment process is described below:

Under edit mode, push the rod with gradually increasing force until the system went into plastic state. (Line ab indicates the elastic control state and curve bc indicates the plastic control state) Then hold the finger's movement until the system goes into the shaping state. (Line cd) In the shaping state move the cylinder rod back and forth by controlling the finger force. (Curve de, ef, fg, gh, hi, ij and jk) Then quickly remove the finger, (Curve kl) let the system go into the elastic state (with a new zero load position --- point l). In the shaping state, when the finger force (proportional to the pressure in the cylinder) is between the upper limit force F_p and lower limit force F_l , the cylinder rod keeps stationary. This can be seen from the vertical line S, gh, ef, etc.

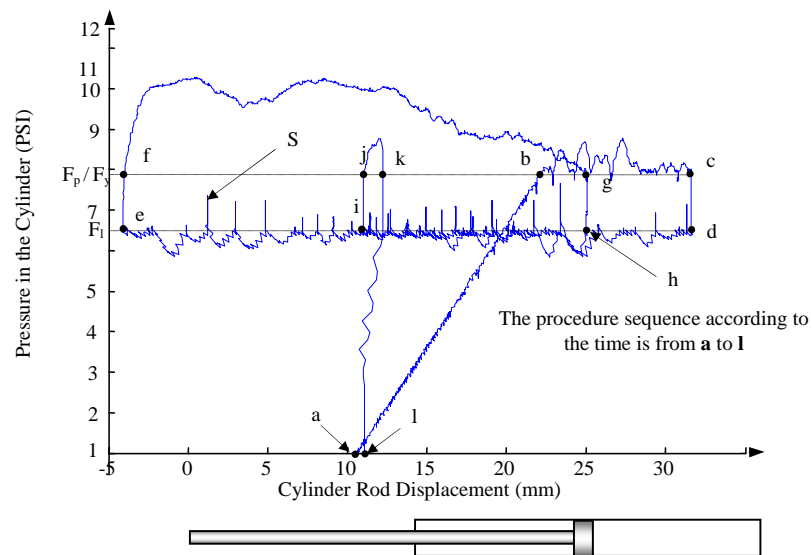


Figure 3-12 Experimental Results

Though the experimental result is obtained under the edit mode, the result is also applicable for the display mode. Since this experiment focused on testing the user gesture interpretation method, two high-speed solenoid valves instead of the conventional solenoid valves were used to make the control states clearer and easier to identify.

3.3 DISPLACEMENT SENSING METHODS

The challenges of displacement measurement lie in both the fabrication of the sensor (micro diameter, sensing range > 50 mm), and mounting the sensor into the cell. Since no suitable off-the-shelf sensor is available, the design of new displacement sensors or alternative estimation technology becomes necessary. In this research, three displacement sensing methods are investigated: PWM displacement estimation, capacitance sensor and the non-contacting resistive displacement sensor.

Displacement sensors have a variety of structures and working principles. Generally speaking, there are three major types of displacement sensors with three working principles: resistive sensor (also known as potentiometer); inductance sensors (LVDT, eddy current sensor, etc); non-contacting potentiometer displacement sensor¹.

Resistive sensors are relatively low cost and have simple structures. Their main drawback is that they are contacting style sensors. With the contacting points always scratching each other during working, they are subject to limited life and poor environmental resistance.

Inductance sensors are non-contacting sensors. The widely used inductance sensors are LVDT, which are precise and robust. However they are relatively high cost because of their complex structure. In addition, they need to use ferrite material as the plunger, so they have relatively poor resistance to environments like acid environments.

A patent on the non-contacting potentiometer sensor can be found early in 1970s. It is also a kind of non-contacting displacement sensor. Related commercialized products can be found at NOVOTECHNIK Company. However due to the structures of the

¹ www.novotechnik.com

existing non-contacting potentiometer sensor, their cost is relatively high and the structure is complex.

There are a lot of other displacement sensors working on the inductance and capacitance. However, their working range is relatively small (0.1mm~10mm). In this research, three displacement sensing methods are investigated. All of these three solutions meet the requirements on size and stroke. They are PWM displacement estimation, capacitance sensor and the non-contacting resistive displacement sensor.

3.3.1 PWM Displacement Estimation

Pulse width modulation (PWM) can be used to control average flow by varying the valve duty cycle on some (usually) fixed base frequency to match the flow requirement.

By controlling the relative amount of time the valve is in the on state, one can vary the average amount of flow as a function of the on time. For example, if a valve can flow 3.0 liters per minute in the full on state, then the valve is cycled so that it is ON for 33% of the time, the valve will flow approximately 33% of the total flow capacity, or about 1 liter per minute. By controlling the pressure and system constraints and characterizing the dynamic performance, a very reliable means of controlling flow can be obtained. With the PWM method, flow can be easily controlled in a range exceeding 10:1, up to a possible 40:1. This ratio of maximum total flow to minimum total flow is sometimes called the "turn-down ratio" of a valve or system. For example, if flow can be controlled between 0.3 and 3.0 liters per minute, then the turn-down ratio is 10:1. More or less resolution can be obtained by altering pressure and frequency, or by changing valve dynamics.

Using pulse width modulation, a bi-state solenoid valve can be used to very effectively control flow over a range exceeding 10:1. The existing problem is that when the base frequency of the PWM is high ($> 100\text{Hz}$), the relationship between the duty cycle and the flow rate is no longer proportional / linear as will be dressed in the following paragraphs.

Experimental system

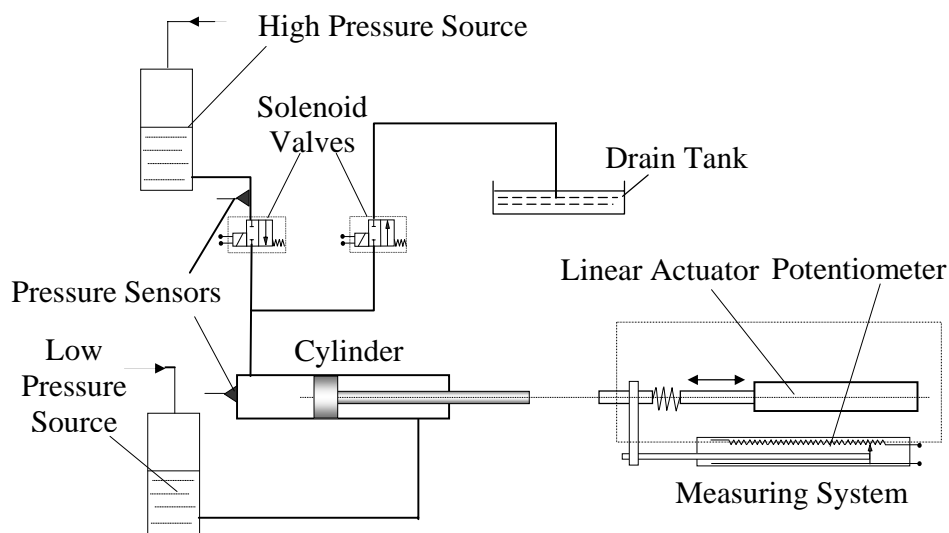


Figure 3-13 Experimental System

The schematic diagram of the experimental system is given in Figure 3-13. An ultra-low friction cylinder is chosen to represent the actuator a cell of the Digital Clay. Two simple on/off solenoid valves are used as the control valves, which have response times around 1.5ms. Two pressure sources, pressurized by regulated compressed air, are applied to drive the cylinder. Two low cost pressure sensors are used to measure the pressure difference across the inlet valve. The information about the components are

listed in table 3-1. Current research focuses on the inlet solenoid valve, so only the inlet valve is controlled using the PWM method. The working fluid is the deionized water.

A computer directly controls the whole system. A digital I/O card and a DAQ card provide the interface between the computer and the experimental system. To improve the performance, Real-time Linux is used as the operating system.

Measuring the Displacement of the Cylinder Rod

A measurement device is designed to measure the final displacement of the cylinder (Figure 3-13). A linear actuator moves the measuring head left until it touches the cylinder rod. The spring between the measuring head and the linear actuator regulates the contacting force. A potentiometer attached to the measuring head measures the displacement of the cylinder rod. The measuring process occurs only after the cylinder stops.

Displacement Response under Constant Across-valve Pressure using PWM Method

The PWM base frequency is set to 200Hz. Seven constant across-valve pressures were applied: 1PSI, 3 PSI...11PSI. For each across-valve pressure, 100 PWM duty cycles from 1% to 100% with an increment of 1% were applied on the inlet valve. After a certain PWM duty cycle is applied, the displacement of the cylinder is measured. The testing process is repeated several times for each across-valve pressure ΔP_v . Mean values are shown in figure 3-14.

To inspect the repeatability and reliability of the tests, the variance corresponding to each ΔP_v is calculated and plotted. The variance for 11 PSI is shown in figure 3-15, which is quite similar to others. From figure 3-15, one can see that the variations are

small, less than 0.05mm for small displacement (<5mm) and less than 2% for large displacement. The small variance indicates that the valve response to the PWM duty cycle is stable and repeatable.

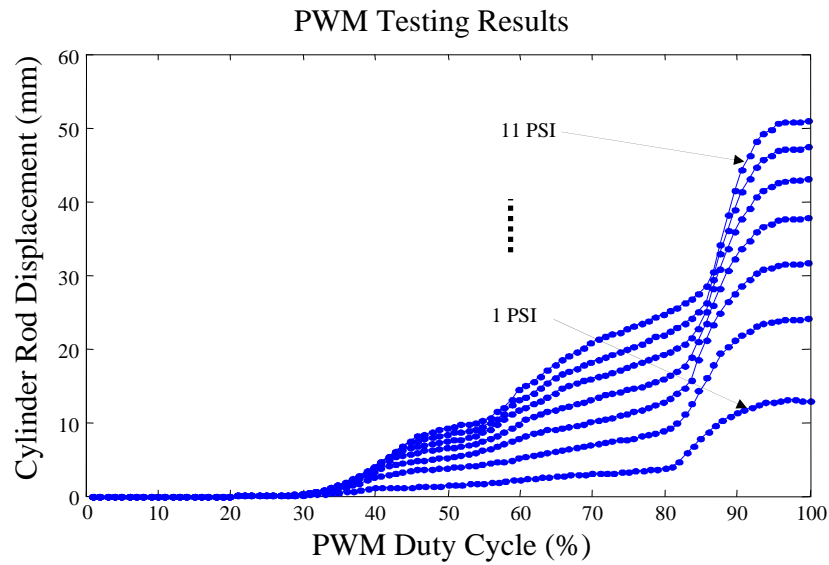


Figure 3-14 PWM Method Testing Results

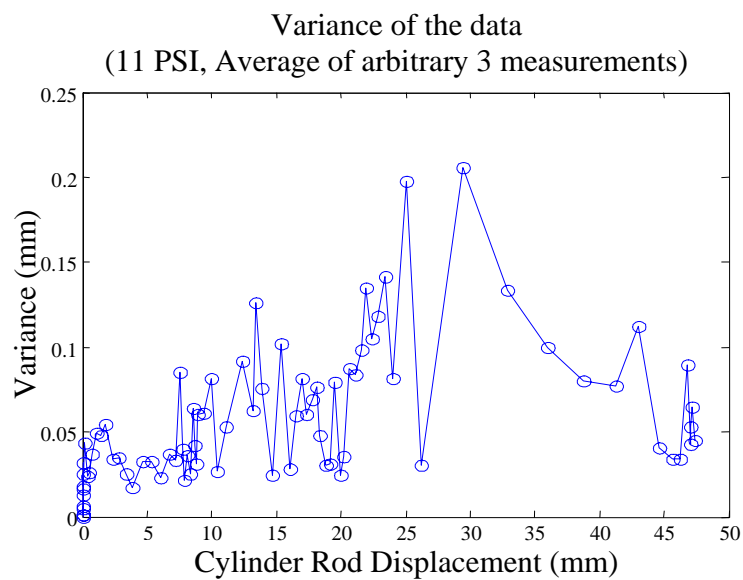


Figure 3-15 Variance for $\Delta P_v = 11$ PSI

Analysis on Solenoid On/off Valve

Theoretical analysis is conducted to gain more understanding of the test results above. The valve used in above experiment has a structure shown in figure 3-16 (Only the NC port and the Common port are used). The free body diagram of the plunger is drawn as shown in Figure 3-16.

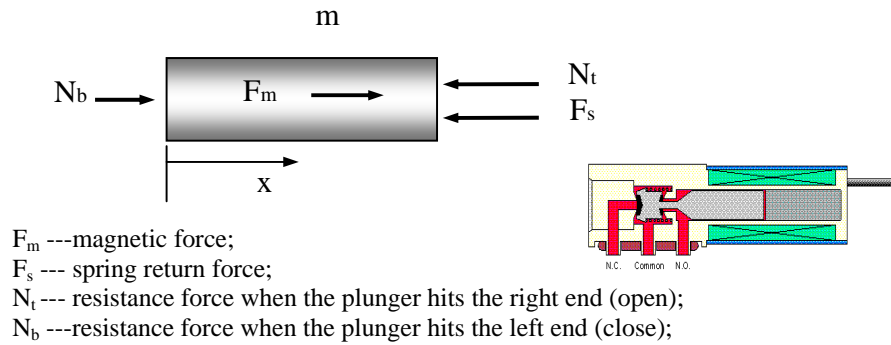


Figure 3-16 Free Body Diagram of the Solenoid Valve

From above free body diagram, the following equations are established:

$$F_m = F_s + N_t - N_b + m\ddot{x}(t) - b\dot{x};$$

$$F_s = F_0 + K_s x(t);$$

$$N_t = K_w \langle x - e \rangle;$$

$$N_b = K_w \langle 0 - x \rangle;$$

Where:

F_0	-----	Spring preload;
K_s	-----	Spring constant;
K_w	-----	Elastic modulus of the cousin;
e	-----	Plunger's stroke;
b	-----	Damping ratio;
m	-----	Plunger's mass;
$\langle x - e \rangle$ and $\langle 0 - x \rangle$		Singular functions.
x	-----	Displacement of the plunger

The magnetic force F_m is calculated as follows:

Voltage balance equation (not considering the effect of the eddy current):

$$U(t) = rI(t) + \frac{d\phi(t)}{dt}, \text{ where: } NI = R\phi; R = \int_{l+e} \frac{dl}{\mu_0 S} + \int_{L_2} \frac{dl}{\mu_0 \mu_r S} \cong \int_{l+e} \frac{dl}{\mu_0 S} = \frac{l+e}{\mu_0 S}$$

$$\begin{aligned} \Rightarrow U(t) &= rI(t) + \frac{Nd\phi}{dt} = rI(t) + \frac{\mu_0 N^2 S}{(l+e)} \frac{dI(t)}{dt} + \frac{\mu_0 N^2 SI(t)}{(l+e)^2} \frac{dx}{dt} \\ &= rI(t) + L_0 \dot{I}(t) + k_1 I(t) \dot{x}(t) \end{aligned}$$

$$\text{Where: } L_0 = \frac{\mu_0 N^2 S}{(l+e)}; \quad k_1 = \frac{\mu_0 N^2 S}{(l+e)^2}$$

$$\text{Hence: } F_m = \frac{B^2 S}{2\mu_0} = \frac{\mu_0 S N^2}{2(l+e)^2} * I^2 = \frac{1}{2} k_1 I^2, \text{ where } B = \frac{\phi}{S} = \frac{NI}{RS}$$

In above equations:

$U(t)$	-----	<i>The voltage applied on the valve</i>
e	-----	<i>The stroke of the plunger (shown in figure 2-7)</i>
l	-----	<i>Resistance of the coil</i>
r	-----	<i>Plunger's stroke;</i>
n	-----	<i>Rounds of the coil</i>
S	-----	<i>Effect area of the magnetic effect on the plunger</i>

Simulation of the trajectory of the plunger is plotted as shown in Figure 3-17 (Matlab Simulink,). Based on the simulation, following approximation is made to simplify further analysis: “Plunger moves at a constant speed when the coil is energized and de-energized.”

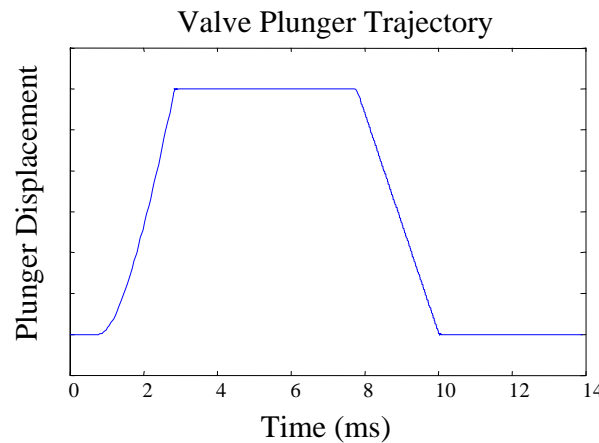


Figure 3-17 Valve Plunger Trajectory Simulation

Explicit Analytic Models for the Valve and Cylinder Motion

Entire working process of the plunger under the PWM driving method can be divided into four phases as shown in Figure 3-18. The shape of the plunger trajectory will now be examined for each phase and an explicit analytical expression for flow and resulting piston motion will be derived. The method will be executed in detail for Phases I and II, and only the solution given for Phases III and IV. Notice that in figure 3-18, there are two vertical axes. The one on the left is the measured cylinder rod displacement and the one on the right is the flow rate corresponding to the cylinder rod displacement.

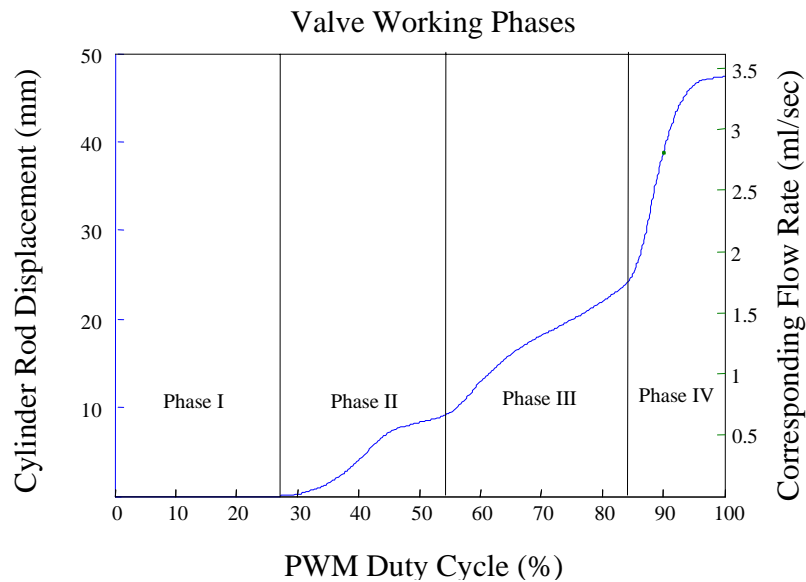


Figure 3-18 Solenoid Valve Working Phases under PWM Method

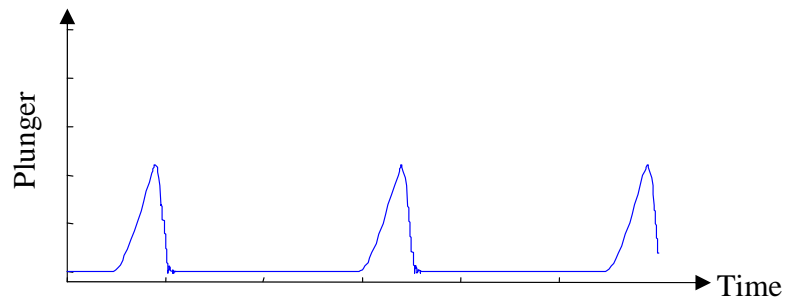
Phase I

During each PWM duty cycle, when the power is on, the plunger will not move immediately since it needs time for the magnetic force to grow to overcome the spring preload. Therefore, during phase I, the plunger does not move; the valve does not open. That explains that when the PWM duty cycle is lower than 27%, the flow rate is zero as

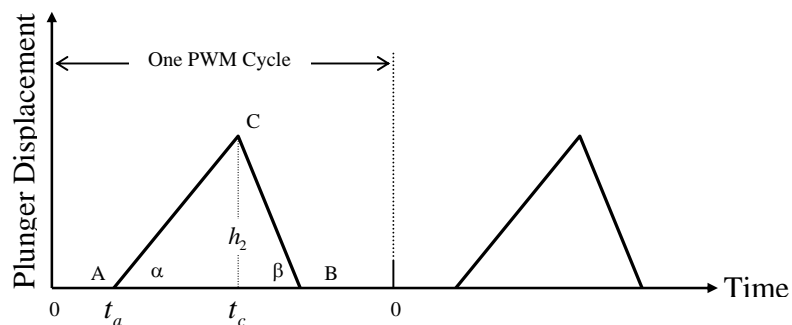
shown in Figure 3-18. (When the PWM period is 5 milliseconds, 27% duty cycle equal to an open time of $5 \times 0.27 \cong 1.4$ milliseconds.)

Phase II

After the magnetic force is bigger than the spring preload, the plunger starts to move and the valve begins to open. During this phase, the plunger does not reach the fully open position (right end in figure 3-16), so there is no magnetic energy stored in the coil. Thus when the coil is de-energized, the plunger moves back immediately until fully closed. So during phase II, the valve is partially opened and fully closed. The plunger's trajectory under this phase is simulated and shown in figure 3-19a.



a. Plunger trajectory simulation under Phase II (Simulink)



b. Approximated plunger trajectory analysis

Figure 3-19 Simulation and Analysis for Phase II

According to the fluid mechanics approximations commonly used for flow through a sharp orifice, the flow rate is: $q = C_d \cdot \sqrt{\Delta P} \cdot A_o$, where, A_o is the area of the valve orifice. Therefore, the displacement of the cylinder is: $y = \int \frac{q}{A_c} \cdot dt$, where, A_c is the area of the cylinder piston.

Therefore, the vertical coordinate of a point on the displacement-duty curve in Figure 3-18 can be calculated as:

$$y = K_1 \cdot \int \frac{q}{A_c} \cdot dt = K_1 \cdot \int \frac{C_d \cdot \sqrt{\Delta P} \cdot A_o}{A_c} \cdot dt,$$

$$= K \cdot \int x \cdot dt$$

Where $K = \frac{C_d \cdot \sqrt{\Delta P} \cdot K_2 \cdot K_1}{A_c}$, and

x	-----	<i>The plunger displacement.</i>
K_1	-----	<i>The number of the PWM circles in 1 second.</i>
K_2	-----	<i>a constant equals to A_o/x</i>
C_d	-----	<i>The discharge coefficient</i>

For a given point on the displacement-duty curve, K_1 , K_2 and C_d are constants, so K is constant. $\int x \cdot dt$ is the area enclosed by the plunger trajectory and the horizontal axis (time axis) as shown in Figure 3-19b. So, the vertical coordinate of a point on the displacement-duty curve in phase II can be calculated as:

$$y = K \cdot S_{II} = K \cdot \text{Area of } \triangle ABC = K \cdot \frac{1}{2} \cdot h_2 \cdot \overline{AB}$$

$$= K \cdot \frac{1}{2} \cdot (t_c - t_a) \cdot \tan \alpha \cdot [(t_c - t_a) + \frac{(t_c - t_a) \cdot \tan \alpha}{\tan \beta}]$$

$$= K \cdot \frac{1}{2} \cdot (t_c - t_a)^2 \cdot \tan \alpha \cdot [1 + \frac{\tan \alpha}{\tan \beta}]$$

$$= C_{II} \cdot (t_c - t_a)^2$$

where :

$$C_{II} = K \cdot \frac{1}{2} \cdot \tan \alpha \cdot \left[1 + \frac{\tan \alpha}{\tan \beta}\right]$$

Here,

- 0 ----- the time that the valve is energized, and also is the beginning of a PWM circle
- t_a ----- the time that the plunger begins to move
- t_c ----- the time that the valve is de-energized

Note that, In the following analysis, above notation always holds.

Phase III:

If the energizing time is long enough, the plunger will reach the right end (Figure 3-16), and the magnetic energy starts to store in the coil. Therefore, when the coil is de-energized, the plunger will not move back until the energy stored in the coil is dissipated to certain amount. Thus there is a delay before the plunger starts to move back (CD in Figure 3-20).

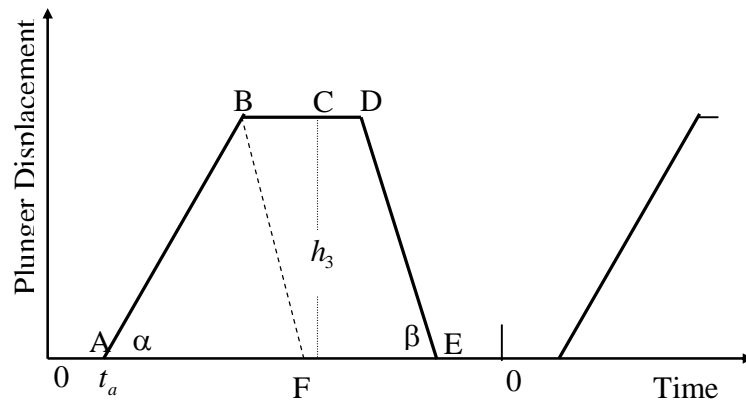


Figure 3-20 Approximated Plunger Trajectory for Phase III

The vertical coordinate of a point on the displacement-duty curve (Figure 3-18) during phase III can be calculated as:

$$y = K \cdot S_{III} = K \cdot (S_{\triangle ABF} + S_{BDEF}) = K \cdot \left(\frac{1}{2} \cdot h_3 \cdot \overline{AF} + h_3 \cdot \overline{BD} \right)$$

$$= C_{II} + K \cdot h_3 \cdot [(t_c - t_b) + f(t_c - t_b)]$$

where $C_{II} = K \cdot \frac{1}{2} \cdot h_3 \cdot \overline{AF}$

Here $f(t_c - t_b)$ is a function describing the closing time delay caused by the coil magnetic energy storage. Therefore, when t_c is bigger than a certain value, due to the saturation, $f(t_c - t_b) = c_m = \text{Constant}$. Thus,

$$y' = C_{II}' + K \cdot h_3 \cdot (t_c - t_b)$$

where

$$C_{II}' = C_{II} + K \cdot h_3 \cdot c_m$$

This can be viewed in the Figure 3-18. At the end of phase III, the slope of the curve is approximately constant.

Phase IV

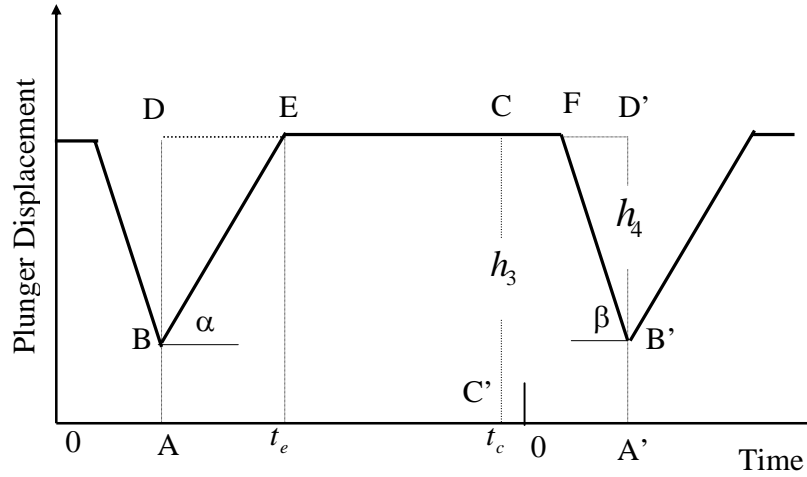


Figure 3-21 Approximated Plunger Trajectory

During phase IV, as the PWM duty increases, the plunger is pulled to open again by the magnetic force before it reaches the close position (left side in Figure 3-16). So in Phase IV, the valve is fully opened and partially closed as shown in Figure 3-21.

The vertical coordination of the point on the displacement-duty curve (Figure 3-18) during phase IV can be calculated as:

$$\begin{aligned}
 y &= K \cdot S_{IV} = K \cdot (S_{ADD'A'} - S_{\Delta BDE} - S_{\Delta FD'B'}) \\
 &= K \cdot (h_3 \cdot \overline{AA'} - \frac{1}{2} \cdot h_4 \cdot \overline{DE} - \frac{1}{2} \cdot h_4 \cdot \overline{FD'}) \\
 &= C_{III} - C_{IV} \cdot (p - t_c - c_m)^2 \\
 \text{where :} \\
 C_{III} &= K \cdot h_3 \cdot p \\
 C_{IV} &= K \cdot \frac{1}{2} \cdot \tan^2 \beta \left(\frac{1}{\tan \alpha} + \frac{1}{\tan \beta} \right)
 \end{aligned}$$

Data Process and Results

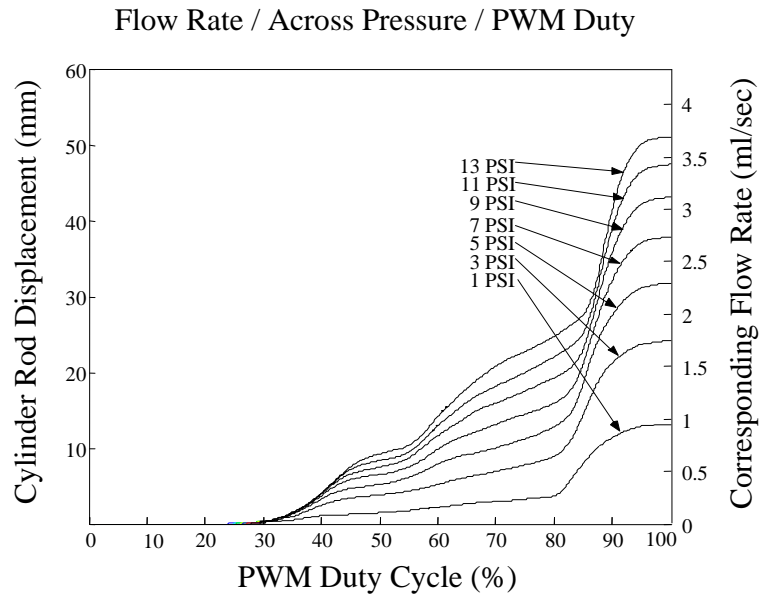


Figure 3-22 Curve Fitting Results

The above analysis provides an explanation and means of calculation of the valve working behaviors under PWM. The actual curve is affected by a lot of factors. For example, the across-valve pressure can cause some delay during valve action. The actual plunger-moving trajectory is not a straight line as approximated above, etc. So the above analysis is only used to provide the analytical structure in which to embed the data by curve fitting. This produces a chart of the flow rate under different across valve pressures is constructed and shown in Figure 3-22.

Speed and position control using PWM

Reverse Process

Due to the complexity of the valve behaviors under PWM control, the lookup table method is adopted to realize the control.

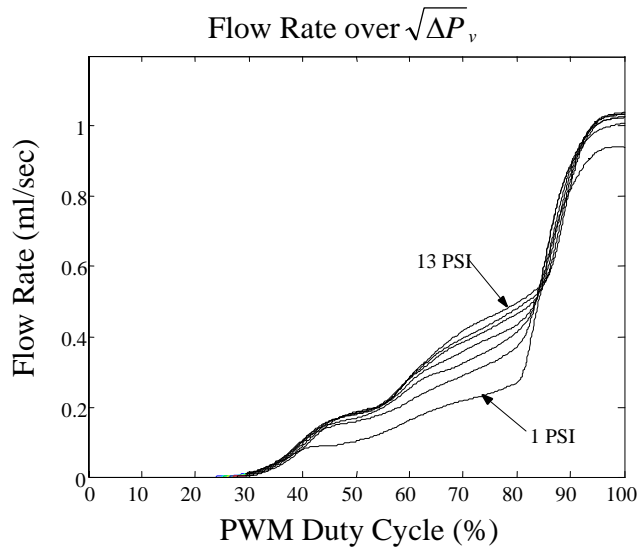


Figure 3-23 Flow Rate Curves Divided by $\sqrt{\Delta P_v}$

The lookup table is built as follows:

1. Construct a table consisting of duty-flow relations/curves corresponding to different across-valve pressure as shown in figure 3-22.

2. Divide each curve by the square root of its corresponding across valve pressure (Figure 3-23)
3. Reverse above duty-flow table to form a flow-duty table (figure 3-24)

The lookup table is used as described below.

1. Measure the across-valve pressure ΔP_v .
2. Calculate the duty-flow curve corresponding to ΔP_v using linear interpolation.
3. Multiply the interpolated desired duty-flow curve by $\sqrt{\Delta P_v}$.
4. Use the calculated curve in step 3 to find the PWM duty according to the required flow rate or cylinder rod speed.

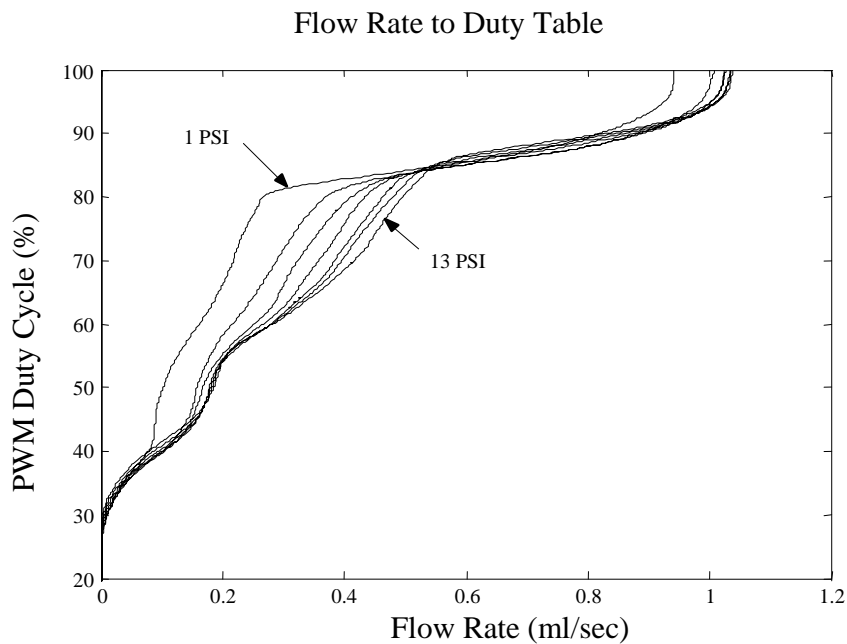


Figure 3-24 Look-up Table of Flow Rate to Duty

Control System Structure & Testing System

The general control structure of the velocity and position control using PWM is shown in Figure 3-25.

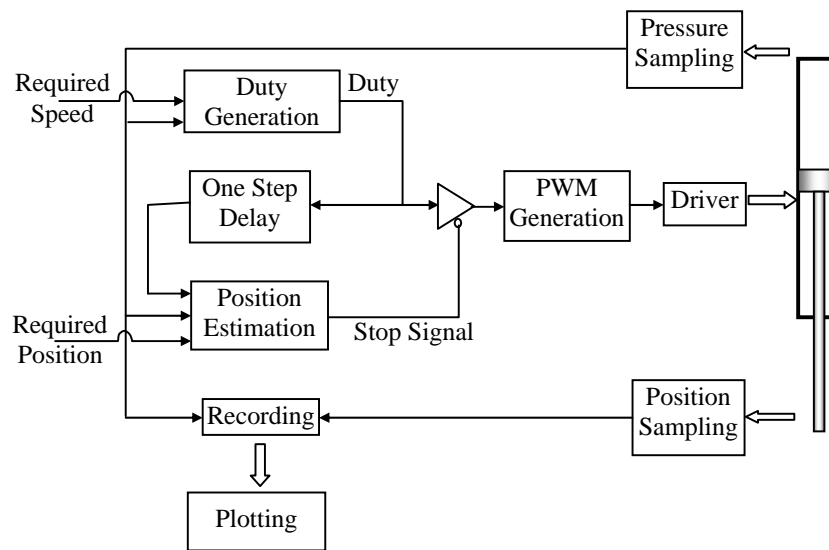


Figure 3-25 Structure of Velocity and Position Control using PWM

A testing system is set up as shown in Figure 3-26 to test the proposed control method.

Hardware information is listed in table 3-1.

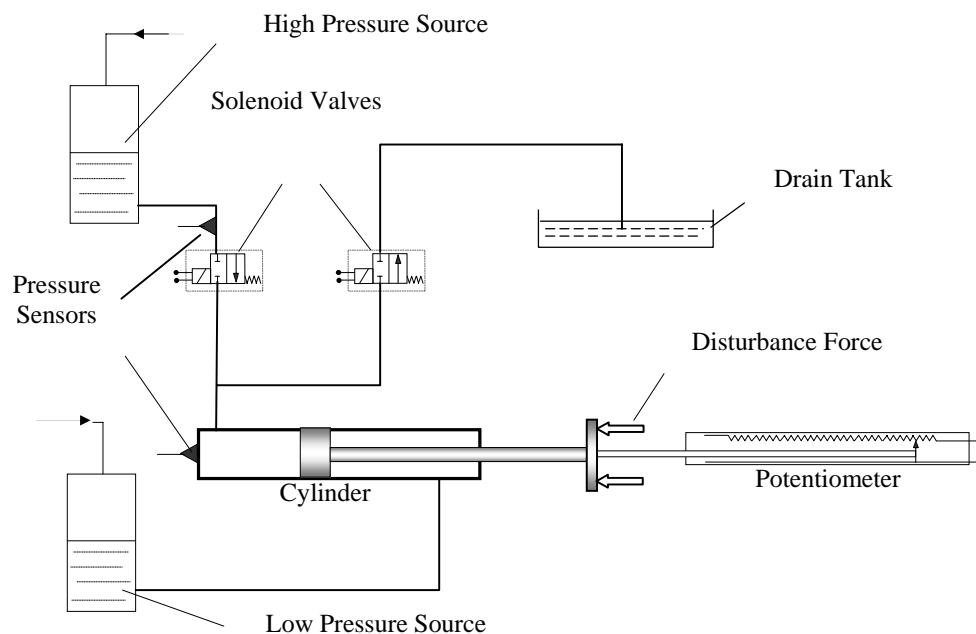


Figure 3-26 Testing System for Control using PWM

The testing is conducted using the following devices and parameters: (Table 3-2)

Table 3-2 Parameters Used in Testing

ITEM	VALUE	UNIT
Required Displacement	62.31	mm
Required Speed	12.46	mm/sec
PWM Base Frequency	200	Hz
PWM Duty Refresh Rate	40	Hz
Sampling Rate	20	kHz
Data Recording Rate	40	Hz
High-pressure Source	13.5	PSI
Low-pressure Source	2.5	PSI

Results for Zero Disturbance Force

The response of the testing system under zero disturbance force is shown in Figure 3-27. The desired displacement is provided for reference (i.e. the dashed line drawn with slope equals to the required speed and ending at the required displacement.) The across valve pressure is sampled by two pressure sensors (Figure 3-26).

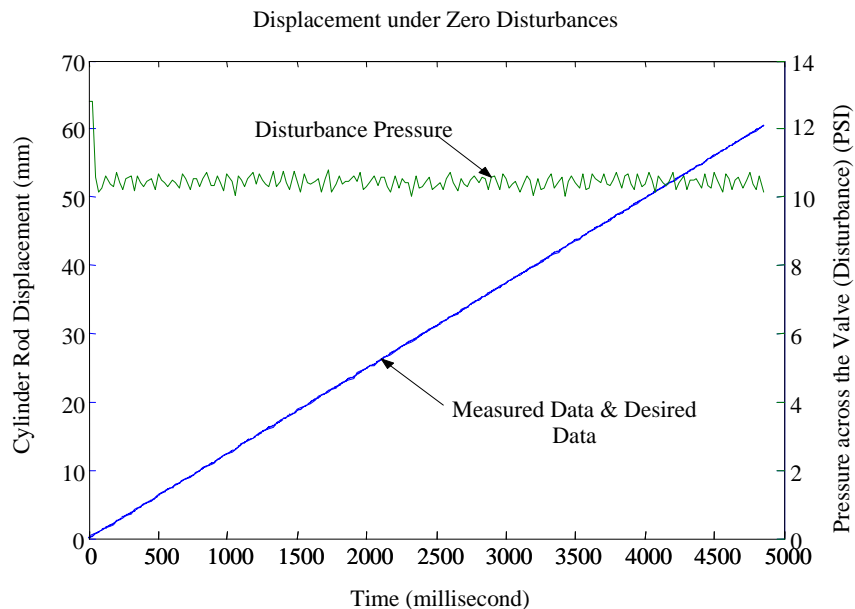


Figure 3-27 Displacement under Zero Disturbance Pressure

As shown in Figure 3-27, the measured data overlaps the desired displacement. To illustrate the goodness of the control result, the absolute error is plotted vs. the desired displacement (Figure 3-28). The absolute displacement error and relative error are calculated as following:

$$\text{Absolute Error} = \text{Measured Data} - \text{Desired Data}$$

$$\text{Relative Error} = \frac{\text{Measured Data} - \text{Desired Data}}{\text{Desired Data}} \times 100\%$$

The testing results show that the absolute displacement error is less than ± 0.2 mm, and the relative error is decreasing quickly as the cylinder rod displacement increases and reaches a value lower than ± 0.5 %.

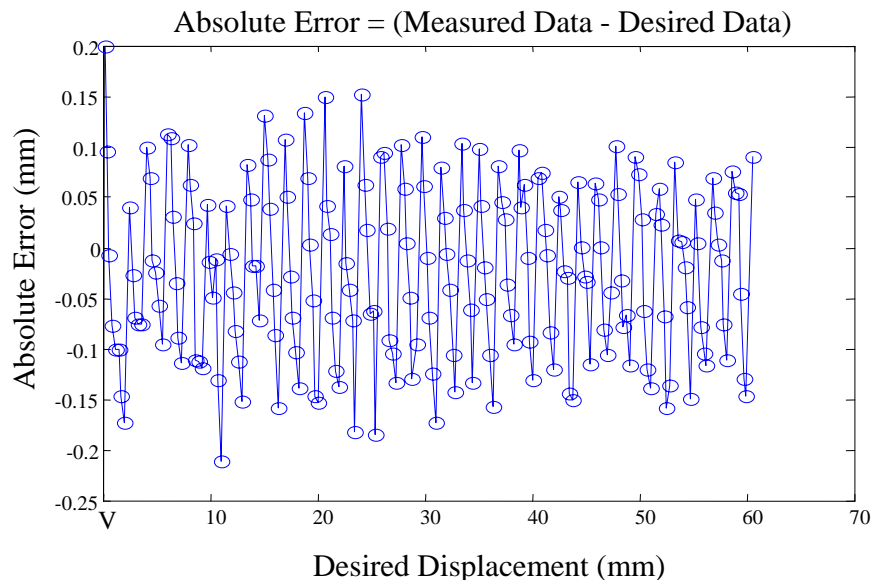


Figure 3-28 Absolute Error vs. Desired Displacement

Results for Varying Disturbance Pressure

Three independent tests are conducted with different types of varying disturbance force acting on the cylinder. Results of the test with small amplitude (5 ~ 10.5 PSI) but high frequency finger force acting on the tip is shown in Figure 3-29. The corresponding absolute errors are shown in Figure 3-30. A test with a comparatively bigger amplitude

(3~10.5 PSI) but low frequency finger force was done but is not shown. Comparing the two results, following can be found: 1) Varying disturbance force acting on the cylinder will reduce the speed and increase the error. 2) The error increases when the finger force's amplitude rises.

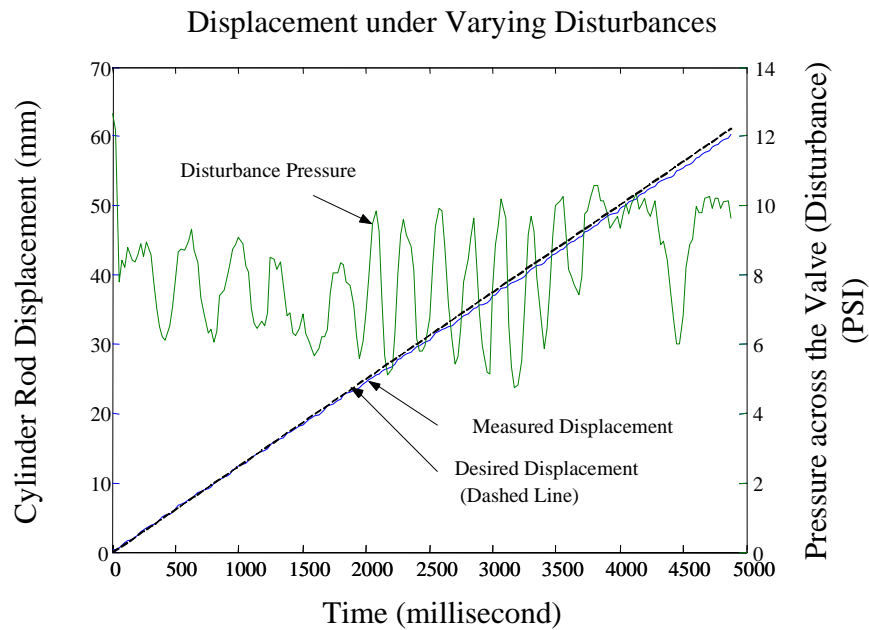


Figure 3-29 Displacement under Varying Disturbance Pressure

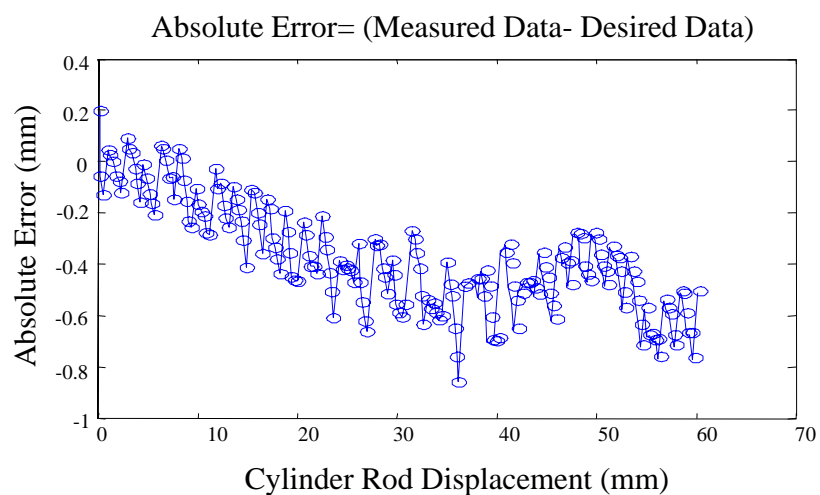


Figure 3-30 Absolute Error vs. Desired Displacement

3.3.2 Capacitive Sensor

An example for the capacitive sensor is shown in Figure 3-31. The key elements are an outer metal film and two symmetrical inner metal films. By measuring the capacitance between the two inner films, the relative displacement between the inner films and outer film can be detected.

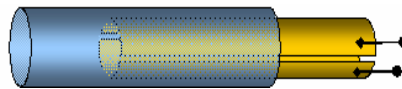


Figure 3-31 Capacitive Sensor Concept

The advantage of this kind of displacement sensor is its simple structure. The drawback is the capacitance variance due to the eccentricity of the inner and outer tubes. The capacitance variance (of the capacitive displacement sensor with the design parameters shown in Figure 3-32) is analyzed and plotted as shown in Figure 3-33. The ratio of capacitance/displacement is around 3.9 pf /mm (for water and 1 pf/mm for oil). Therefore, the calculated capacitance variance will cause 0.5 mm error (for water) and 3.8 mm error (for oil)

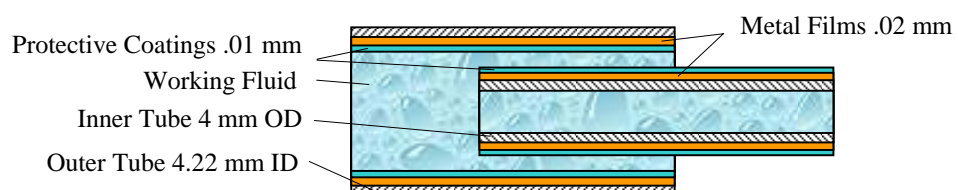


Figure 3-32 Proposed Capacitive Sensor Dimensions

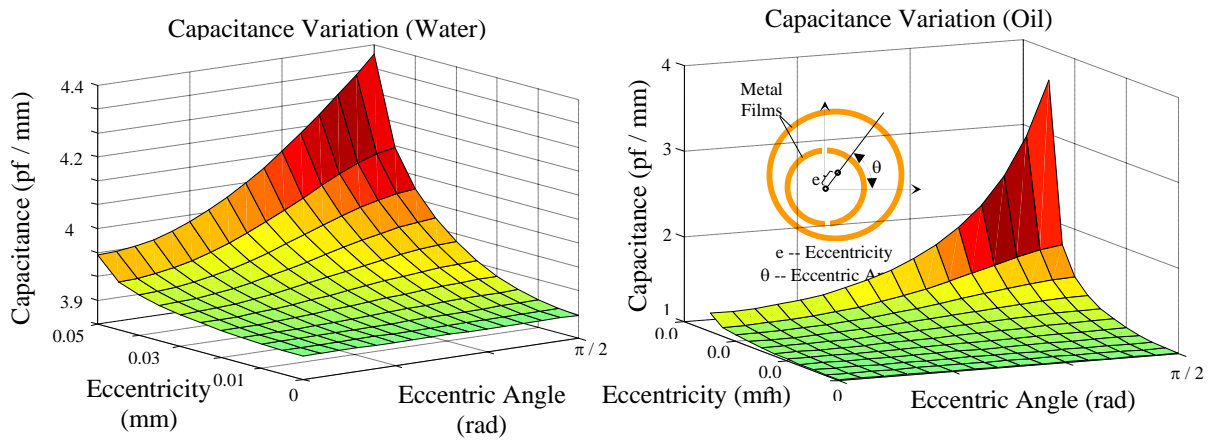


Figure 3-33 Capacitance Variation Due to the Eccentrics

3.3.3 Concept of Non-contacting Resistive Displacement Sensor

An example for the non-contacting resistive displacement sensor is shown in Figure 3-34. This concept is not original, but it provides a good combination of the advantages of capacitive sensor and resistive sensor.

As shown in Figure 3-34, the displacement sensor consists of: 1) a resistive film 2) a conductive metal film, and 3) a conductive metal ring.

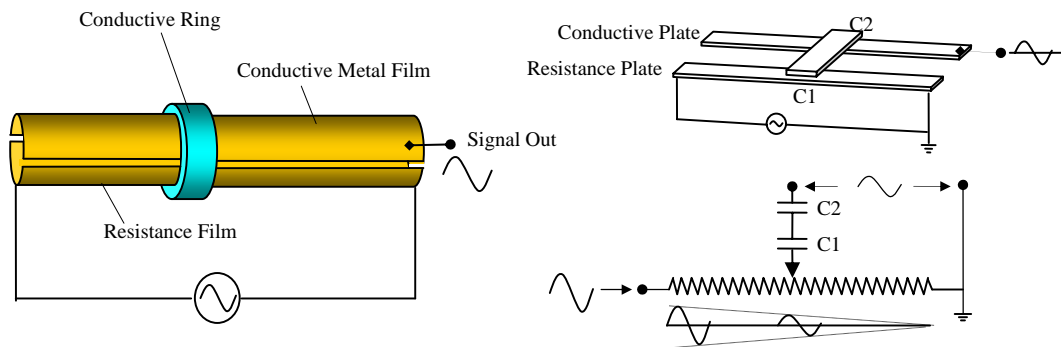


Figure 3-34 Non-contacting Resistive Displacement Sensor

A high frequency alternating voltage is applied across the resistive film. By sensing the amplitude of the alternating voltage on the conductive film, the relative position of the metal ring can be detected. The electrical schematic circuit of the sensor is shown in Figure 3-34, where R is the impedance of the measurement instrument, $C1$ is the capacitance between the conductive ring and the resistive film, and $C2$ is the capacitance between the metal ring and the conductive film. This is a high-pass filter. Therefore, if the frequency of AC excitation is high enough, a small capacitance variation will not affect on the amplitude of the output signal.

3.4 DESIGN OF MICRO ACTUATOR

For the 2.5D formable body structure of Digital Clay, linear hydraulic actuator can be used since the actuation is one dimensional. Given the requirements on the compact size (i.e. diameter < 5 mm, stroke > 50 mm), it is very difficult to find a suitable hydraulic actuator. Bellows fabricated using MEMS technology provide an alternative solution. However their actuation range is limited due to the buckling problem. Hence it is necessary to design a micro fluidic actuator.

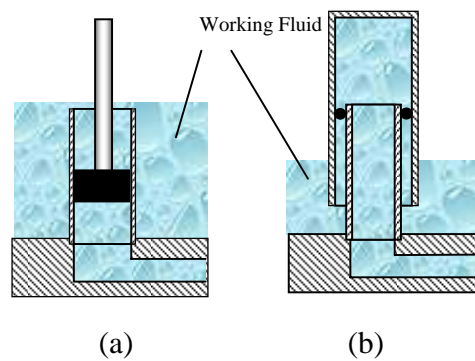


Figure 3-35 Solutions for Actuators of Digital Clay

As shown in Figure 3-36, two alternative solutions for the actuator are proposed and studied. Experiments show that either rubber o-ring or graphite seal can provide excellent seal, but the graphite seal can reduce the friction greatly. For solution a, the retraction of the actuator can be achieved either by spring or pressurized fluid. For solution b, applying negative pressure (vacuum) can make it retract. Due to their simple structure, both two solutions can easily meet the requirements on diameter and stroke. Further research shows that for configuration b, the cavity problem is found when applying the vacuum to make the actuator retract. Therefore configuration a is chosen as the solution for the actuator of Digital Clay.

3.4.1 Displacement Sensor Embedded Micro Actuator

Currently, the only way to get a displacement sensor embedded is to attach a standalone sensor to the cylinder. This will increase the size, the complexity and the cost of the cylinder-sensor assembly. Due to the space limitation, design of a new space saving sensor embedded actuator becomes necessary. As discussed before, non-contacting resistive sensor provides a good potential. But the structure needs to be modified to fit to the cylinder type actuator and the special working principle (i.e. the dielectric is changing from time to time). The novel displacement sensor embedded actuator introduced here is an integrally combined cylinder with a displacement sensor. The space occupied by the embedded displacement sensor is negligible due to its structure. In other words, the cylinder itself is a displacement sensor, or the displacement sensor itself is a cylinder.

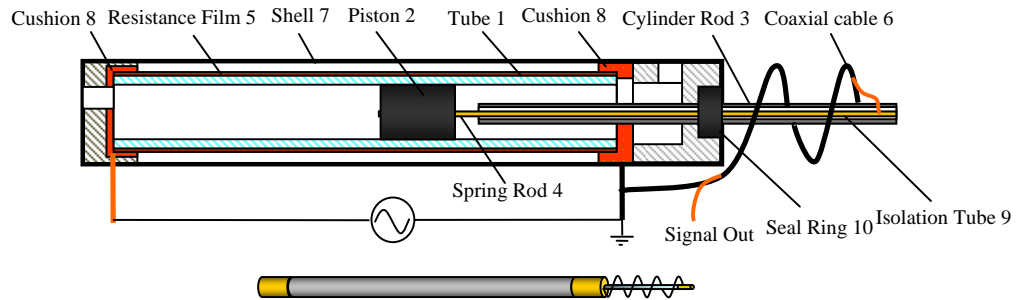


Figure 3-36 Micro Cylinder With Displacement Sensor Embedded

As shown in Figure 3-37, the actuator comprises: a non-conductive precision tube 1, a graphite/metal piston 2, an electrically conductive hollow cylinder rod 3, an electrical conductive spring rod 4, a resistive film 5, a coaxial cable 6, a shell 7, two electrical conductive cushions 8, an isolation tube 9, and a graphite seal ring 10.

More specifically,

1. The tube 1 and the piston 2 are fitted with a minor gap between them;
2. The rod 4 is fixed to the piston 2 coaxially with electrical conductivity;
3. The other end of the rod 4 is coaxially fitted into the tube 9;
4. Tube 9 is coaxially is fitted into the hollow cylinder rod 3;
5. The axially uniform resistive film 5 is deposited on the outside of the tube 1;
6. The core of the coaxial cable 6 leads the flexible wire 4 to the signal output, and the shield of coaxial cable 6 connects the ground;
7. A shell 7 is fixed outside the tube 1 to provide protection;
8. Two electrically conductive cushions 8 lead the two ends of the film 5 to the excitation inputs;
9. The seal ring 10 seals the cylinder rod 3.
10. The coaxial cable 6 may be placed inside tube 1, either in the front cylinder chamber or in the rear cylinder chamber.
11. The rod 4 is hard to compress along the axial direction but flexible. It can reduce the friction caused by the misalignment between piston 2 and tube 1.

The working principle is described as follows.

Apply an alternating voltage across the resistive film 5 as shown in Figure 3-37. The amplitude of the alternating voltage along the film will have a distribution as shown in Figure 3-34. When the piston 2 moves inside the tube, the alternating voltage will be coupled out by the capacitance between the piston 2 and the metal film 5 and be sent out through the Flexible rod 4 and the cable 6.

The advantages of this actuator are obvious:

1. Simple structure;
2. Micro size can be easily achieved: the outside diameter can be less than 2 mm;
3. Low cost;
4. Excellent linearity along a long working range;
5. Excellent hazard environment resistance. All the components here have a wide variety of selection of materials. By selecting proper materials, this invention can resist hazardous environments such as acid working environments.

Some preliminary tests are performed on the proposed sensor embedded actuator. For the actuator, the leakage through the graphite piston and glass cylinder bore is found negligible, and the friction is tiny (the piston will drop down inside the glass bore by its own gravity if put the actuator vertically). To preliminary test the non-contacting sensor, A LVDT is linked to the proposed displacement sensor as shown in figure 3-38. The measure probe of the displacement sensor is moved back and forth. Both the data from the proposed sensor and the LVDT are recorded and compared.

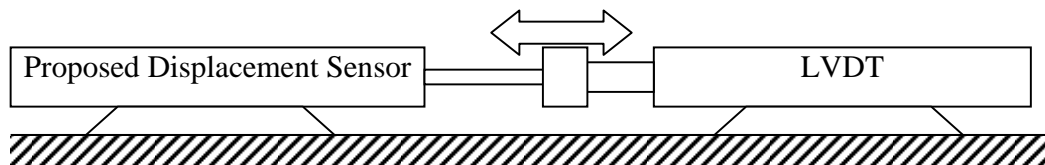


Figure 3-37 Test Setup on the Non-contacting Resistive Sensor

The test results are shown in figure 3-39. The data from the LVDT is used as the reference data (horizontal axis), and the data from the sensor is put along the vertical axis. From the figure, one can see that except the start and the end of the stroke, the proposed sensor is quite linear. For further illustration, results of the linear curve fitting is also presented in figure 3-40.

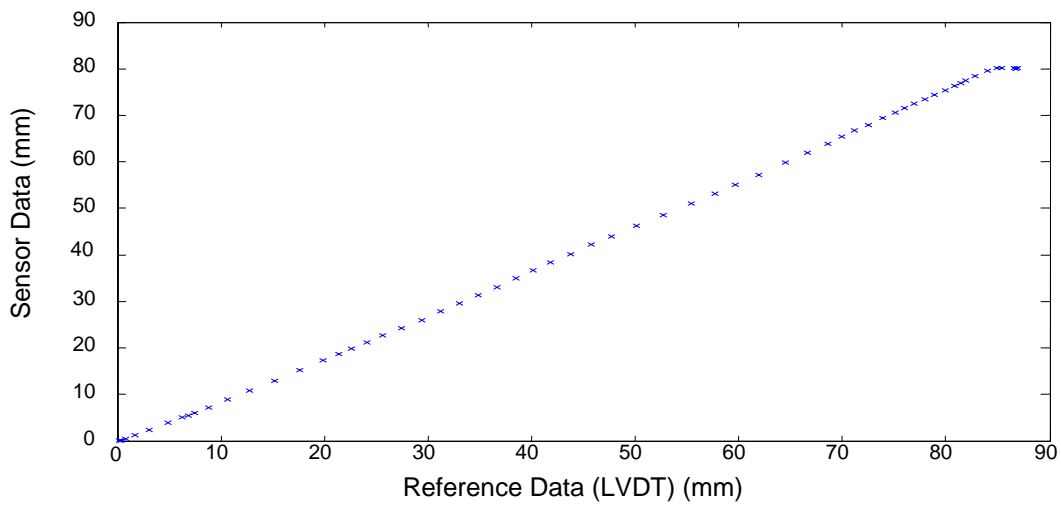


Figure 3-38 Test Results for the Non-contacting Resistive Sensor

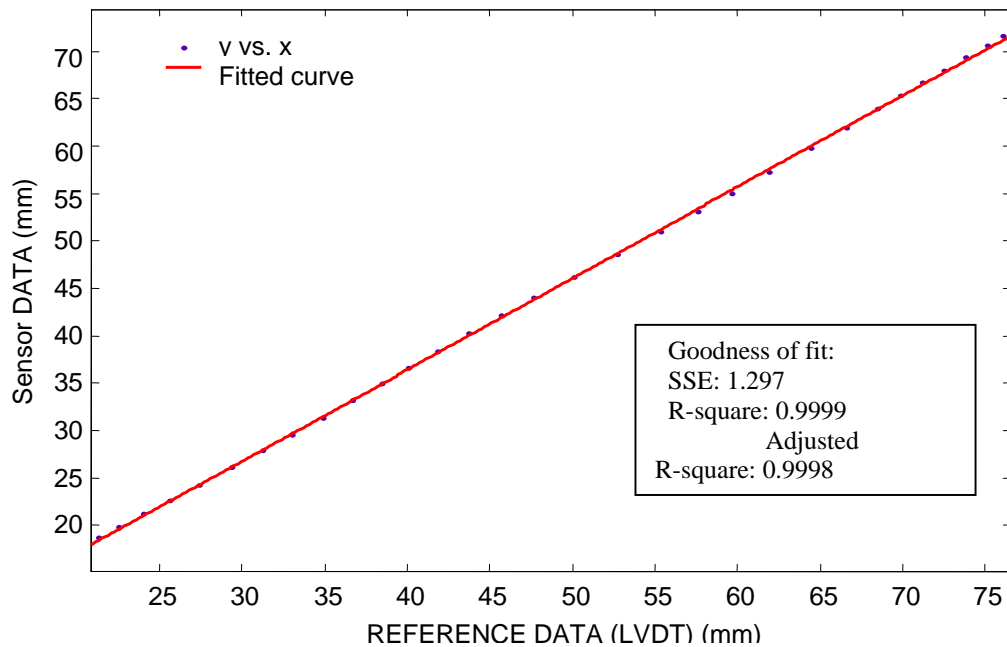


Figure 3-39 Curve Fitting Results for the Non-contacting Resistive Sensor

3.5 CONCLUSION

Digital Clay is a novel 3D computer input/output device. The cell is the elementary unit of the Digital Clay. In this chapter, complete cell level control is discussed and good results are shown. More specifically,

1) The experimental system constructed using conventional devices is sufficient for testing the cell level control for the single cell system of Digital Clay,

2) Electrical low-pass filter is better than hydraulic filter in suppressing the undesired frequencies in the pressure signal that is affected by the on-off valve,

3) To provide haptic effect, cell level control for the single cell Digital Clay system is essentially displacement control based on the pressure (caused by the user's pressing force) feedback,

4) To simulate / mimic a point on a material surface, the system must be able to switch between several control states. Moreover, by introducing a special control state -- shaping state, Digital Clay can realize the adding or subtraction of volume like real clay.

5) By carefully designed intelligent procedure, Digital Clay can understand the user's intention expressed just by the user's gesture.

6) Experimental results demonstrated and elaborated the success of the control on the single cell Digital Clay, and furthermore, proved the feasibility of the concept of Digital Clay..

Besides the cell level control, the displacement sensing technologies are investigated. PWM displacement estimation method is discussed first. Testing results confirmed the feasibility and accuracy of the proposed PWM velocity control and displacement estimation method for hydraulic systems involving solenoid valves. However, drifting of

the solenoid valve and pressure sensor parameters requires recalibration, which prevents this method to be applied on the large numbered cell array. Therefore, design on physical displacement sensors is necessary.

Potentiometer is kind of contacting sensor and takes a big space, so it is not considered. The capacitive sensor has simple structures, but they are too sensitive to the environmental variation. LVDT style sensor are too complicate and of high cost. Finally, a novel non-contacting resistive sensor is introduced and selected as the displacement sensor for Digital Clay. Non-contacting resistive sensor has high accuracy, and requires very small space to be embedded into the actuator. Based on the displacement sensor and the actuator structure for Digital Clay, a novel displacement sensor embedded actuator is provided.

CHAPTER 4

MULTI-CELL ARRAY OF DIGITAL CLAY

In this chapter, research on conceptual designs for the structure and control of the cell array of Digital Clay are investigated. Cell array forms the working surface of Digital Clay. Due to the large number of cells in the cell array, challenges are found both with the mechanical actuation structure and control methods. By conventional hydraulic means, one actuator needs two simple on/off valves to control it. Therefore, for a 600x600 cell array, at least 720,000 on/off valves are required. In this chapter, a novel hydraulic “matrix drive” structure is introduced which can greatly reduce the number of control valve needed. (e.g. in above example only 1201 is needed, almost 600 times less). Based on the Fluidic Matrix Drive structure, control methods are studied. More specifically, the basic Matrix Drive control methods, the dynamic cell level controller reformation and the dynamic computing resource allocation are investigated.

4.1 OVERVIEW

Digital Clay studied in this research utilizes the planar pin-rod matrix array known as “bed of nails” concept as depicted in Figure 4-1. The tips of the vertically actuated pin-rods form the tangible working surface. The rods of the actuators (in this research, the hydraulic cylinders) also help to form the object being displayed. Due to the one dimensional type of the actuators, Digital Clay under planar pin-rod matrix array concept can only display objects in a 2.5 D form. That means the Digital Clay cannot display laterally concaved objects. However, since the planar pin-rod matrix array concept is

relatively easy to realize at the current stage, it is the only structural form being used by all following research.

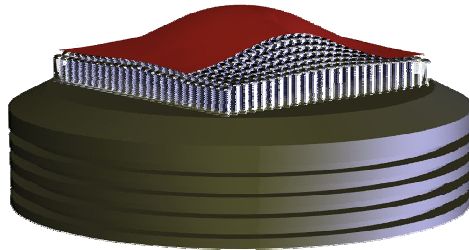


Figure 4-1 Planar Pin-rod Array Concept

A single cell of Digital Clay is essentially an intelligent hydraulic system. The structure and control of this kind of intelligent hydraulic system is relatively conventional compared to the large scale cell array that forms the working surface of the Digital Clay. As the ultimate goal, Digital Clay will use a cell array with the size ranging from 100x100 to 1000x1000 or even more to achieve a good resolution. Due to the large scale of the cell array, scalability and controllability become big problems. This chapter focuses on the approaches to solve the scalability and controllability problems.

The structure of the cell array is quite different from the simple stacking-up of discrete single cells. As mentioned in chapter 3, each single cell of Digital Clay needs 2 control valves, 1 pressure sensor, 1 displacement sensor and 1 cell level controller. Therefore, a 1000x1000 array will need millions of components. Meanwhile, huge computing resource is required to control the system. These requirements prevent the Digital Clay from being practical. Therefore, research on both the mechanical design and control architecture is carried out and presented in this chapter.

For the mechanical structure, efforts are put on the design and optimization of the hydraulic driving circuit. The objective of the design is to reduce the complexity of the hydraulic channels as well as to reduce the number of control valves needed. A concept similar to the Matrix Drive for an LED array is proposed and studied in this chapter.

Control for cell array is the surface level control. The surface level control is responsible for achieving the best fit to the desired surface. It is dependent on the implementation of Digital Clay under control but that will be hidden from both the higher and lower level of control software. Interaction between neighboring cells might be critical for the reliable operation. Challenges in surface level control can be found as 1) huge, real-time computation; 2) large, high speed communication and 3) complicate and real-time control. Solutions for above problems are provided.

Requirements for the Cell Array of Digital Clay

Digital Clay requires a large scale cell array to be actuated under control. The Mechanical structure and control architectures are investigated in this chapter. Per the ultimate goal, requirements for the cell array of Digital Clay can be found as below:

Requirements on the hydraulic system structure and the control hardware:

Compact size: The hydraulic system occupies the major space of the Digital Clay. To reduce the size of Digital Clay is mainly to make the hydraulic circuit and the control hardware compact.

Open to Scale Up: Limited by the research resources, fabrication of a large scale cell array system is not practical at current research stage. However, the hydraulic system structure and the control hardware investigated and designed in this research are all

targeted at a large scale system, i.e. all the hardware designs should be readily to expand to a large scale system.

Requirements on the control:

Controllability: The large scale array should be able to control using existing technology.

Scalability: The control method proposed need to be applicable when the scale of the cell array expands.

Stability: The system should be stable given reasonable disturbances.

Outline of this chapter is listed below:

In this chapter, a novel Fluidic Matrix Drive is introduced first. Based on the concept of the matrix drive, several control methods is provided and discussed for effective control of the drive structure. More specifically, a simplified model of matrix drive is discussed followed by three control methods: the one-time refresh method, gradual refresh method and the gradual approximation refresh method. After that, details surface level control for Digital Clay is introduced. The experimental system is given. Solenoid valve noise filtering problem is discussed. Finally, conclusions are given.

4.2 HYDRAULIC “N² BY 2N” MATRIX DRIVE

An important issue that must be addressed for a large-scale hydraulic planar pin-rod matrix array is the complexity of the system including hardware and control loops. Under conventional methods, to actuate a typical $N \times N$ pin-rod matrix such as those driven by servomotors, each pin-rod must be controlled individually. That will require an amount of control hardware and information proportional to N^2 . Such scheme works perfectly well if the size of the matrix array is small.

But for a high-resolution display with a large number of actuators as required by Digital Clay, the required hardware and information load could make the system uncontrollable and impossible for manufacturing.

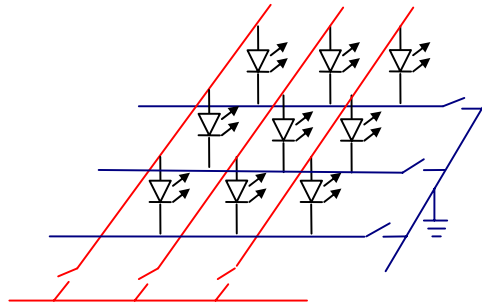


Figure 4-2 Matrix Drive for LED array

To solve the problem, a scheme that is commonly used in CMOS and LCD displays called "Matrix Drive" is investigated. As shown in Figure 4-2, it is composed of an N channel switch positioned orthogonally at both ends of the LED array. To actuate a certain LED, each switch needs to be turned on in the corresponding horizontal and vertical channels, as a Boolean "AND" operation. The advantage of this drive method is that it can greatly reduce the number of required control components (valves, etc.). However, since hydraulic actuator of the Digital Clay is quite different from the LED or other electrical device, this method needs to be modified before applying.

As shown in Figure 4-3, an " N^2 by $2N$ " Fluidic Matrix Drive structure is designed to drive the cell array. The " N^2 by $2N$ " Fluidic Matrix Drive structure is a novel structure for large scale fluidic actuator array. It is so called because each actuator of an $N \times N$ hydraulic actuator array can be independently driven using only $2N$ control valves (e.g. 200 valves can drive 100×100 actuators).

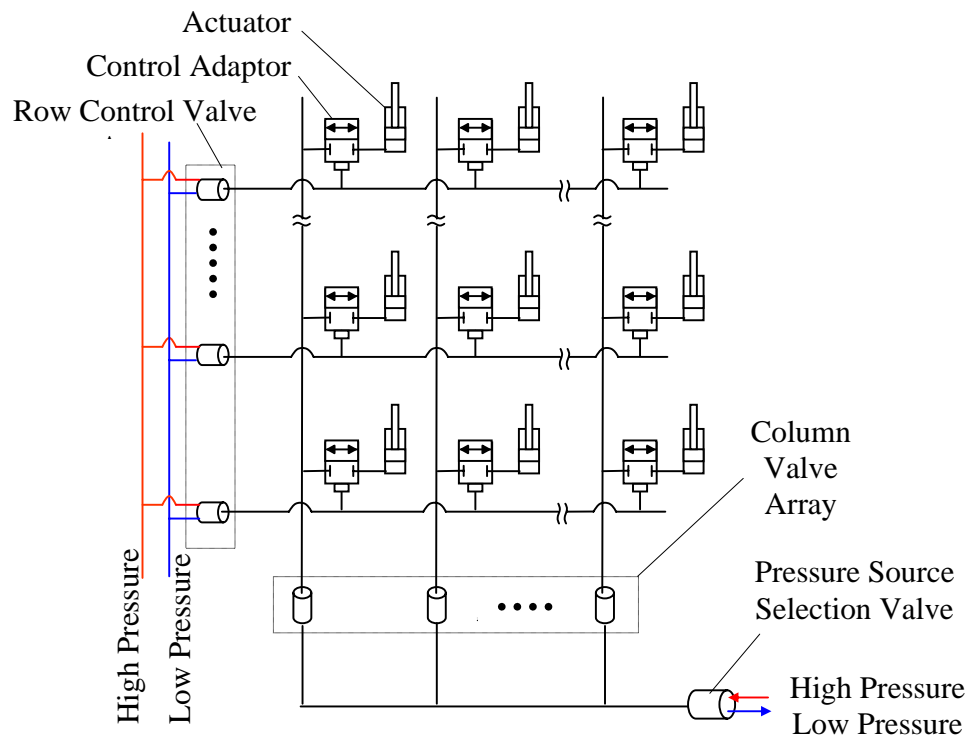


Figure 4-3 “N² by 2N” Fluidic Matrix Drive Concept

In above “N² by 2N” Fluidic Matrix Drive structure, the row control valves and the pressure source selection valve are 3 port / 2 way on/off valves. The common ports of these valves are connected to the actuation system, while the other two ports are connected to the high pressure source and low pressure source respectively. The hydraulic actuators displayed in Figure 4-3 are single acting actuators with pressure return.

When a row control valve is not powered, the control ports of the control adapters in that row will be subject to the high-pressure as shown in Figure 4-4a. (The normally open port of the row control valve connects the high-pressure). These control adapters then will block the fluid channels from the column control valves to the hydraulic actuators in

that row. Therefore these hydraulic actuators will not move despite of the status (on or off) of the column control valves.

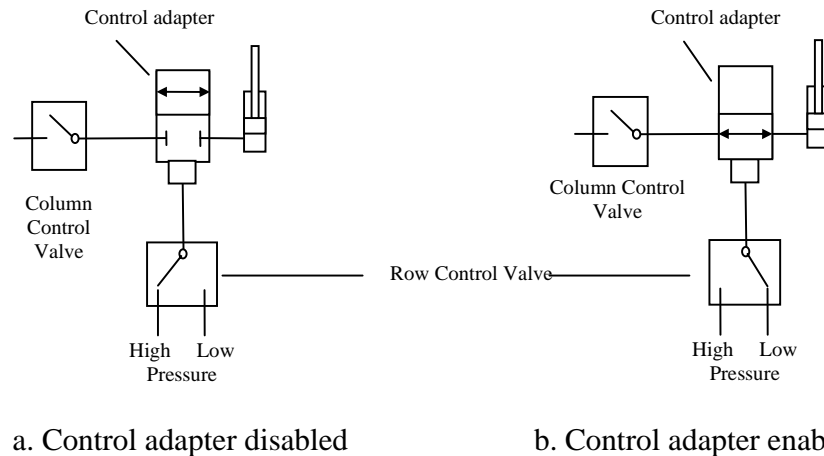


Figure 4-4 Working Principle of “ N^2 by $2N$ ” Fluidic Matrix Drive

When a row control valve is energized, the control ports of the control adapters in that row will be subject to the low-pressure (atmosphere or vacuum) (Figure 4-4b). These control adapters will enable the fluid channels from the flow control valves to the hydraulic actuators in that row. Therefore, the displacement of each hydraulic actuator in that row can be adjusted by its corresponding column control valve.

When the pressure source selection valve connects the high-pressure, a hydraulic actuator will extend (given the corresponding row control valve and column control valve are powered), and vice versa. By powering the row control valves one by one (or in certain manners an interlace scan), the entire array of hydraulic actuators can be controlled.

Note: Though the above schematic circuit is for a single acting hydraulic actuator (with certain return mechanism like spring), some minor modifications can make it suitable for double acting cylinder array as shown in figure 4-5.

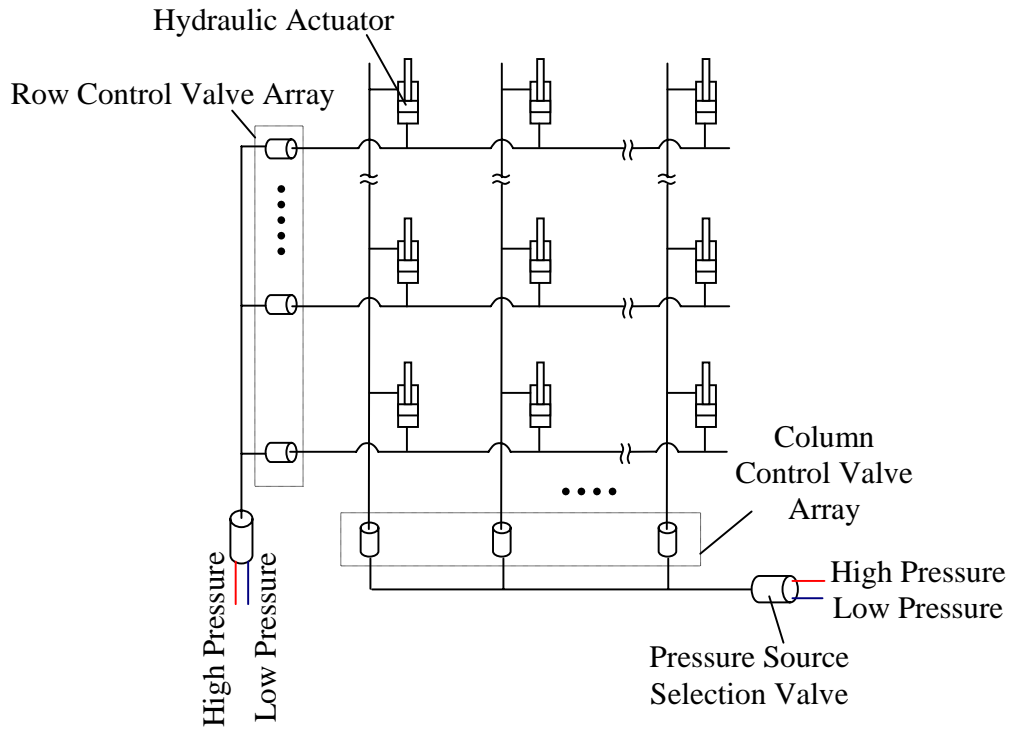


Figure 4-5 “ $N^2 - 2N$ ” Fluidic Matrix Drive for Double Acting Actuator

4.3 SURFACE REFRESH METHODS FOR THE FLUIDIC MATRIX DRIVE

Three control methods based on the Fluidic Matrix Driver will be discussed in this section: one-time refreshing, gradual refreshing and gradual approximation refreshing. No matter which control method is used, the basic principle to control the cell array based on the Fluidic Matrix Driver is to open the row control valves and the column control valves in a certain pattern to achieve the desired surface.

4.3.1 Model of the Fluidic Matrix Drive Node

As shown in Figure 4-6, one node of the Fluidic Matrix Drive can be simplified as two on-off valves serially linked together. The control adapter is simplified as an on/off valve that is controlled by its corresponding row control valve. Note that there is a

pressure source selection valve linking to the column control valve, which is not shown in this figure. Based on the matrix drive structure and the simplified node model, the flow rate can be described as the function of duty cycles applied on the valves:

$$q = f(\delta_1, \delta_2);$$

Where, δ_1 and δ_2 are the duty cycles applied to the valves. Therefore, the displacement of the actuator is: $c = k \cdot q = k \cdot f(\delta_1, \delta_2) = g(\delta_1, \delta_2)$. (k is a constant) Note that, the phase difference between the PWM waves on the two valves can also affect the flow rate. However, this affection can be isolated and avoided by synchronizing the PWM waves and carefully increasing the compliance of the pipe between the two valves.

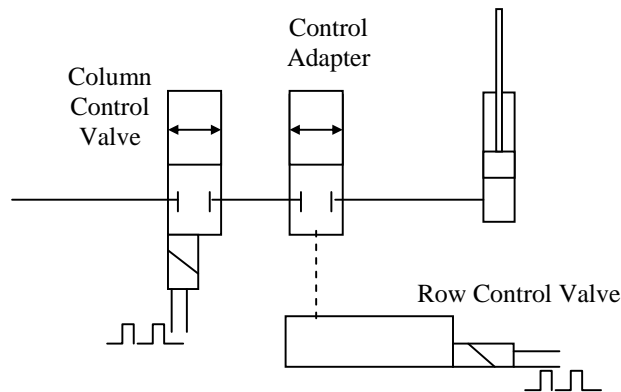


Figure 4-6 Simplified Node Model

4.3.2 Matrix Representation of the Basic Control

For the efficiency of the illustration, several terms are defined here before further discussions: 1) Row refreshing cycle (RRC) is the process for one row being fully refreshed. 2) Surface refreshing cycle (SRC) is the process for the whole surface being fully refreshed. An SRC is composed of one or several RRC. 3) Operation Θ is an operation subjected to following rule:

$$\mathbf{A} = \begin{bmatrix} a_1 \\ \vdots \\ a_i \\ \vdots \\ a_n \end{bmatrix}; \text{ and } \mathbf{B} = [b_1 \quad \dots \quad b_j \quad \dots \quad b_n];$$

$$\text{Then } \mathbf{A} \Theta \mathbf{B} = \begin{bmatrix} \mathbf{g}(a_1, b_1) & \mathbf{g}(a_1, b_2) & \dots & & \\ \mathbf{g}(a_2, b_1) & & & & \\ \vdots & & \ddots & & \\ & & & \mathbf{g}(a_i, b_j) & \\ & & & & \end{bmatrix}$$

In above definition, $g(x, y)$ depicts the relationship between input duty cycles and the fluid volume passing through the actuator ports. It depends on variables such as pressure drop, discharge coefficient, etc. Obviously, this is not an operation in the domain of linear algebra. It describes the mechanism of the Fluidic Matrix Drive. Due to the large amount of actuators, in practice, the relationship $g(x, y)$ can be estimated using displacement feedback. The estimation method will be discussed later.

If, during a row refreshing cycle, the PWM duty cycles of the column control valve array are represented by a column vector $\mathbf{A1}$, and the on/off status of the row control valve array are represented by a row vector $\mathbf{B1}$, then the displacement change of the cell array after that RRC can be expressed as: $\mathbf{C1} = \mathbf{A1} \Theta \mathbf{B1}$. For example, for the 5x5 cell array: **(For the simplicity, assume $g(x, y) = x*y$ in the following examples)**

$$\text{If } \mathbf{A1} = \begin{bmatrix} 0.1 \\ 0.2 \\ 0.3 \\ 0.4 \\ 0.5 \end{bmatrix}; \text{ and } \mathbf{B1} = [0 \quad 1 \quad 0 \quad 0 \quad 0]; \text{ Then } \mathbf{C1} = \begin{bmatrix} 0 & 0.1 & 0 & 0 & 0 \\ 0 & 0.2 & 0 & 0 & 0 \\ 0 & 0.3 & 0 & 0 & 0 \\ 0 & 0.4 & 0 & 0 & 0 \\ 0 & 0.5 & 0 & 0 & 0 \end{bmatrix}$$

Note that, in $\mathbf{B1}$, “0” means not enabled, “1” means enabled.

Obviously, if the desired cell displacement after a surface refreshing cycle is represented by a matrix C, then we can decompose C into two matrixes A and B, which represents the control actions needed for column and row control valves. Take the 5 x 5 cell array for example, if the desired final surface matrix:

$$C = \begin{bmatrix} 0.2 & 0.1 & 0.3 & 0.2 & 0.3 \\ 0.3 & 0.2 & 0.4 & 0.4 & 0.5 \\ 0.4 & 0.3 & 0.5 & 0.6 & 0.7 \\ 0.5 & 0.4 & 0.6 & 0.8 & 0.3 \\ 0.6 & 0.5 & 0.7 & 0.5 & 0.6 \end{bmatrix}$$

Then the control applied to the control valves can be calculated as:

$$C = A * B = \begin{bmatrix} 0.2 & 0.1 & 0.3 & 0.2 & 0.3 \\ 0.3 & 0.2 & 0.4 & 0.4 & 0.5 \\ 0.4 & 0.3 & 0.5 & 0.6 & 0.7 \\ 0.5 & 0.4 & 0.6 & 0.8 & 0.3 \\ 0.6 & 0.5 & 0.7 & 0.5 & 0.6 \end{bmatrix} * \begin{bmatrix} 1 & 0 & 0 & 0 & 0 \\ 0 & 1 & 0 & 0 & 0 \\ 0 & 0 & 1 & 0 & 0 \\ 0 & 0 & 0 & 1 & 0 \\ 0 & 0 & 0 & 0 & 1 \end{bmatrix}$$

\uparrow 1st RRC \uparrow 2nd RRC • • • • •

\leftarrow 1st RRC
 \leftarrow 2nd RRC

Therefore during the first RRC, the first row control valve shall open, while the others remain closed. At the same time, synchronized PWM duty cycles of [0.2 0.3 0.4 0.5 0.6] shall be applied to the column control valves.

The above control method is the simplest method that needs least calculations. As a fact, it also is the method used to refresh LED arrays and monitors. If the refreshing speed is fast enough, there will be no problem. However, since fluidic systems has much bigger hysteresis than electrical systems, this method will make the refreshing process

too obvious, and the user can easily feel the low speed of row by row refreshing. Therefore, optimizations are investigated to raise the refreshing speed.

Proposed here are three refresh methods: single step method, multi-sub-step method and multi-step approximation method.

4.3.3 One-time Refresh Method

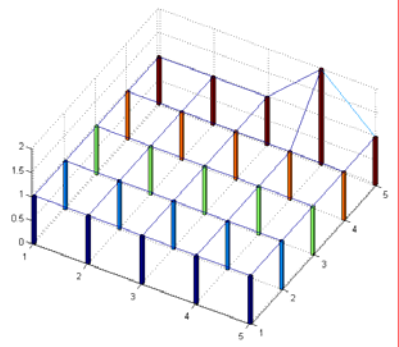
By the one-time refresh method, actuators are controlled to reach their final positions (determined by the surface matrix) row by row and in one step. The whole surface is refreshed row by row. A row will not be refreshed until the actuators in previous row are all in final position. Or in other words, the final surface is achieved through only 1 SRC. Here is an example:

$$\text{Suppose } C = \begin{bmatrix} 0 & 1 & 2 & 3 & 4 \\ 0 & 0 & 1 & 2 & 3 \\ 0 & 0 & 0 & 1 & 2 \\ 0 & 0 & 0 & 0 & 1 \\ 0 & 0 & 0 & 0 & 0 \end{bmatrix} \text{ is the final surface matrix desired.}$$

If the maximum speed of the actuator is 1 unit/sec, and the row refreshing settling time (i.e. the time for valves to stably open and close) is 0.1 sec. Note: The equilibrium position of each pin-rod is 1. The vectors for controlling the valve arrays in the first RRC are A1 and B1, and the achieved surface matrix is C1.

$$A1 = [0 \ 0 \ 0 \ 1 \ 0]^T; \quad B1 = [0 \ 0 \ 0 \ 0 \ 1];$$

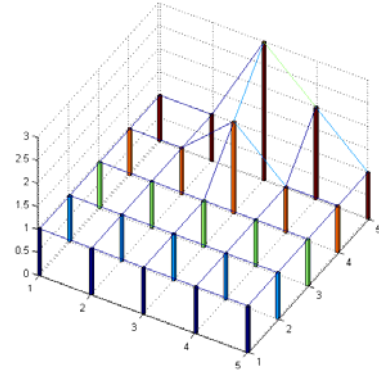
$$C1 = A1 \ominus B1 * t_1 = \begin{bmatrix} 0 & 0 & 0 & 0 & 0 \\ 0 & 0 & 0 & 0 & 0 \\ 0 & 0 & 0 & 0 & 0 \\ 0 & 0 & 0 & 0 & 1 \\ 0 & 0 & 0 & 0 & 0 \end{bmatrix}; \text{ where } t_1 = 1 \text{ sec}$$



The vectors for controlling the valve arrays in the 2nd RRC are A2 and B2, and the achieved surface matrix is C2.

$$A2 = [0 \ 0 \ 1 \ 1 \ 0]'; \quad B2 = [0 \ 0 \ 0 \ 0.5 \ 1];$$

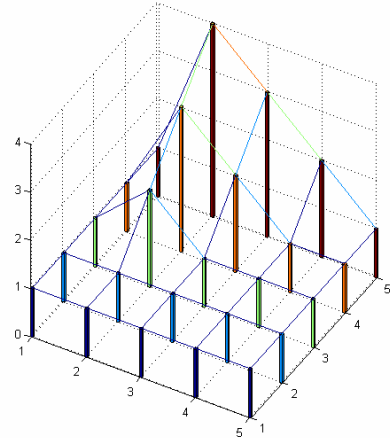
$$C2 = C1 + A2 \Theta B2 * t_2 = \begin{bmatrix} 0 & 0 & 0 & 0 & 0 \\ 0 & 0 & 0 & 0 & 0 \\ 0 & 0 & 0 & 1 & 2 \\ 0 & 0 & 0 & 0 & 1 \\ 0 & 0 & 0 & 0 & 0 \end{bmatrix}; \quad \text{where } t_2 = 2 \text{ (sec)}$$



The vectors for controlling the valve arrays in the 3rd RRC are A3 and B3, and the achieved surface matrix is C3.

$$A3 = [0 \ 1 \ 1 \ 1 \ 0]; \quad B3 = [0 \ 0 \ 1/3 \ 2/3 \ 1];$$

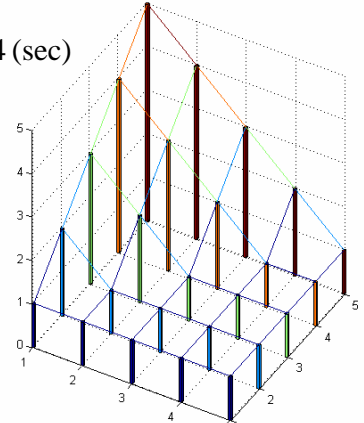
$$C3 = C2 + A3 \Theta B3 * t_3 = \begin{bmatrix} 0 & 0 & 0 & 0 & 0 \\ 0 & 0 & 1 & 2 & 3 \\ 0 & 0 & 0 & 1 & 2 \\ 0 & 0 & 0 & 0 & 1 \\ 0 & 0 & 0 & 0 & 0 \end{bmatrix}; \quad \text{where } t_3 = 3 \text{ (sec)}$$



The vectors for controlling the valve arrays in the 4th RRC are A4 and B4, and the achieved surface matrix is C4. C4 is the final desired surface matrix.

$$A4 = [1 \ 1 \ 1 \ 1 \ 1]; \quad B4 = [0 \ 0.25 \ 0.5 \ 0.75 \ 1];$$

$$C4 = C3 + A4 \Theta B4 * t_4 = \begin{bmatrix} 0 & 1 & 2 & 3 & 4 \\ 0 & 0 & 1 & 2 & 3 \\ 0 & 0 & 0 & 1 & 2 \\ 0 & 0 & 0 & 0 & 1 \\ 0 & 0 & 0 & 0 & 0 \end{bmatrix}; \text{ where } t_4 = 4 \text{ (sec)}$$



Therefore the total time = $t_1 + t_2 + t_3 + t_4 + 4 * \text{Row Refreshing Settling Time} (= 0.1) = 10.4 \text{ sec.}$

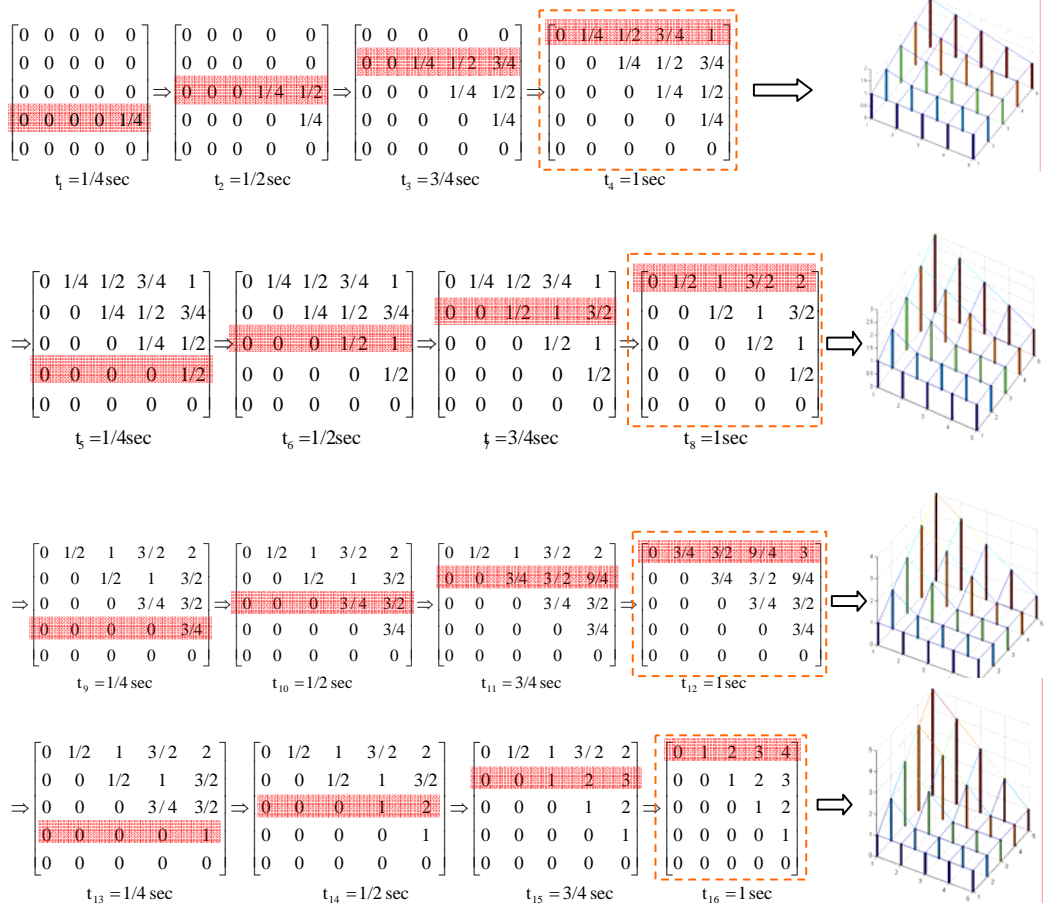
The advantage of the one-time refreshing method is the simplicity. The problem is the bad visual effects due to obvious discontinuous movement of the pin-rods. Therefore, the gradual refreshing method is studied.

4.3.4 Gradual Refresh Method

By gradual refresh method, the final desired surface is gradually achieved through several intermediate surfaces. In other words, there are several SRCs involved to achieve the final surface. For example,

$$\text{Suppose } C = \begin{bmatrix} 0 & 1 & 2 & 3 & 4 \\ 0 & 0 & 1 & 2 & 3 \\ 0 & 0 & 0 & 1 & 2 \\ 0 & 0 & 0 & 0 & 1 \\ 0 & 0 & 0 & 0 & 0 \end{bmatrix} \text{ is the desired surface matrix.}$$

If the maximum speed of the actuator is 1 unit / sec, by the gradual refreshing method, it will take 11.6 seconds to fulfill the task as shown below. Note: The equilibrium position of each pin-rod is 1.



Therefore, the total time = $t_1 + t_2 + \dots + t_{16} + 16 * \text{Row Refreshing Settling Time (0.1)}$
= 11.6 sec

As one can see that by gradual refreshing method, the visual effect is improved. However, this refreshing method is more complicated than one-time refreshing method and when the number of the intermediate surfaces increases, the total surface refreshing time will increase due to the increasing of the number of row refreshing cycles. In above example, 4 sub-steps are applied, therefore the total row refreshing settling time is $4 * 4 *$

0.1 = 1.6 seconds. But if 40 intermediate surfaces are required, the total row refreshing settling time will be $40 * 4 * 0.1 = 16$ seconds. Note: The more intermediate surfaces are applied, the smoother the surface transition appears.

4.3.5 Gradual Approximation Refresh Method

Surface refreshing cycles of both one-time refreshing method and gradual refreshing method are essentially the same: row refreshing cycles are processed one by one or, in other words, cylinders are actuated row by row, using the column and row matching method. When a certain row is being refreshed, others are just waiting. Therefore, if all the rows can be refreshed at the same time, the total refreshing time may be reduced. The basic principle for the gradual approximation refreshing method is to refresh the whole surface at the same time instead of refreshing row by row. That requires all the row control valve and column control valve to open at the same time. Obviously, if during the refreshing process, the PWM duty cycles are fixed, the columns or rows of the surface matrix will be dependent to each other. (In linear algebra, the rank of the matrix will be 1, because the matrix is the product of a column vector and a row vector.) Therefore, several intermediate surfaces are needed. In other words, the PWM duty cycle for each valve needs to be changed before the actuator reaches the final position.

Note that, this refresh method is currently still under investigation. But due to its big advantage (as will be shown in the following), it is still worth to mention here.

$$\text{For example, suppose } C = \begin{bmatrix} 0 & 1 & 2 & 3 & 4 \\ 0 & 0 & 1 & 2 & 3 \\ 0 & 0 & 0 & 1 & 2 \\ 0 & 0 & 0 & 0 & 1 \\ 0 & 0 & 0 & 0 & 0 \end{bmatrix} \text{ is the surface matrix desired.}$$

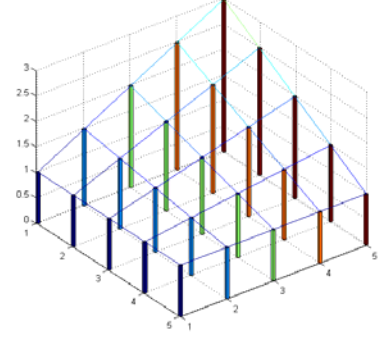
Suppose the maximum speed of the actuator is 1 unit/sec, and the equilibrium position of each pin-rod is 1.

The first intermediate surface is:

$$A1 = [1 \quad 3/4 \quad 1/2 \quad 1/4 \quad 0]^T; \quad B1 = [0 \quad 1/4 \quad 1/2 \quad 3/4 \quad 1];$$

$$C1 = A1 \ominus B1 * t_1 = \begin{bmatrix} 0 & 0.500 & 1.00 & 1.500 & 2.0 \\ 0 & 0.375 & 0.75 & 1.125 & 1.5 \\ 0 & 0.250 & 0.50 & 0.750 & 1.0 \\ 0 & 0.125 & 0.25 & 0.375 & 0.5 \\ 0 & 0 & 0 & 0 & 0 \end{bmatrix};$$

where $t_1 = 2$ sec



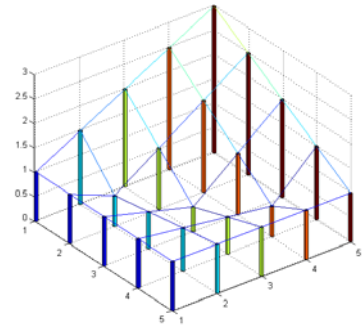
The second intermediate surface can be:

$$C2 = C - C1 = \begin{bmatrix} 0 & 0 & 0 & 0 & 0 \\ 0 & -0.75 & -0.5 & -0.25 & 0 \\ 0 & -0.50 & -1.0 & -0.5 & 0 \\ 0 & -0.25 & -0.5 & -0.75 & 0 \\ 0 & 0 & 0 & 0 & 0 \end{bmatrix}$$

This is achieved by:

$$\begin{bmatrix} 0 & 0.500 & 1.00 & 1.500 & 2.0 \\ 0 & 0.375 & 0.75 & 1.125 & 1.5 \\ 0 & 0.250 & 0.50 & 0.750 & 1.0 \\ 0 & -0.125 & -0.25 & -0.375 & 0.5 \\ 0 & 0 & 0 & 0 & 0 \end{bmatrix}_{t_2 = 3/4 \text{ sec}} \Rightarrow \begin{bmatrix} 0 & 0.500 & 1.00 & 1.500 & 2.0 \\ 0 & 0.375 & 0.75 & 1.125 & 1.5 \\ 0 & -0.250 & -0.50 & -0.250 & 1.0 \\ 0 & -0.125 & -0.25 & -0.375 & 0.5 \\ 0 & 0 & 0 & 0 & 0 \end{bmatrix}_{t_3 = 1 \text{ sec}} \Rightarrow \begin{bmatrix} 0 & 0.500 & 1.00 & 1.500 & 2.0 \\ 0 & -0.375 & 0.25 & 0.875 & 1.5 \\ 0 & -0.250 & -0.50 & 0.250 & 1.0 \\ 0 & -0.125 & -0.25 & -0.375 & 0.5 \\ 0 & 0 & 0 & 0 & 0 \end{bmatrix}_{t_4 = 3/4 \text{ sec}}$$

After above refreshing steps, we can get a surface depicted in the figure below.



Finally apply:

$$A2 = \begin{bmatrix} 1 & 3/4 & 1/2 & 1/4 & 0 \end{bmatrix}; \quad B2 = \begin{bmatrix} 0 & 1/4 & 1/2 & 3/4 & 1 \end{bmatrix};$$

$$C3 = C1 + C2 + A2 * B2 * t_5 = \begin{bmatrix} 0 & 1 & 2 & 3 & 4 \\ 0 & 0 & 1 & 2 & 3 \\ 0 & 0 & 0 & 1 & 2 \\ 0 & 0 & 0 & 0 & 1 \\ 0 & 0 & 0 & 0 & 0 \end{bmatrix}; \quad \text{where } t_5 = 2 \text{ sec}$$

Therefore, the total time = $t_1 + t_2 + \dots + t_5 + 5 * \text{Row Refreshing Settling Time } (0.1) = 7$ sec

Note: If we use $25 * 2 = 50$ valves for this application, it also needs 4 seconds to generate the required surface.

From above example, one can see that the intermediate surfaces usually are not proportional to the final surface, but the superposition of these intermediate surfaces yields the final surface. The method is called gradual approximation refreshing method, because these intermediate surfaces are chosen such that their shapes are close to the final surface. By this approach, the total refreshing time can be reduced and a gradually changed surface can be achieved. In addition, though above discussions are based on the linear algebra (i.e. $g(x, y) = x * y$), they are also applicable if $g(x, y)$ is in other forms.

The problem foreseen in this method is the decomposition of the desired surface matrix into intermediate surface matrices. Since it is out of the scope of this research, the solutions to the problem will be left for future research.

4.4 CONTROL OF THE FLUIDIC MATRIX DRIVE

The control architecture of Digital Clay using Fluidic Matrix Drive is constructed from the modified decentralized control architecture described before. The overall

control architecture for the Fluidic Matrix Drive is shown in Figure 4-7. Due to the specialty of the Fluidic Matrix Drive, the cell level controller is different from the cell level controller for the single cell system. It composed of valve controllers, surface refresh coordinator and hot area processor as shown in Figure 4-8. Instead of large amount of cell level controller embedded in every cell, one or several scan coordinator and a hot area processor perform the cell level control through two valve controller arrays. The information flow between each control level also can be found in Figure 4-7. Definitions of the terms and symbols can be found in table 4-1.

Table 4-1 Table of Definitions of Terms and Symbols

TERM /	DEFINITION
[X]	Absolute displacement matrix for the cell array. Note: this is also the equilibrium position for every cell.
[ΔX]	Relative or increment displacement matrix for the cell array
[V]	Velocity matrix for the cell array
[P]	Pressure matrix for the cell array
[H]	Haptic information matrix for the cell array. The value (1,2 or 3) of each element in the matrix has following meaning: 1 --- elastic state, 2 --- plastic state, 3 --- shaping state
[MP]	Material property matrix for the cell array. Note: At the current stage, it defines the elastic modulus matrix for each cell.
GUI	Graphical User Interface
Haptic Process	The control process that generates the haptic interaction between the user and the Digital Clay

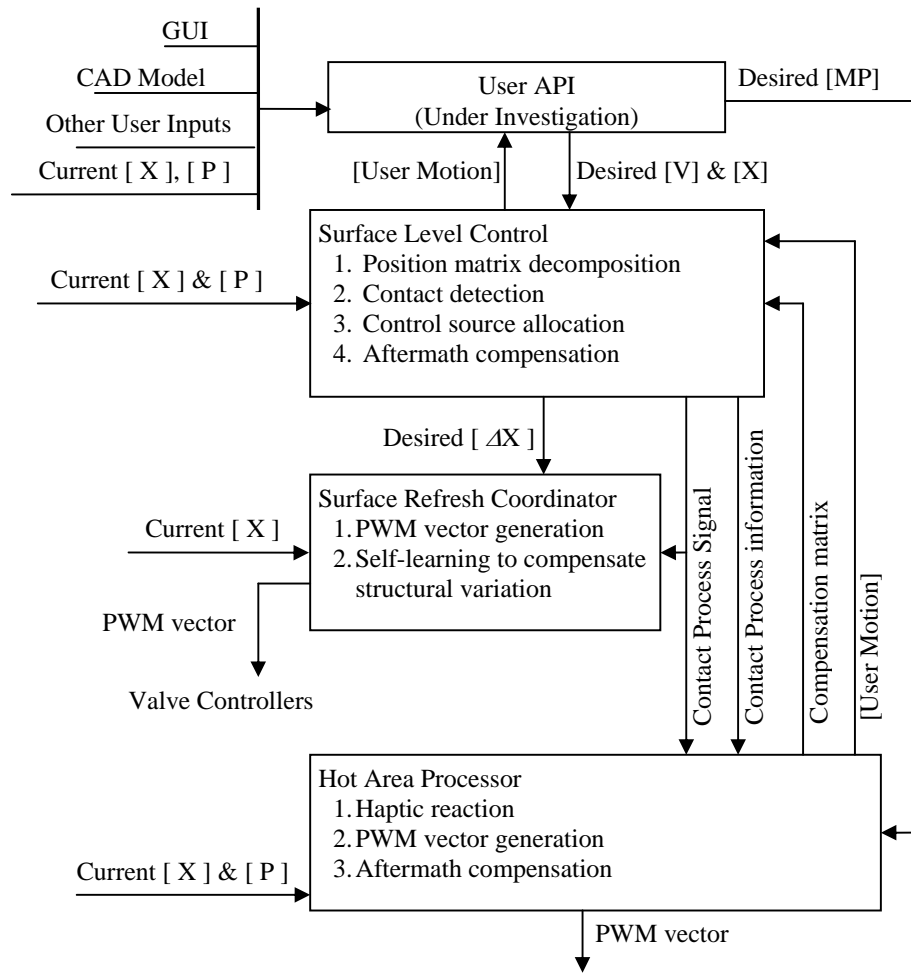


Figure 4-7 Control Architecture for the Fluidic Matrix Drive

4.4.1 User API

The top application level is represented by the user application programming interface (User API) software, which generates desired displacement matrix [X], desired [V] to the surface level controller and desired Material Property matrix [MP] to the haptic processor in the cell level controller as shown in Figure 4-7. The user API will be developed by the computer science group in Georgia Tech.

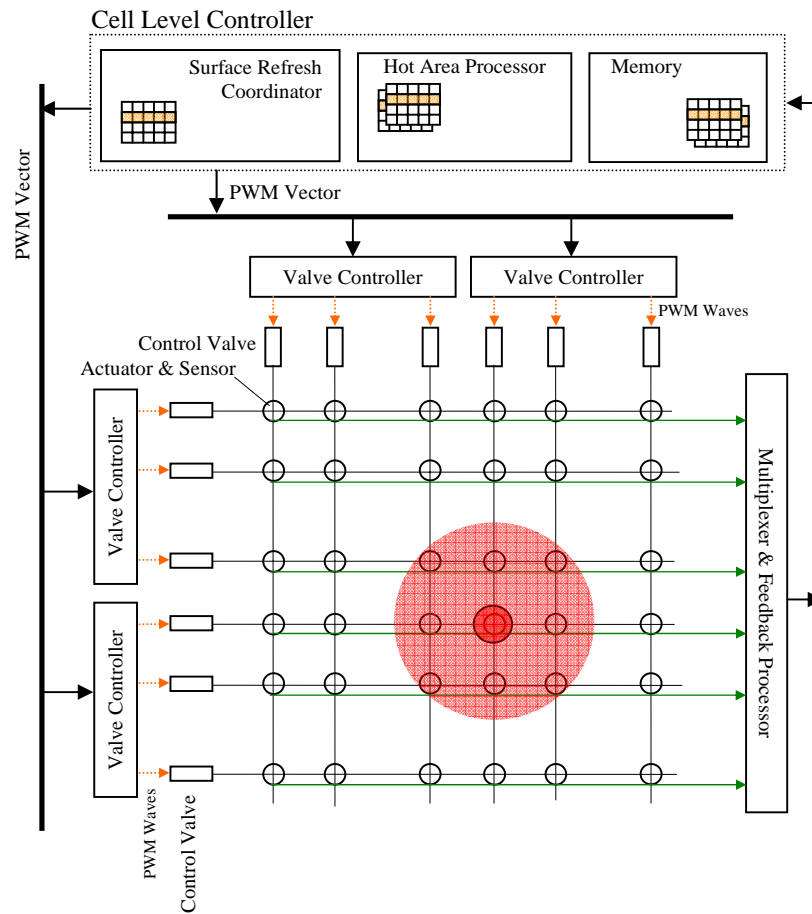


Figure 4-8 Low Level Control Architecture

The information from the user API is mainly about global surface parameters, as well as virtual material property for each cell. Pressure matrix [P], displacement matrix [X] and user motion matrix [user motion] of the cell array will be sent back to the user API for the host PC's reference and for further editing purpose (i.e. save, undo, redo, etc.) User API also takes other inputs such as GUI, CAD models, keyboard and mouse inputs.

Interfacing the surface level control with the user API is a cooperative work with computer science group. The objective of this part is to study and provide the surface level control mechanism and corresponding parameters for computer science group to build the connection from the user API to surface level control and vice versa.

4.4.2 Surface Level Control

Surface level control is responsible for achieving the best fit to the ideal surface. It is dependent on the implementation of Digital Clay. The surface level control will be hidden from both the Fluidic Matrix Drive, the architecture of the surface level control is constructed as shown in Figure 4-9. Details on the functions of the surface level control are described below.

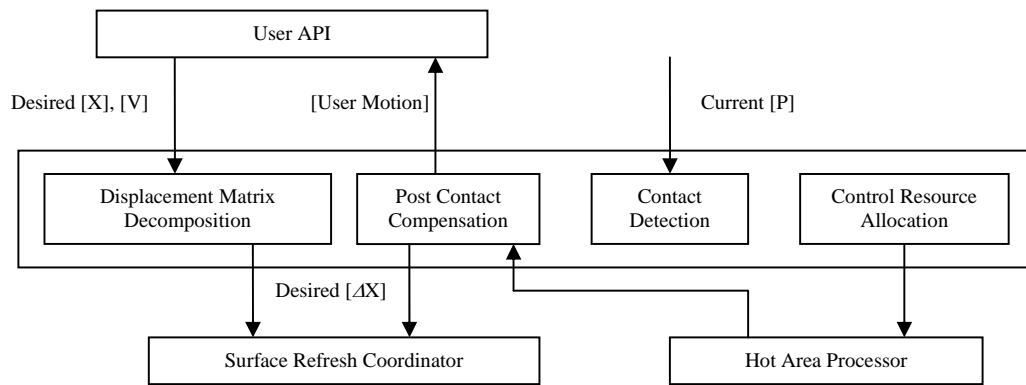


Figure 4-9 Surface Level Control Functional Block Diagram

Displacement matrix decomposition

The desired displacement matrix $[X]$ received from the user API represents the surface shape after a certain period. The desired velocity matrix $[V]$ describes the dynamic transient between the current surface and the final surface, i.e. how the current shape changes to the desired surface described by $[X]$. As discussed before, there are three surface refresh methods. For the gradual refresh method and the gradual approximation refresh method, the desired displacement matrix $[X]$ needs to be decomposed into a set of intermediate matrices. This work will be done by the surface level control based on the desired $[X]$ and the desired speed matrix $[V]$. The decomposed intermediate matrices will be sent to the surface refresh coordinator to execute.

Contact detection

The surface level control will frequently monitor the pressure matrix [P] change to detect if the cell array is touched by the user. The pressure measurement needs to be filtered before a contact can be determined.

Control resource allocation

Categorized by whether the user contacts the working surface or not, there are two display methods: 1) passive display, if there is no interaction between the user the Digital Clay, and 2) active display, if the user contacts the working surface and the Digital Clay needs to provide haptic interface.

During the passive display, the working surface is refreshed by the refresh coordinator. However, under most circumstances, Digital Clay works under the active display. If the user contacts the Digital Clay, most of the cells still operates under passive display; only the cells in a small area will work in the active display. That is because the area the user hands have limited area ($< 0.04 \text{ m}^2$) compared with that of the cell array ($0.5\sim 2 \text{ m}^2$)

The surface level control frequently monitors the pressure of each actuator. Once a pressure change is detected that is due to the user contacting the actuator, that actuator will be defined as the hot spot. When a hot spot is defined, the surface level controller will define a hot area including the hot spot and its neighboring actuators. Then the surface level controller passes the hot spot and the hot area information to the hot area processor, halts the surface refresh coordinator and enables the hot area processor. During the haptic interaction, the user's motion is frequently received from the hot area

processor and sent to the user PAI in the forms of $[P]$, $[X]$, and the user motion matrix $[user\ motion]$.

Post contact processing

After the active display terminates, there will be a surface discrepancy since the hot area is changed during the process while the rest of the surface is remain unchanged or delayed. Therefore making up of the discrepancy is necessary. To solve this problem, the user API will generate the ultimate make up surface matrix and send it to the surface level controller to generate several intermediate matrices for the surface refresh coordinator to execute.

4.4.3 Surface Refresh Coordinator

The surface refresh coordinator takes the desired displacement increment matrix $[\Delta X]$, and generates the corresponding PWM duty cycles for both column and row valve controller arrays. Details of the work are described below.

At the beginning of a surface refresh cycle, surface refresh coordinator first receives the displacement increment matrix from the surface level controller. Displacement increment matrix $[\Delta X]$ carries the displacement increments for each actuator during the next surface refresh cycle. The $[\Delta X]$ and the time period (usually fixed) during which the $[\Delta X]$ need to be fulfilled are determined and given by the surface level controller. Depending on the refresh method used, the surface refresh coordinator generates PWM duty cycle vector. Once a set of PWM vectors are sent out, the surface refresh coordinator will continuously monitor the displacement feedback $[X]$. When the current surface refresh cycle ends, (i.e. the time period is over) no matter whether the desired $[X]$

is achieved or not, control valves will be closed. If there is any discrepancy between the current $[X]$ and the desired $[X]$, the correction factors will be calculated and stored to compensate the PWM duty cycles generated during the next surface refresh cycle. At the same time, the surface level controller will consider the discrepancy when generating the next $[\Delta X]$

As one can see, the last step is actually a self learning process with the feedback of the discrepancy. Because of the structural variation between discrete cells, theoretically generated PWM duty cycles will not fit for all cells. Moreover, other factors like temperature and aging will also change the dynamic properties of the cell array.

4.4.4 Hot area Processor

Hot area processor deals with the haptic reaction once an area is detected to be touched by the user.

Hot area processor determines the displacement of each actuator based on the current pressure matrix $[P]$, the current displacement matrix $[X]$ and the material property matrix $[MP]$. The working principle is similar to the single cell system discussed before.

Once the user motion stops, the hot area processor will report the results to the surface level controller. The surface level controller will determine the desired displacement matrix (the compensation matrix) in order to make the surface not included in the hot area consistent to the hot area. Note that, the surface not included in the hot area ceases or delays moving during the hot area processing. Then the surface refresh coordinator will be enabled and the hot area processor will be disabled. The calculated compensation matrix will be processed and sent to the surface refresh coordinator. After the compensation is made, everything will be set back to the passive display.

During the process, user motion will be frequently sent to the surface level controller and the user PAI for reference.

4.4.5 Valve Controller

The valve controller provides interfaces between the control valves and the cell level controller as shown in figure 4-10. The valve controller first recognizes and receives the corresponding section of the PWM duty cycle flow on the data bus. Then the received PWM duty cycles are translated into corresponding PWM waveforms and sent to the valve drivers. The translation will not occur, unless the newly received PWM duty cycles are different from the existing ones.

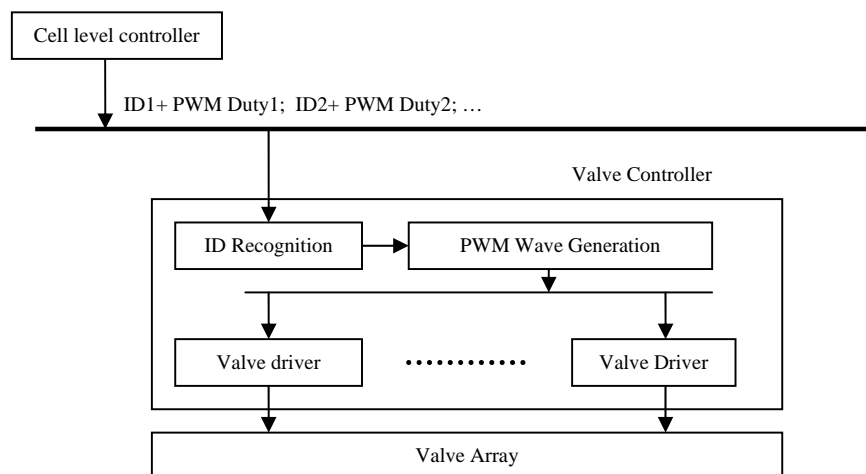


Figure 4-10 Valve Control Functional Block Diagram

4.5 CONCLUSIONS

At the current stage of the actuation technology, planar pin-rod matrix array concept is the most suitable for construction of the working surface of Digital Clay and is first introduced. To be able to drive a pin-rod matrix array that consists of large number of

actuators, the Fluidic Matrix Drive is proposed. By using the Fluidic Matrix Drive, not only is the number of the control valves reduced but also the amount of control resource needed is reduced. The Fluidic Matrix Drive is suitable for the actuator array that consists of either single acting or double acting actuator array.

To control the Fluidic Matrix Drive, three control methods to realize the surface refresh are proposed. One-time refresh method is the most straight forward and simplest method. The drawback is the slow refresh speed and bad visual effect caused by the discontinuity change of the working surface. Gradual refresh method takes more time than one-time refresh method, but provides a visually continuous changing surface. If well designed, gradual approximation refresh method can provide continuously changing surface as fast as one time refresh method.

Control architecture for Digital Clay using fluidic matrix drive is a little different from the control structure proposed in chapter 3. Cell level controller may need to control a set of cells instead of just one cell. Passive display and haptic display are controlled by different processors inside the cell level control system. Concepts on the general control architecture, functions of the User API, the surface level controller, the cell level controller are presented. Relationship and information flows between the important control mechanisms are proposed and described in detail.

CHAPTER 5

IMPLEMENTATION OF THE CELL ARRAY SYSTEM

In this chapter, technologies and implementations to realize the cell array of Digital Clay are investigated. Digital Clay by its hardware is composed of an array of subsystems and the peripherals. Modular subsystem designs and implementations for Digital Clay are introduced in this chapter. More specifically, the method to deploy an array of displacement sensor embedded actuators is discussed; realizations for the Fluidic Matrix Drive are investigated; structural design of large scale pressure sensor array is introduced and the multiplexing circuits that reduce the number of data acquisition channels are investigated.

5.1 OVERVIEW

The Planar pin-rod matrix array concept has the advantage of practice and structural simplicity. Therefore, it is the most common structure used in research. Under this concept, Digital Clay's working surface is formed by the top ends of the hydraulic actuators in a linear pattern.

Ultimately, Digital Clay will have a cell array containing 100x100 to 1000x1000 cells to achieve a good resolution. Thus, the structural scalability and the controllability are main problems for the realization of Digital Clay. Solutions for the scalability and controllability on the conceptual level are provided in the previous chapter. This chapter focuses on the implementations to realize the Digital Clay regarding the scalability requirement.

For the mechanical structure realization, 1) modular design of functional blocks of Digital Clay is introduced; 2) Fluidic Matrix Drive hardware structural design is discussed; and 3) actuator and sensor related structures are investigated.

For the control hardware, embedding methods for pressure and displacement sensors are described. Sensor embedding methods include the arrangement of position and pressure sensors and their corresponding signal conditioning circuits. Through a conventional approach, a 1000x1000 array needs 1,000,000 displacement sensors and pressure sensors and corresponding signal conditioning circuits. In this research, several approaches are investigated to simplify the hardware and to reduce the data acquisition channels as well.

Requirements for the Implementation of Cell Array System

Digital Clay requires a large scale cell array to be actuated under control. According to the ultimate goal, the requirements for the implementation of the cell array system can be summarized as:

Design for Large Scale: This requires every subsystem to be as identical and simple as possible. Highly integrated systems are preferred under this requirement.

Design for Manufacturing: Digital Clay will finally need mass production technology. For the sake of long term development and later commercialization, the hydraulic system structure and the control hardware investigated and designed in this research should be practical and easy to manufacture using proper methods such as MEMS.

Outline of this chapter:

The mechanical structural designs for large scale cell array are discussed first. That includes the introduction to the functional modules, design of the control adapter, design of the time sequence for the Fluidic Matrix Drive structure, construction of the displacement sensor embedded actuator array assembly, and design of a pressure sensor mounting base.

Then the electronic system of the Digital Clay is introduced. This includes introduction to the electrical functional blocks, designs of the signal filter and multiplexer for the pressure sensor array, and the designs of multiplexer and signal conditioner for the displacement sensor array.

Finally, conclusions are given.

5.2 MECHANICAL STRUCTURE DESIGN FOR LARGE SCALE CELL ARRAY

Mechanical system of the cell array consists of the hydraulic circuit boards, the actuator-sensor array assembly, mounting base for sensor arrays, and some auxiliary function blocks. Per its ultimate goal, Digital Clay will have thousands or millions of cells in order to provide a high resolution surface. Therefore, organically combining cells to form a functional array with compact size, scalability and mass production ability, is the main objective of the design of mechanical system.

In this section, the construction of actuator array and the matrix drive for hydraulic system will be discussed; the design of mounting blocks for sensor arrays will be investigated; and the realization of the mechanical system using the stereolithography technology will be introduced.

5.2.1 Functional Modules of The Mechanical System

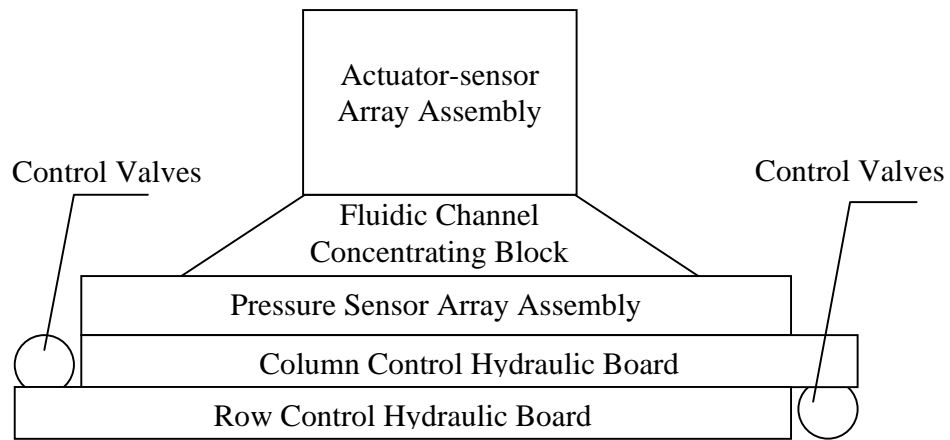


Figure 5-1 Functional Modules of Digital Clay

As shown in Figure 5-1, the mechanical system is proposed consisting of five functional modules for easy fabrication, easy assembling and easy maintenance: 1) Row control hydraulic board, 2) Column control hydraulic board, 3) Pressure sensor array assembly, 4) Fluidic channel concentrating block, and 5) Actuator-sensor array assembly.

Row control hydraulic board is a functional module with following features: 1) hydraulic channels for row control action, 2) control chambers of the control adapters, and 3) seats for the row control valve array are built on the board.

Column control hydraulic board is a functional module with following features built inside the board: 1) hydraulic channels for the column control action, 2) working chambers of the control adapters, and 3) seats for column control valve array.

Pressure sensor array assembly consists of the pressure sensor array and a mounting base for the pressure sensor array. The mounting base provides fittings to mount pressure sensors and the channels linking the inlet ports of the pressure sensors to the corresponding actuators. Though the pressure sensor mount and the pressure sensors

can be made on one wafer, it is not cost effective to do so and the size of the pressure sensor array is also limited due to the limitation on the wafer size.

Fluidic channels concentrating block concentrates the hydraulic channels into a small area to achieve a higher spatial resolution. This block provides a set of channels that have large center distance at bottom side and small center distance at top side.

Actuator-sensor array assembly is the assembly of displacement sensor embedded actuator array.

5.2.2 Design of the Control Adapter

Control adapter is the key element to realize the “ N^2 by $2N$ ” Fluidic Matrix Drive. The structure of the control adapter has several alternative solutions as shown in Figure 5-2. Control adapter is responsible for adjusting the flow rate between the actuator and the column control valve. The operation of the control adapter is controlled by its corresponding row control valve.

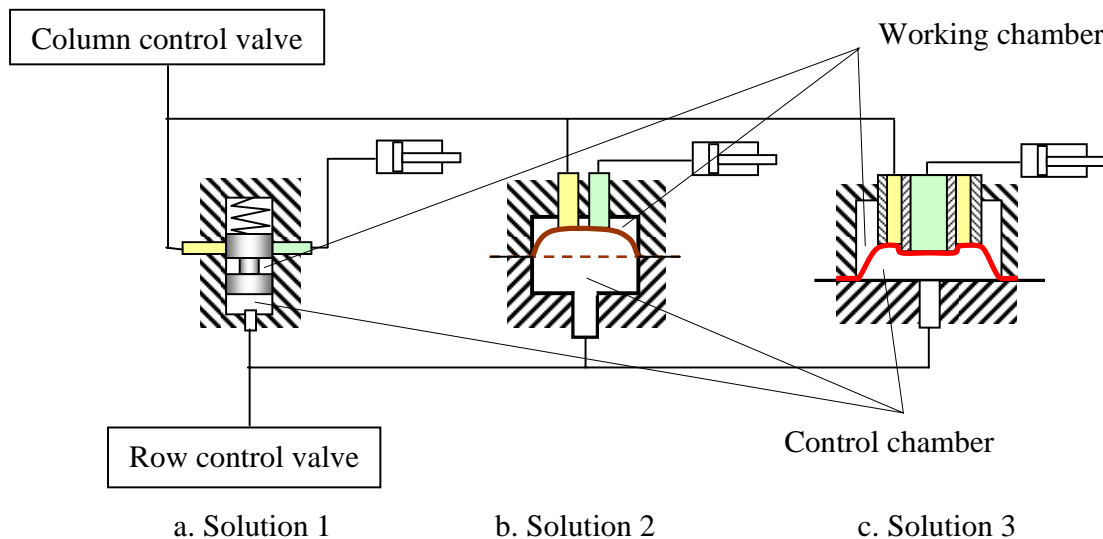


Figure 5-2 Solutions for Control Adapter Structure

As shown in Figure 5-2a, the control adapter of in solution 1 is composed of a working chamber, a control chamber, an H-style spool, two passive channels, and a return spring. Two passive channels link to the working chamber. The working chamber and control chamber are separated by the H-style spool. When the control channel is connected to the high pressure, the spool will move towards the working chamber and block the fluid path. When the control channel is connected to the low-pressure, the return spring will push the spool back and enable the fluid path.

As shown in Figure 5-2b, control adapter of solution 2 is composed of a working chamber, a control chamber, a membrane, and two passive channels. Two passive channels are placed in the working chamber in parallel. The working chamber and the control chamber are separated by the membrane. When the control chamber is connected to the high-pressure source, the membrane will move towards the working chamber and block the fluid path. When the control chamber is connected to the low-pressure source, the membrane will move back and enable the fluid path.

By solution 3 (Figure 5-2c), the control adapter is composed of a working chamber, a control chamber, a membrane, and two coaxial passive channels. The working chamber and the control chamber are separated by the membrane. When the control chamber is connected to the high-pressure source, the membrane will move towards the working chamber and block the fluid path. When the control channel is connected to the low-pressure source, the membrane will move towards the control chamber and enable the fluid path.

Comparison of above three solutions is listed in Table 5-1, and solution 2 and 3 are further considered as the potential solutions.

Table 5-1 Comparison of Solutions for Control Adapter

	SOLUTION 1	SOLUTION 2	SOLUTION 3
Simplicity	Complex	Simplest	Simple
Discrete components*	Spool and spring	Membrane	Membrane
Tolerance for moving parts	Strict	No	No
Response time	Slow	Fast	Fast
Orifice size	Large	Small	Large
Pulsation when close/open**	No	Large	Small

* The components needed other than the bases that are built using SLA technology

** Will be discussed below

A problem found during experiments is the pulsation that occurs when the control adapter opens and closes. The structures for these two solutions used in experiments are shown in Figure 5-3. Investigation shows that when the membrane moves, the residue volume in the working chamber will go into or out from the output channel that links to the actuator, which causes the actuator to pulsate. The residue volume tends to go into or out from the output channel instead of input channel, because the pressure in the supply channel is usually higher than the output channel. During the experiment, this clearly viewed phenomenon compromises the visual effect and the haptic effect. Note: The input channel links to the column control valve and the output channel links to the actuator.

From Figure 5-3, the residue volume in solution 2 is obviously larger than that of solution 3, given that the orifices of both solutions are the same. Therefore, solution 3 is chosen for the control adapter.

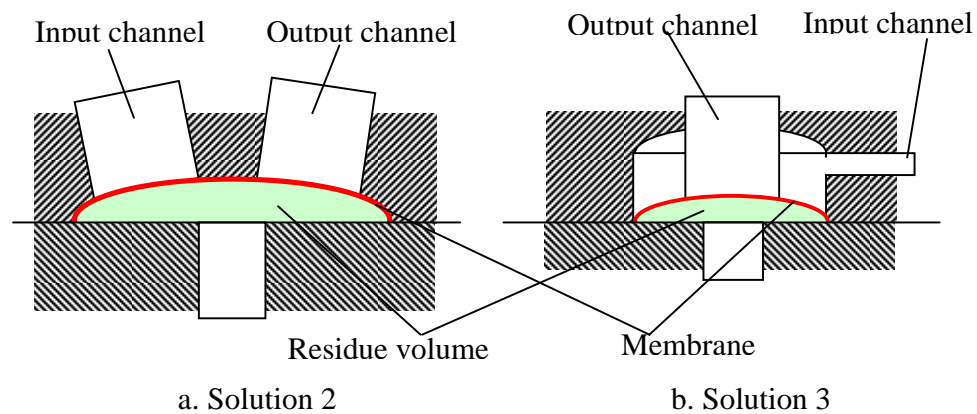


Figure 5-3 Residue Volume in the Control Adapter

5.2.3 Time Sequence for “N2 by 2N” Matrix Drive

By Fluidic Matrix Drive, actuators are actuated using the column and row matching method. Therefore, the control time sequence for the row valves and column valves is critical. In addition, carefully designed time sequence also helps to reduce the pulsation caused by the residue volume in the control adapter. This can be achieved by following method: before the control adapter closes, keep the pressure in the input channel lower than that in the output channel by linking the column control valve to the low pressure tank; before the control adapter opens, keep the pressure in the input channel higher than that in the output channel by linking the column control valve to the high pressure source. By that method, part of the residue volume will go through the input channel and relief the pulsation.

As shown in Figure 5-4, for example, when an actuator extends to the required position, the column control valve will be closed a little later after pressure selection valve selects the low pressure tank and the row control valve closes (i.e. the control

adapter closes). By that means, some of the residue volume can be squeezed into the input channel, which will relief the pulsation problem.

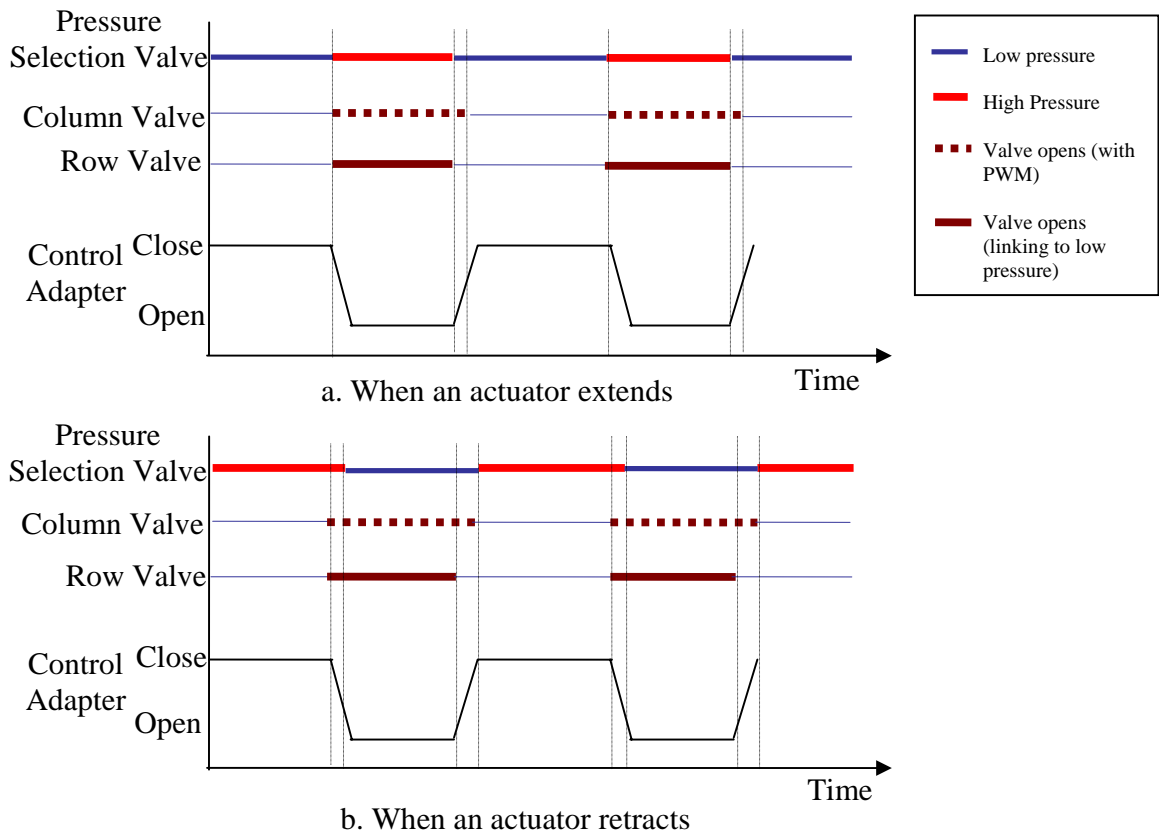


Figure 5-4 Timing Table for Row, Column and Pressure Selection Valves

5.2.4 Displacement Sensor Embedded Actuator Array Assembly

Linear hydraulic cylinder type actuators are used in this research, because cylinders can convert hydraulic power into linear motion/force and their structure is simple.

Categorized by the acting type, there are two types of hydraulic cylinders: single acting and double acting. As shown in Figure 5-5a), double acting cylinder using the differential of two pressures (applied to its two ports) to work. Single acting cylinder (Figure 5-5b) can be extended using pressure and returned by spring of a constant return

pressure. A double acting cylinder needs at least two 3 port / 2 way on/off valves, therefore is not considered in this research. Spring return single acting cylinders use springs to return, which will increase the complexity of the actuator.

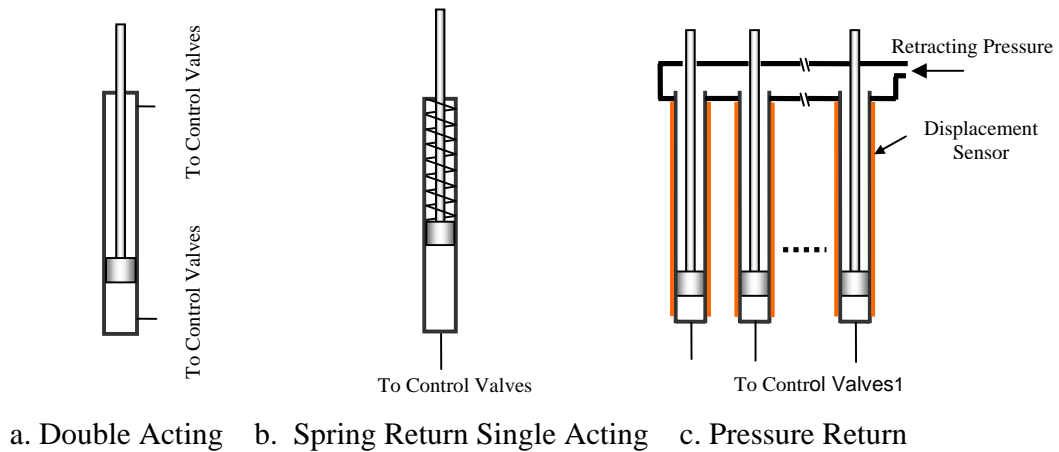


Figure 5-5 Structures of Actuator Arrays for Digital Clay

Therefore, pressure return single acting cylinders are adopted. A solution for the arrangement of actuators is provided, as shown in figure 5-5c. The upper ports of the actuators are connected to a constant pressure source, and their lower ports are connected to corresponding control valves. To extend the actuator, one can simply apply a pressure higher than the return pressure at the lower port of the actuator, and vice versa. The advantage of this configuration is the simplicity. The return mechanism can be easily realized even the size of the array is very large. The potential problem may be the limited return force compared to the double acting cylinders. However due to the working principle for Digital Clay to provide the haptic display, mentioned problem will not affect the performance of Digital Clay.

5.2.5 Pressure Sensor Array Mounting Base

Micro miniature pressure sensors are commonly built using MEMS Technology. An example of such pressure sensor can be found in the PS40 serial pressure sensor provided by Honeywell. These pressure sensors have the signal conditioner and amplifier built on a small die along with the pressure gauge. Though the small scale pressure sensor array can be built on a single wafer, it is practically impossible to build a large scale pressure sensor array on a single wafer due to the cost and the size limitation of the wafer. However, mounting large number of micro miniature pressure sensors onto a relatively large size mounting base is possible as discussed below.

Currently, two cost effective mounting solutions are investigated. In both solutions, for each pressure sensor, the mounting base provides a main through channel for the working fluid to passing through and a branch channel linking the main channel to the input port of the pressure sensor.

As shown in Figure 5-6, solution 1 is made of stamped, machined, or cast metal plates. The two plates have channels shown in Figure 5-6. They are bonded to each other by means such as solder or epoxy. The pressure sensor then is bonded onto the top plate using low temperature solder. The leads are connected to the PCB on the top of the top metal plate.

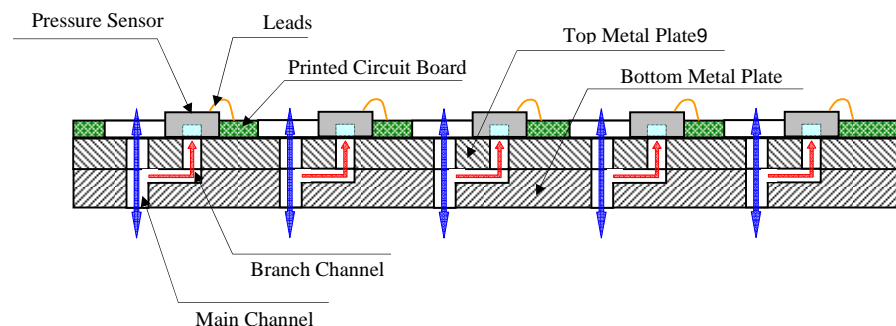


Figure 5-6 Mounting Base per Solution 1

Another alternative solution is to build the mounting base using stereolithography technology as shown in Figure 5-7. The pressure sensor is bonded to the mounting base by epoxy. The leads are connected to the PCB on the top of the mounting base. At the current stage, solution 2 is adopted since it is easy to realize due to the small quantity production. An assembled 5 x 5 pressure sensor array is also shown in figure 5-7.

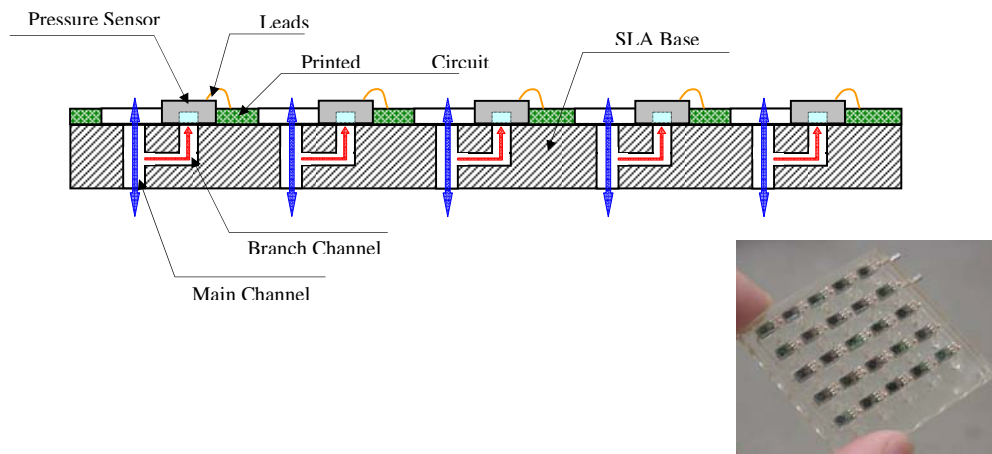


Figure 5-7 Mounting Base per Solution 2

5.3 ELECTRONIC SYSTEM FOR CELL ARRAY

Electronic system drives the on-off valves, multiplexes and conditions the signals from the sensor arrays, and provides other necessary interfaces to controllers and host PC. The functional block diagram of the electronic system is shown in Figure 5-8.

Due to the large number of sensors (and the large number measurements), multiplexing is necessary before the sensor outputs being sent to A/D converters of controllers. The pressure sensor signal has an undesired noise frequency around 200 Hz. But since the low pass filter can be made miniaturize, so a low pass filter is provided for

each pressure sensor. The filtered signals have a low frequency (< 10 Hz), so it can be simply multiplexed using digital switches.

The displacement sensors for Digital Clay have outputs similar as LVDTs', the same signal conditioners as LVDTs' are applied. Due to the size and cost of those signal conditioners, displacement feedback signals are first multiplexed to fewer channels before being sent to signal conditioners. Since the unconditioned signal from the displacement sensors are AC signals with a frequency around 10 KHz, design of the multiplexer with interference rejection is critical. Note: Though 10 KHz is not high, thousands these signals do provides a big interference as will be discussed in the following sections.

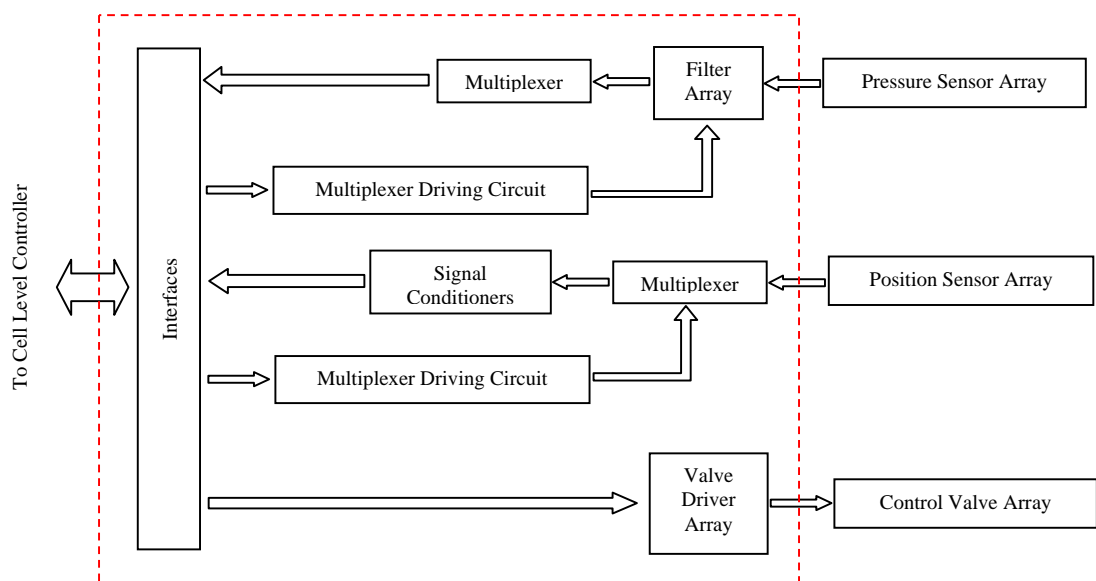


Figure 5-8 Functional Block Diagram of the Electronic System

The on-off valve driver turns the command signal from controller into a big current signal with a certain form that is used to drive the on-off valve to achieve faster response. The structure of the driver depends on the type of the on-off valve used. In this research,

micro miniature solenoid valve is chosen as the control valve. Therefore, a kind of “spike and hold” driver is adopted.

Details of these subsystems are given in the following sections.

5.3.1 Pressure Sensor Signal Filtering and Multiplexing

The pressure signal contains a big noise generated by 1) The sudden on / off of the column control solenoid valve and 2) The on / off of the control adapter (controlled by the row control valve)

To get the desired signal, a low-pass filter is provided for each pressure sensor. The signal multiplexing and filtering scheme is shown in figure 5-9. It is necessary to point out that large number of high frequency signals can cause interference between sensor outputs during multiplexing (as can be seen from the analysis on the displacement signal multiplexing in the following sections). But signals after the filters (representing the external force) contain only low frequencies. Therefore, the signal is filtered first and then sent to the multiplexer as shown in Figure 5-9.

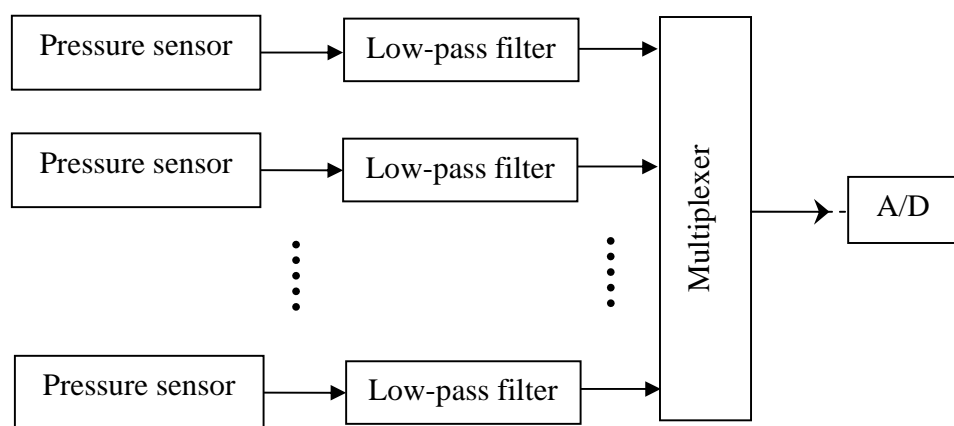


Figure 5-9 Pressure Sensor Signal Filtering and Multiplexing

The multiplexer for pressure signals is simply composed of the matrix array of digital switches as shown in Figure 5-10. By the column and row matching method, feedback of certain pressure sensor can be read by the A/D converter.

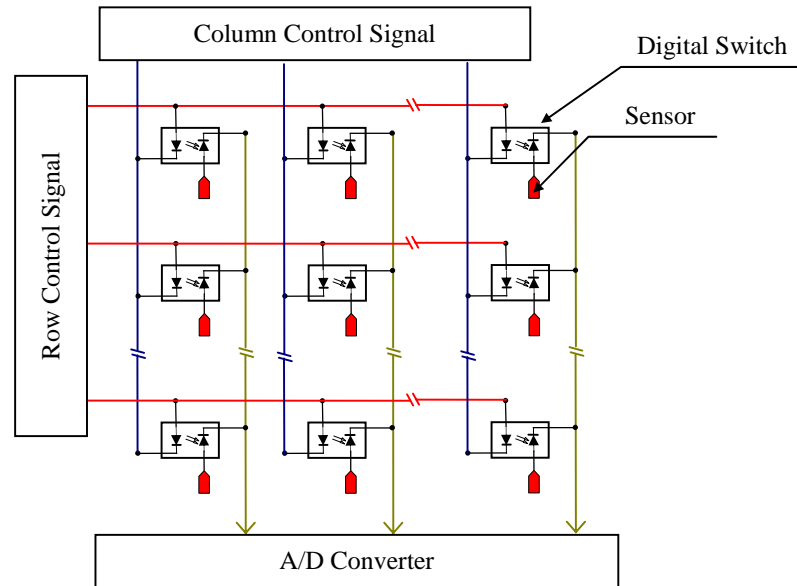


Figure 5-10 Multiplexing Scheme for the Pressure Sensor Array

5.3.2 Displacement Sensor Signal Conditioning and Multiplexing

Non-contacting resistive displacement sensor has been discussed in chapter 3. The displacement of the moving piston can be detected by comparing the amplitudes of the AC signal and the AC excitation voltage. The principle of the signal conditioner used to turn the AC signal into a DC voltage proportional to the displacement is shown in Figure 5-11.

Similar to the pressure sensor array, thousands and even millions of displacement sensors will be used to get the position feedback of each actuator. Due to the large quantity, it is costly to provide a signal conditioner for each sensor. Furthermore, the size

of the signal conditioner is relatively big, which also prevents the application of one conditioner for each other. Therefore, multiplexing technology is investigated to reduce the number of the signal conditioners. As shown in figure 5-12, a multiplexer solution is provided as several sensors sharing one signal conditioner using digital switches. Each time only one sensor is connected to the signal conditioner. The displacement sensors used in this research are based on capacitance coupled alternating voltage. The frequency of the alternating voltage is around 10 KHz. Therefore, keeping each sensor's output unaffected by others is critical for this solution.

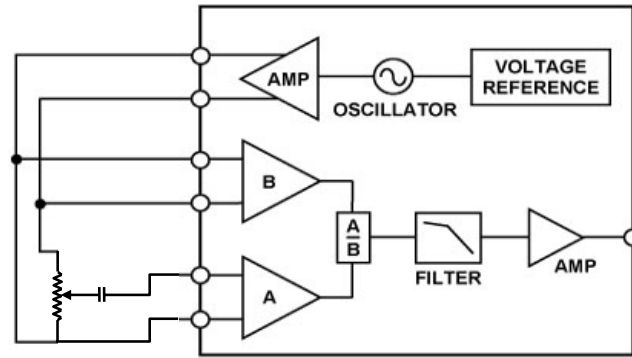


Figure 5-11 Functional Block Diagram of Signal Conditioner for Displacement Sensor

Simple Multiplexing Scheme

A simple multiplexing scheme is provided as shown in figure 5-12. The resistive film provides a resistor. For the i^{th} sensor, the capacitance between the graphite piston and the resistive film is simplified as a capacitor C_i . Other capacitances caused by shielding are lumped to a capacitor C_{gi} . The parasitic capacitance of the digital switch is represented by a capacitor C_s . R is the resistor used to suppress the noise.

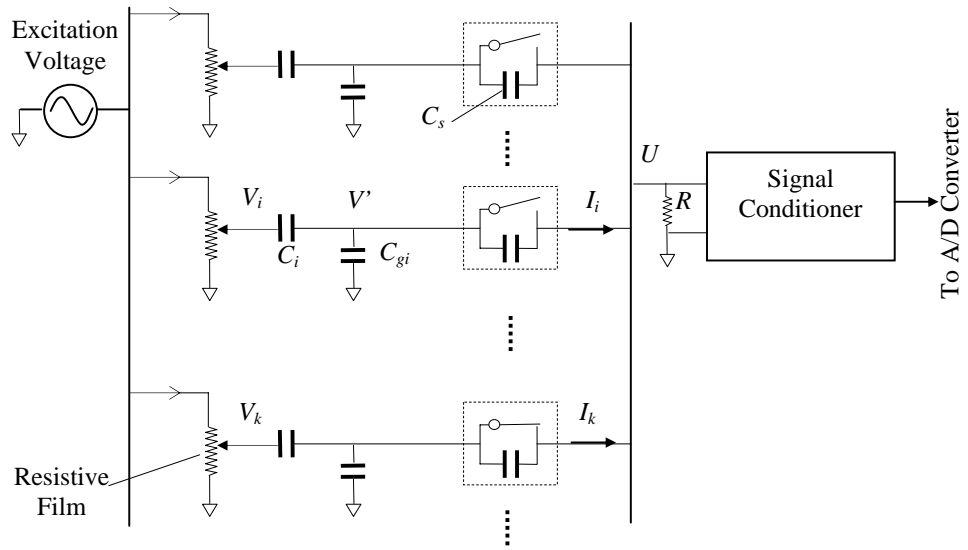


Figure 5-12 Simple Multiplexing Scheme

Assume the k^{th} switch is activated and all others are deactivated. Then the current I_i from any inactive switches to the signal conditioner can be calculated as:

$$\begin{cases} (V_i - V')C_i s = V' C_{gi} s + I_i \\ I_i = (V' - U)C_s s \end{cases} \quad \text{..... (5-1)}$$

Equation (5-1) yields:

$$I_i = \frac{C_s s}{C_i + C_{gi} + C_s} [C_i V_i - (C_i + C_{gi})U] \quad \text{..... (5-2)}$$

The current I_k from the active switch to the signal conditioner can be calculated as:

$$I_k = (C_k V_k - (C_k + C_{gk})U)s \quad \text{..... (5-3)}$$

Where, U is the voltage presented to the signal conditioner.

Since $U/R = \sum I_i + I_k$, we have:

$$\begin{aligned}
C_k V_k + \sum \left(\frac{C_s C_i}{C_i + C g_i + C_s} \cdot V_i \right) \\
= \left[\frac{1}{R s} + \sum \frac{C_s (C_i + C g_i)}{C_i + C g_i + C_s} + (C_k + C g_k) \right] \cdot U
\end{aligned}
\quad \dots\dots (5-4)$$

Note that, in above summations, $i = 1, 2, 3, \dots, n$, $i \neq k$. (n is the total amount of sensors)

In practical, $C_i = C_k = C_1$ and $C g_i = C g_k = C_2$. Furthermore, phase angles of V_i and V_k are equal. (i.e. $V_i = \|V_i\| \sin(\omega t)$; $V_k = \|V_k\| \sin(\omega t)$). Therefore,

$$\begin{aligned}
(\|V_k\| + \frac{C_s}{C_1 + C_2 + C_s} \sum \|V_i\|) \sin(\omega t) \\
= \left[-\frac{1}{C_1 R \omega} \cdot j + \frac{(C_1 + C_2 + n C_s)(C_1 + C_2)}{C_1 (C_1 + C_2 + C_s)} \right] \cdot \|U\| \sin(\omega t + \phi)
\end{aligned}
\quad \dots\dots (5-5)$$

Let:

$$\begin{aligned}
a &= \frac{C_s}{C_1 + C_2 + C_s}; \quad b = -\frac{1}{C_1 R \omega}; \\
d &= \frac{(C_1 + C_2 + n C_s)(C_1 + C_2)}{C_1 (C_1 + C_2 + C_s)}
\end{aligned}$$

Equation (5-5) yields:

$$\|U\| = \frac{\|V_k\| + a \cdot \sum \|V_i\|}{\sqrt{b^2 + d^2}}
\quad \dots\dots (5-6)$$

MATLAB simulates the result as given in figure 5-13. The parameters used in the simulation according the real system are: 1) number of sensors: 10, 100 and 1000, 2) $C_1 = 18\text{pf}$, 3) $C_2 = 30\text{pf}$, 4) $C_s = 0.3\text{ pf}$ and 5) $R = 1\text{M}\Omega$. The simulation shows a comparison of amplitudes of the desired AC signals with $C_s=0.3\text{ pf}$ (solid lines) and $C_s = 0\text{ pf}$ (i.e. ideal switch with no parasitic capacitance, the dashed line). Note that the

simulation describes the worst situation that is the sensor output of active channel is from 0 ~ 10 volt, while all the inactive channels' outputs are at the maximum value: 10 volt.

From figure 2-6, big offsets are found between the measured values (affected by the crosstalk) and the ideal value. Though the parasitic capacitance for each switch is only 0.3 pf, there are large amount of such capacitances linking together in parallel which form a very big capacitance. This big capacitance couples the not desired signal to the signal conditioner.

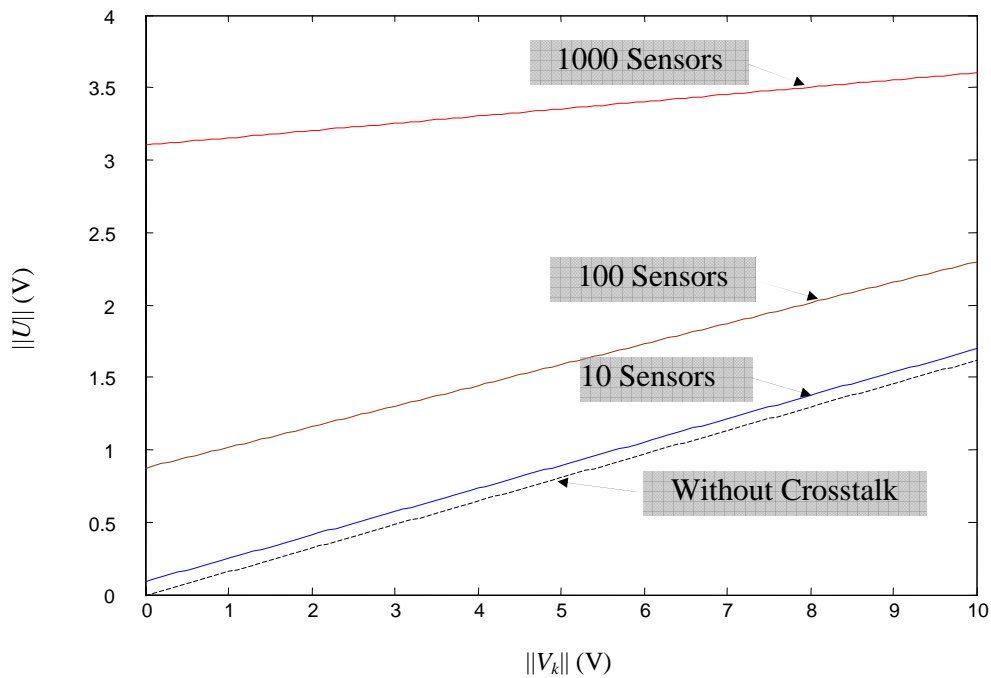


Figure 5-13 Matlab Simulation Result

Solutions for the Displacement Sensor Multiplexing

Several solutions for solving the crosstalk problem are investigated. A solution and its schematic circuit are shown in figure 5-14. The idea is to ground the sensor signal before the digital switch using a grounding resistor R_g .

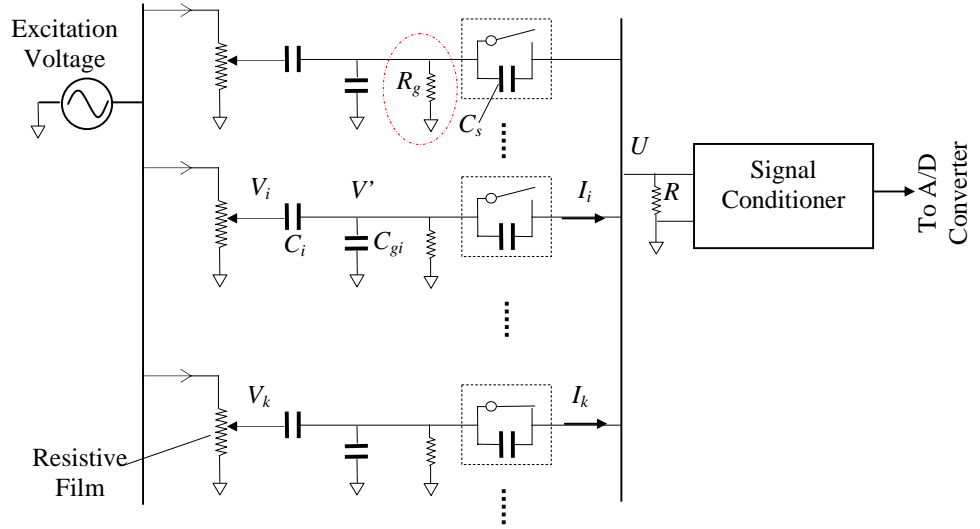


Figure 5-14 Multiplexing Scheme Solution 1

Assume the k^{th} switch is activated and all others are deactivated. The current from any inactive switches (I_i) and from the active switch (I_k) to the signal conditioner can be calculated as:

$$\begin{cases} (V_i - V') \cdot C_i s - \frac{V'}{R_g} = I_i \\ \frac{V'}{C g_i R_g s + 1} \\ (V' - U) \cdot C_s s = I_i \end{cases} \quad \text{..... (5-7)}$$

Equation set (5-7) gives:

$$\begin{cases} I_i = \frac{R_g C_i C_s s^2 \cdot V_i - (R_g C_i s + R_g C g_i s + 1) C_s s \cdot U}{R_g (C_i + C g_i + C_s) s + 1} \\ I_k = C_k V_k s - (C_k s + C g_k s + \frac{1}{R_g}) \cdot U \end{cases} \quad \text{..... (5-8)}$$

Since $U/R = \sum I_i + I_k$, and $C_i = C_k = C_1$ and $C g_i = C g_k = C_2$.

$$\begin{aligned} U/R = & \frac{R_g C_1 C_s s^2 \cdot \sum V_i - (n-1)(R_g C_1 s + R_g C_2 s + 1)C_s s \cdot U}{R_g (C_1 + C_2 + C_s)s + 1} \\ & + C_1 V_k s - (C_1 s + C_2 s + \frac{1}{R_g}) \cdot U \end{aligned} \quad \dots\dots (5-9)$$

Let $V_i = \|V_i\| \sin(\omega t)$; $V_k = \|V_k\| \sin(\omega t)$; $U = \|U\| \sin(\omega t + \phi)$, we have:

$$\begin{aligned} & \{ R_g (C_1 + C_2)(C_1 + C_2 + nC_s) \cdot s^2 \\ & + [(\frac{R_g}{R} + 2)(C_1 + C_2) + (\frac{R_g}{R} + n)C_s] \cdot s \\ & + (\frac{1}{R_g} + \frac{1}{R}) \} \cdot \|U\| \cdot \sin(\omega t + \phi) \end{aligned} \quad \dots\dots (5-10)$$

$$= R_g C_1 [C_s \cdot \sum \|V_i\| + (C_1 + C_2 + C_s) \cdot \|V_k\|] s^2 + C_1 \|V_k\| s \sin(\omega t);$$

Let:

$$\begin{cases} a = R_g (C_1 + C_2)(C_1 + C_2 + nC_s) \\ b = (\frac{R_g}{R} + 2)(C_1 + C_2) + (\frac{R_g}{R} + n)C_s \\ c = \frac{1}{R_g} + \frac{1}{R} \\ d = R_g C_1 (C_s \cdot \sum \|V_i\| + (C_1 + C_2 + C_s) \cdot \|V_k\|) \\ e = C_1 \|V_k\| \end{cases}$$

Since $s = j\omega$, We get:

$$(-a\omega^2 + b\omega \cdot j + c) \|U\| = -d\omega^2 + e\omega \cdot j \quad \dots\dots (5-11)$$

That is:

$$\|U\| = \frac{\sqrt{(e\omega)^2 + (d\omega^2)^2}}{\sqrt{(b\omega)^2 + (c - a\omega^2)^2}} \quad \dots\dots (5-12)$$

MATLAB gives the simulation result as shown in figure 5-15, with all parameters the same as used in the simple multiplexing scheme, and the grounding resistor is 20KΩ.

For the array with 10, 100 sensors, the measured signals overlap the ideal signal (i.e. not affected by the crosstalk). Though for the 1000 sensor array, the result at the small voltage (e.g. $V_k < 2$ V) is not good, but given the fact that the initial working position of sensor can be set at 3 V or more, the problem is easy to solve by sacrificing some of the working range as shown in figure 5-15.

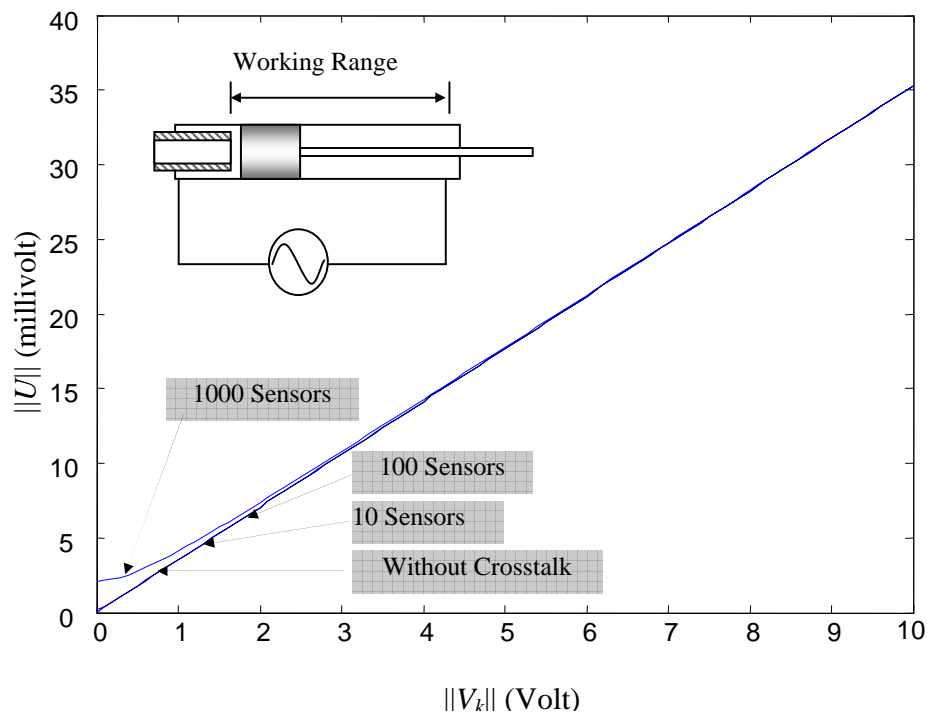


Figure 5-15 Results of the Multiplexer

Other solutions are also investigated. One solution is to numerically compensate the interference by computer. Since the model of the multiplexing system is known, the desired actual signal can be calculated based on all other inactive channels' outputs sensed and stored in the memory by using certain algorithm. However, this method will increase computation load of the computer and if there is any error in the previous feedback, the current data will be inaccurate and the error will accumulate.

Using two digital switches (or a Single Throw Double Position switch) in one channel is another alternative solution as shown in figure 5-16. When a channel is deactivated, one of the switches is shut down, and the other is on to ground the signal from the sensor to the ground before it is coupled to the data bus. The main problem is the cost and complexity inherently in this solution.

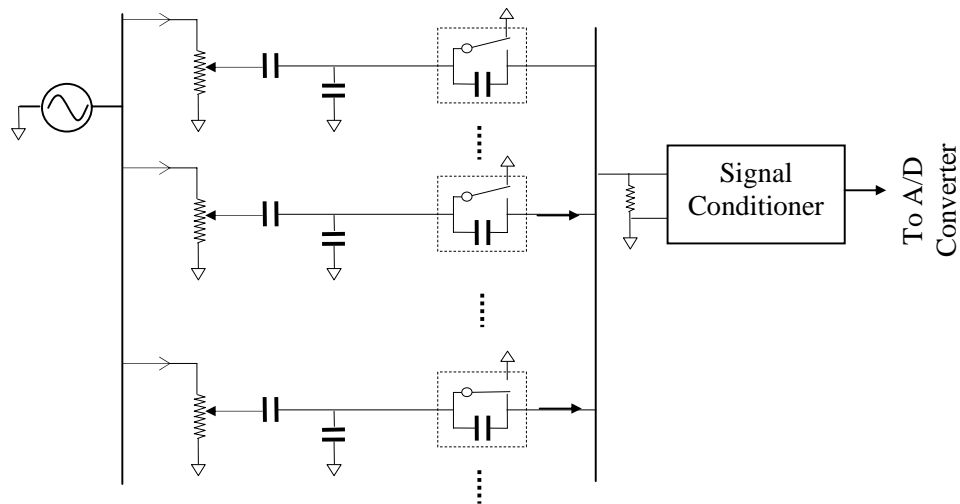


Figure 5-16 Multiplexing using STDP Switch

Therefore, the first solution using a grounding resistor is adopted for multiplexing the displacement sensor array.

5.4 CONCLUSION

In this chapter, details on the implementation of the multi cell array Digital Clay are discussed. To simplify the design, manufacturing and maintenance, which are critical for a large size subsystem array like Digital Clay, mechanical structure of Digital Clay is organized into 5 modular functional blocks. The function of each block is discussed in this chapter. Solutions for the key element of the Fluidic Matrix Drive --- the control adapter are investigated. The coaxial type solution for the control adapter is chosen for

its structural simplicity and its low residual volume. Based on the hardware, the time sequence table is provided to control the Fluidic Matrix Drive. The structure of single acting, constant pressure return actuator array is chosen for Digital Clay. Structural design of the actuator- displacement sensor assembly and the pressure sensor array assembly are discussed in details. The SLA mounting base for pressure sensor array is preferred at the current research stage due to accessibility to the SLA equipment. (Using SLA is preferred for its fast fabrication speed)

The general structure for the electronic system for Digital Clay is discussed. Details on the pressure sensor filtering, pressure sensor multiplexing and position sensor signal conditioning and multiplexing are investigated. Two multiplexer circuits for displacement sensor are theoretically analyzed and the better one is chosen. Simulation shows the feasibility and efficacy of using the chosen solution for multiplexing up to 1000 displacement sensors.

CHAPTER 6

5 X 5 CELL ARRAY PROTOTYPE OF DIGITAL CLAY

In this chapter, designs and approaches are investigated to realize the Digital Clay with a small but scaleable array (the 5x5 cell array prototype). Stereolithography (SLA) technology is first introduced. Based on the research presented in chapter 5, components and subassemblies of the 5x5 cell array prototype are designed and constructed mainly using SLA technology. Designs for the functional blocks of the electronic system of the prototype are also introduced in this chapter. Control for the prototype is presented finally.

6.1 OVERVIEW

To evaluate the research and design for Digital Clay, prototypes are needed. Due to the limited research resources, it is impossible and unnecessary to build a large scale cell array prototype of Digital Clay at the current stage. Therefore a small sized but scalable 5x5 cell array prototype is constructed and presented in this chapter. The research and technologies discussed in previous chapters are applied in building the prototype.

To reduce the time and cost, a rapid prototyping technology is considered known as stereo lithography. Stereo lithography is a technology that allows user to create solid, plastic, three-dimensional objects from CAD drawings in a short amount time. It can greatly reduce the prototyping time for design, manufacturing and assembling, especially for complex components. More importantly, it can fabricate parts with channels built inside, which can not be fabricated using conventional machines. Since the prototype of

Digital Clay does not require high pressure, by choosing the right resin, most components can be built with enough strength using SLA.

The main features and the design objectives of the prototype are described below. To reduce the cost and the complexity caused by the duplicated components (but still keep the scalability), the prototype consists of a 5 x 5 array of actuators in a linear pattern. The grid size of the cell array (center to center) is 5mm determined largely by the 4 mm OD precision glass tubes are used as the actuator cylinder. The cell array is driven by using Fluidic Matrix Drive. Micro miniature solenoid valves are used as the control valves. Non contacting resistive sensors and modified pressure sensors are used to gather the displacement and the chamber pressure of the actuators. Signals are filtered by 5th order low pass filters to get noise-free feedback. “Spike and hold” over-driver for control valves are used to improve the response and performance of the solenoid valves.

The Outline of this chapter is organized as below.

The stereo lithography technology is first briefly described. The mechanical system and the electrical system of the prototype are then introduced separately. The control and the experimental results are provided followed by conclusions.

6.2 STEREOLITHOGRAPHY TECHNOLOGY (SLA)

Stereo lithography is the most widely used rapid prototyping technology. It can create solid, plastic, three-dimensional objects based on designed CAD models in a short amount of time. It provides a fast and easy way to create plastic prototypes and special tools, verify design ideas and concepts, and to mass produce products, etc. Stereo lithography builds plastic parts layer by layer by tracing a laser beam on the surface of a liquid photopolymer. The photopolymer quickly solidifies wherever the laser beam

strikes the surface of the material. After one layer is finished, the part is lowered a small distance into the photopolymer vat and a second layer is traced right on top of the first. The self-adhesive property of the material causes the layers to bond to one another and eventually form a complete, three-dimensional object after many such layers are formed.

Stereo lithography can provide the best accuracy surface finish of the various rapid prototyping technologies. There is a big selection of materials commercially available, which have different material properties mimicking those of several engineering thermoplastics. The technology also well known for the ability to provide large sized objects.

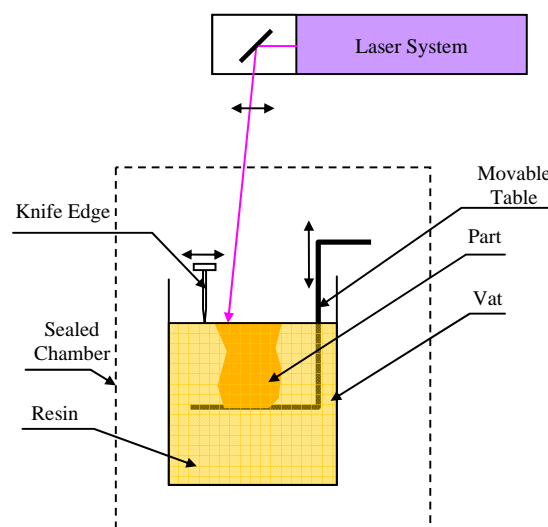


Figure 6-1 The Stereo Lithography Machine

As shown in Figure 6-1, an implementation used by 3D Systems and some foreign manufacturers mainly consists of a moveable table, or elevator, a vat filled with polymer, and a laser system. Initially, the elevator is at a position just below the surface of the polymer resin. The polymer resin will turn from a liquid form into a solid form when certain light applied on it. Usually, an ultraviolet light is used to harden the

photopolymer resin. But resins that work with visible light are also available. The system is sealed to prevent the escape of fumes from the resin. The stereolithography machine used to build the Prototype is shown in Figure 6-1.

The working principle of SLA is briefly described as following:

- Create a 3-D model of the desired parts in a CAD program
- A piece of software slices the CAD model up into thin layers, usually 0.1mm to 0.2 mm per layer.
- The 3-D printer's laser "paints" one of the layers, exposing the liquid plastic in the tank and hardening it. (The photopolymer is sensitive to ultraviolet light, so when the laser touches the photopolymer, the polymer hardens.)
- The elevator drops down into the vat a small distance and the laser paints the next layer
- This process repeats, layer by layer, until the model is complete
- Once the run is complete, rinse the objects with a solvent and then "cure" them in an ultraviolet oven that thoroughly cures the plastic.

Stereo lithography allows user to create almost any 3D shape. The only caveat is the need for structural integrity during the building process. In some cases, it is necessary to add internal bracing to a design so that it does not collapse during the printing or curing phases. The prototypes used in this research, are mainly built using stereolithography technology. By choosing the proper resin (such as SLA 10120), the parts can both achieve mechanical strength and chemical resistive.

6.3 MECHANICAL SYSTEM OF THE 5X5 PROTOTYPE

The 5x5 cell array prototype is a fully functional prototype for verifying and testing previous research and design concepts of the Digital Clay. The mechanical system prototype consists of five functional modules discussed in chapter 4 and built principally using the stereo lithography technology. Each functional module will be introduced from

the bottom one to the top one in the following paragraphs. Miniature o-rings are used to seal the interfaces between these modules. (Usually, the bottom one of the conjunct faces will have bored holes to accommodate the O-rings and the upper one is a flat face)

6.3.1 Row Channel Hydraulic Board and Column Channel Hydraulic Board

As shown in Figure 6-2, row channel hydraulic board is a solid block consisting of docking for the row control valve array, row control channels and the lower portion of control adapter. Shown in Figure 6-3, the column channel hydraulic board consists of docking for the column control valve array, column channels, upper portion of control adapters, and interface for pressure sensor array dock.

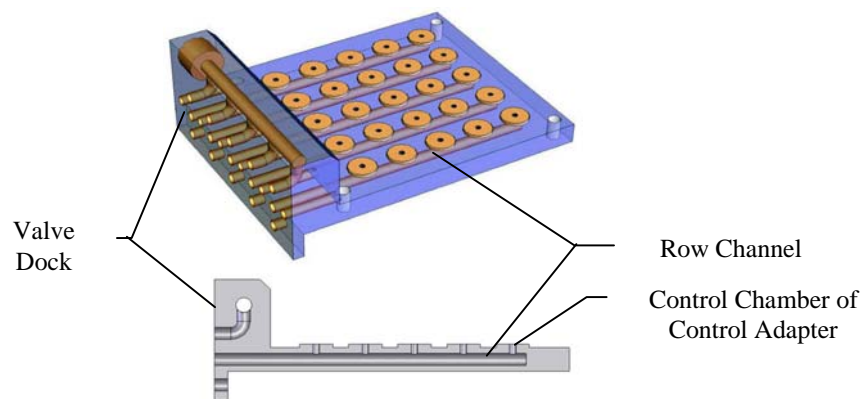


Figure 6-2 Row Channel Hydraulic Board

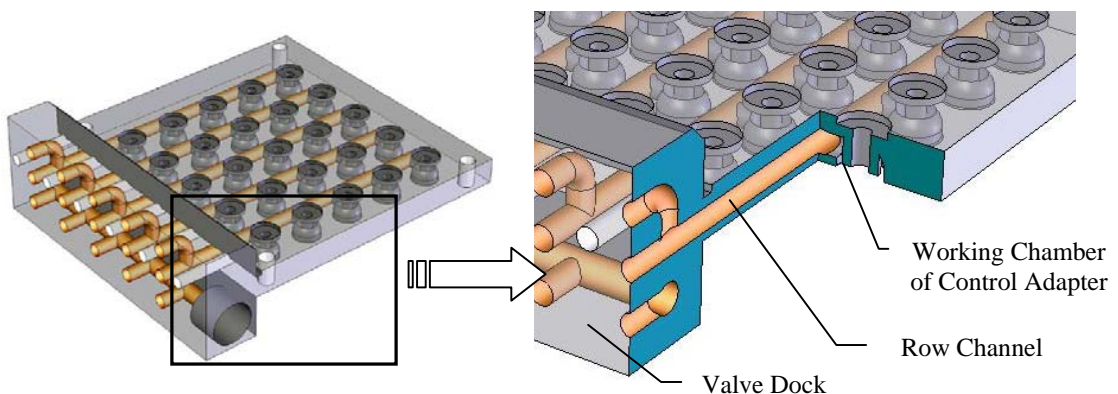


Figure 6-3 Column Channel Hydraulic Board

The assembly of the row-column channel hydraulic boards is shown in figure 6-4.

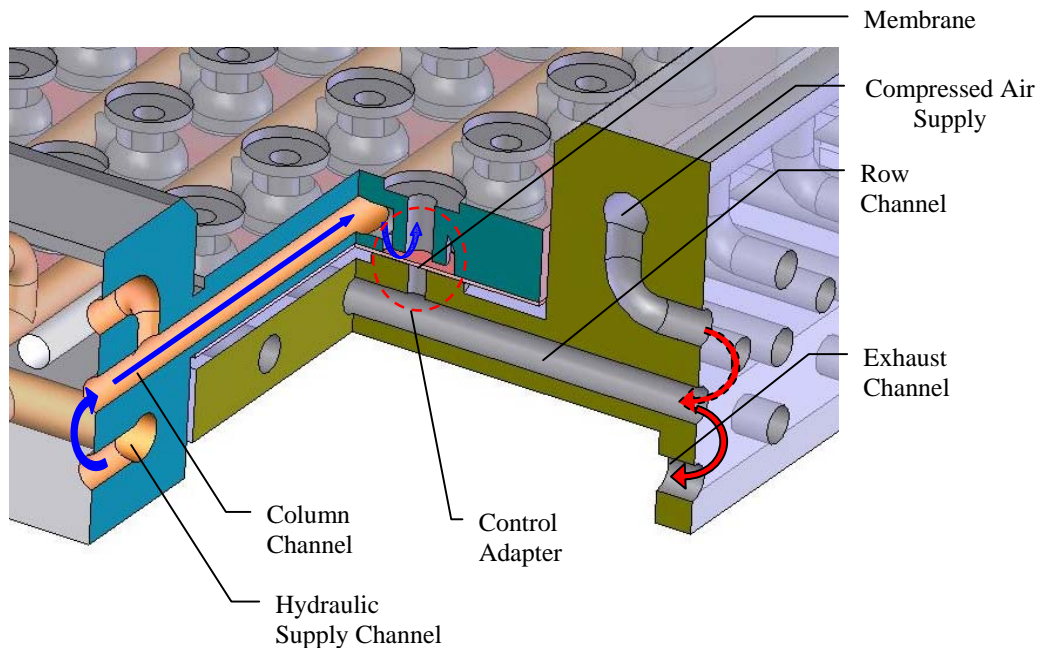


Figure 6-4 Assembly of the Row-Column Channel Hydraulic Boards

Compressed air is used as the control adapter driving fluid. The normally open ports of the row control valves are connected to the compressed air source through the compressed air supply channel. The common ports of the valves are linked to each row of control adapters. When the control valves are not powered, high pressure is present at control chamber of each control adapter through the control valves. Therefore, control adapters are normally closed. When the row control valve is powered, the pressure in the control adapter is released through the normally closed ports of the valve to the exhaust channel. Therefore, the membrane of the control adapter is released and the control adapter is open. The hydraulic fluid from the hydraulic supply channel can pass through the column control valve, the column channel and the control adapter into the actuator, as shown in Figure 6-4. The flow rate of the hydraulic fluid is affected by both the column control valve and the control adapter.

Row channel hydraulic board and column channel hydraulic board are fabricated using the SLA technology and the fabricated parts are shown in Figure 6-5.

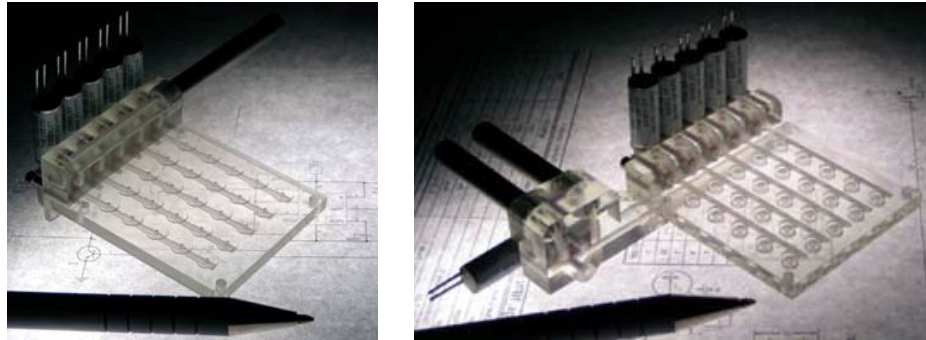


Figure 6-5 Row and Column Channel Hydraulic Boards

6.3.2 Pressure Sensor Array Mounting Base

Pressure sensor can be made very small using MEMS technology. However, due to the cost and time, commercialized pressure sensors are considered for this prototype. After systematically searching the market for available pressure sensors, Honeywell 40pc series pressure sensors were chosen. The die of the sensor has a size around 3 x 5 x 2 mm. Therefore they can be put beside each actuator, since the cell array grid size before the channel condensing block is 7.62 mm. This pressure sensor also has signal conditioning and amplifying circuits built on board, which greatly simplifies the electrical system of the prototype. For this prototype, the SLA board is used as the mounting base for the pressure sensors. To simplify the assembly process, several features are designed. Firstly, we use silver conductive glue instead of solder to connect the leads on the die to the copper pins on the SLA board. This is mainly because the leads on the die have low melting point, therefore low temperature connecting method is required. Secondly, small grooves are designed to make sure when gluing the leads, the conductive glue will not

stick to each other. Since each sensor has one power port and one ground port, there are silver glue filled grooves on the back of the SLA board linking all the power ports together and all the ground ports together. The pressure sensor array mount and the illustration of sensor mounting method are provided as shown in Figure 6-6.

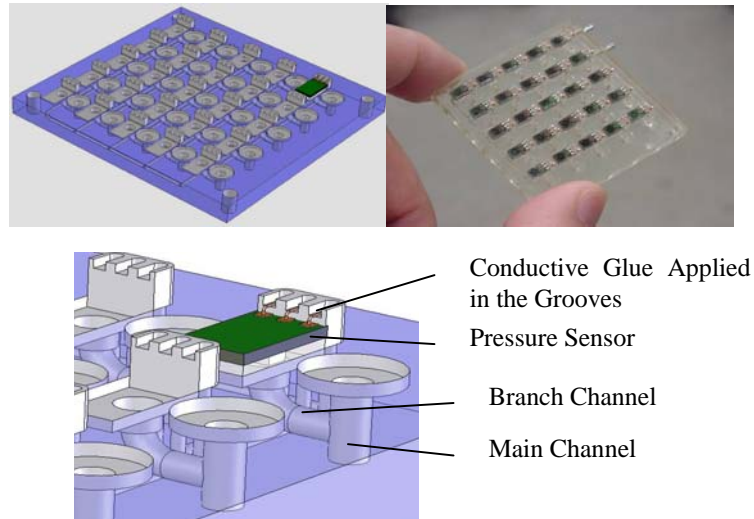


Figure 6-6 Pressure Sensor Array Block

6.3.3 Hydraulic Channel Concentrating Block

Hydraulic channel concentrating block concentrates the hydraulic channels into a small area to achieve a higher spatial resolution. The hydraulic channel concentrating block provides a set of channels that have a big grid distance at bottom side and a small grid distance at top side.

The grid size of the array before the hydraulic channel concentrating block is around 8 mm, which gives space for the control valves, pressure sensors and other components. After the hydraulic channel concentrating block, the grid size is reduced to 5 mm, which provides a better spatial resolution for the working surface. The 3D CAD model and the fabricated component are shown in Figure 5-7.

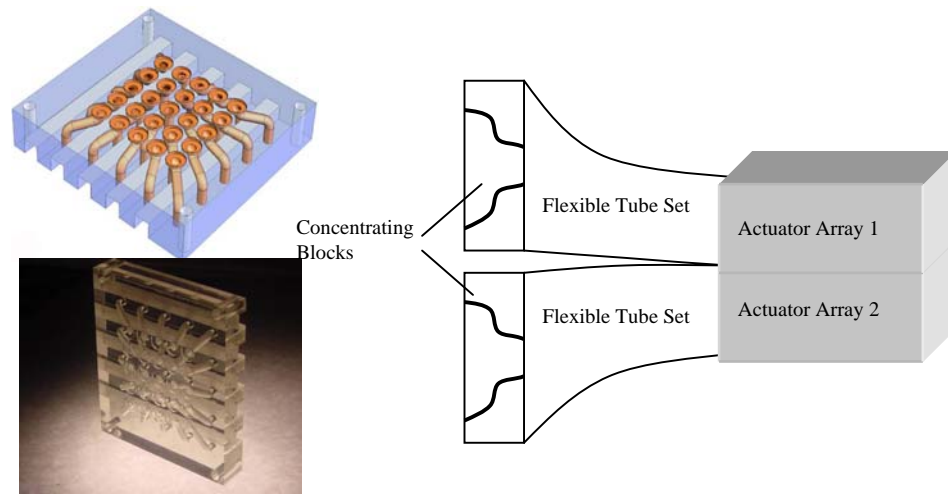


Figure 6-7 Channel Concentrating Block

In order to fulfill the scalability requirement, a set of flexible tubes may be used to link the actuator array and the concentrate block as shown in the lower part of Figure 6-7. The flexible tube set is composed of an array of parallelly arranged plastic tubes. By that means, several actuator arrays can be put together to form a larger actuator array (i.e. a bigger working surface)

6.3.4 Displacement Sensor Embedded Actuator Array Assembly

The actuator used in the prototype has displacement sensor embedded. As shown in Figure 6-8, 25 actuators are arranged in a 5x5 array with the center distance of 5 mm. The bottom ends and the top ends of the glass bores are bonded to the bottom plate and top pressure chamber using conductive epoxy respectively. The alternating excitation voltage is applied to the conductive epoxy as shown in Figure 6-8. Return pressure are provided by the regulated compressed air. A PTFE sealing board seals both the top pressure chamber and the actuator rods. Coiled coaxial cables lead the sensor outputs to the multiplexer. Note that, there are alternative ways to construct the displacement sensor embedded actuator array. For example, the actuator array can also be constructed

using conventional o-ring seal. However from the viewpoint of mass productive, here only the solution assembled using epoxy bonding is depicted. Its 3-D solid CAD model and the physical assembly are shown in Figure 6-8.

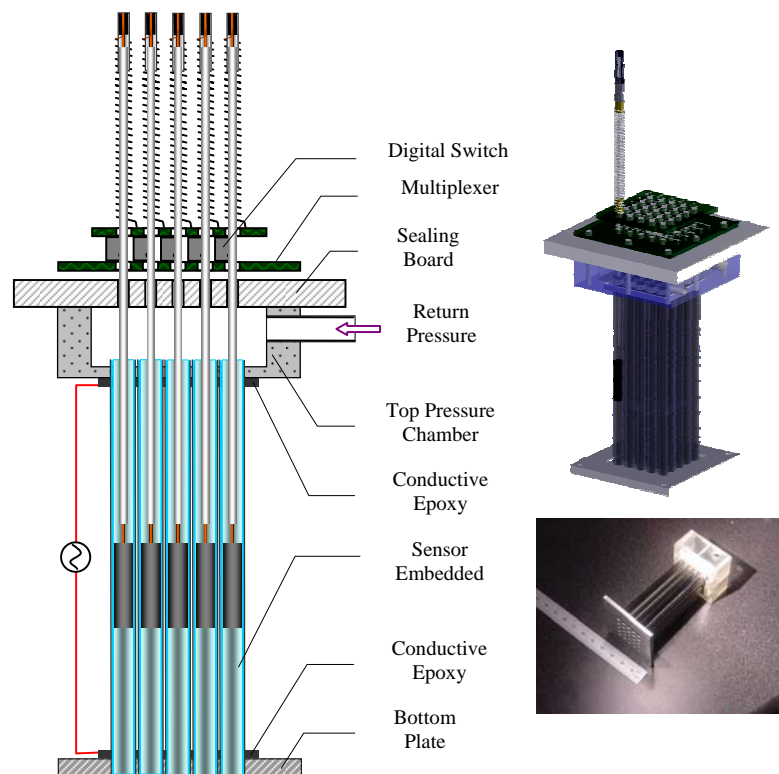


Figure 6-8 Displacement Sensor and Actuator Block

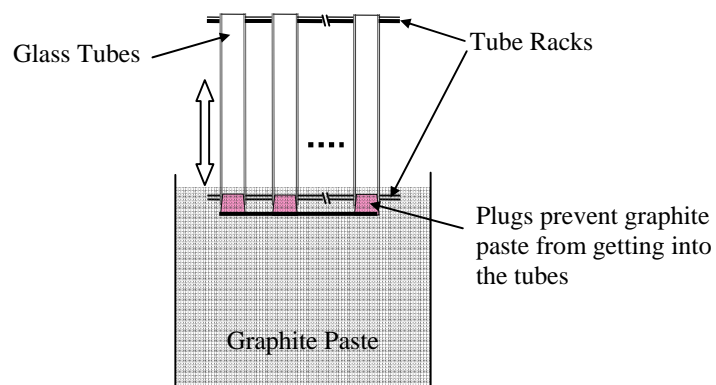


Figure 6-9 Dip-coating Method for Massive Production

For the displacement sensor, its accuracy depends on the uniformity of the film. The film can be deposited using sputtering technology, dipping into a solution such as graphite paste, or e-beam coating. By these methods, thousands of glass tubes can be coated at one time which greatly simplifies the production and reduce the cost. For instance, the coating process using dipping method is shown in figure 6-9. After the glass tubes (cylinder bores) are assembled, the cylinder bore array is immersed into the graphite paste, and raised until only the bottom of the anode is in contact with the paste to allow momentary drainage, and then removed. The total dip-time is 1 to 2 seconds. No matter how many glass tubes are involved, they are coated in one time.

6.4 CONTROL HARDWARE

As mentioned before, electrical system of Digital Clay includes pressure sensor multiplexer and filter array, displacement sensor multiplexer and conditioners, on-off valve over-drivers, and other auxiliary interfaces. The layout of the electrical system for the 5x5 prototype is shown in Figure 6-10.

6.4.1 “Spike and Hold” Over-driver

The control valve is one of the key components for Digital Clay. In this prototype, micro solenoid valves are used. To improve the control valves' time response, the “spike and hold” driving circuit is applied. The basic idea is that applying a high voltage (usually 2-4 times the rated voltage of the valve being driven) to activate the valve for a very short time (usually 0.5-1ms) then applying a low voltage (1/2 the rated voltage of the valve being driven) to hold the valve open until the command signal is off. The relationship of the input signal and output voltage is shown in left part of Figure 6-11, and the schematic circuit is given as shown in right part of Figure 6-11. Experiment

showed that the open time is reduced from 2 ms to 0.6 ms, and the close time is reduced from 2 ms to 1 ms.

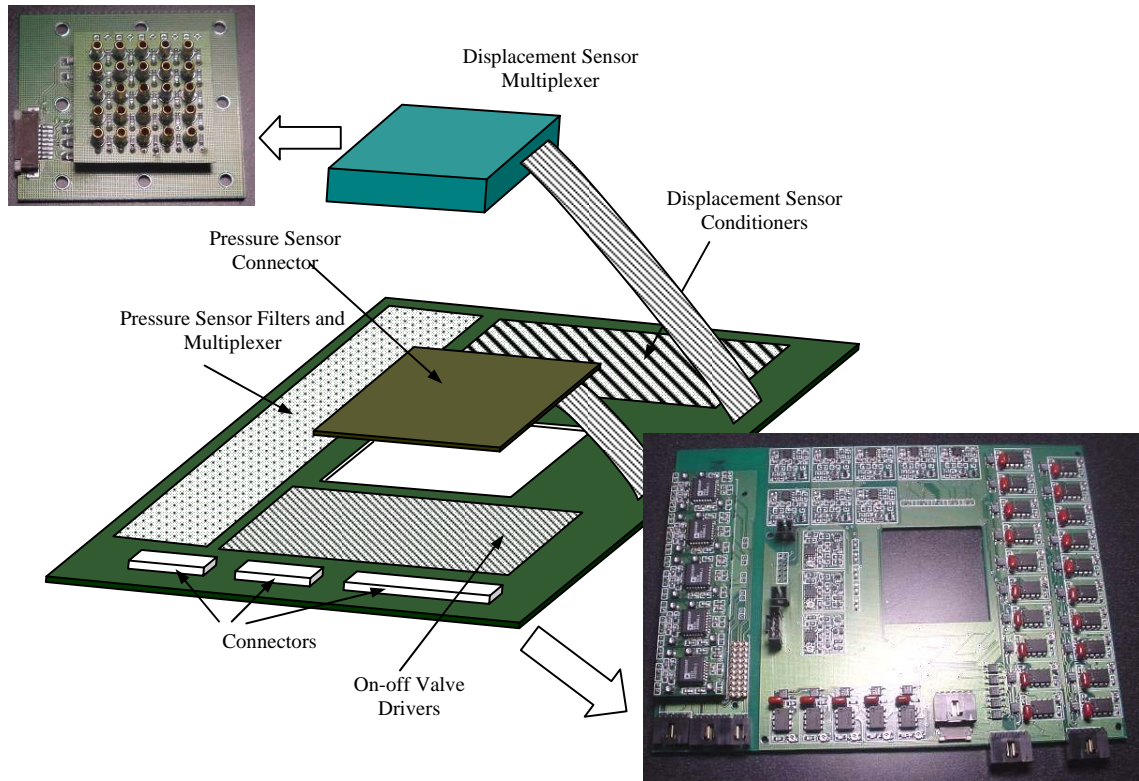


Figure 6-10 Control Hardware for Multi-cell Array

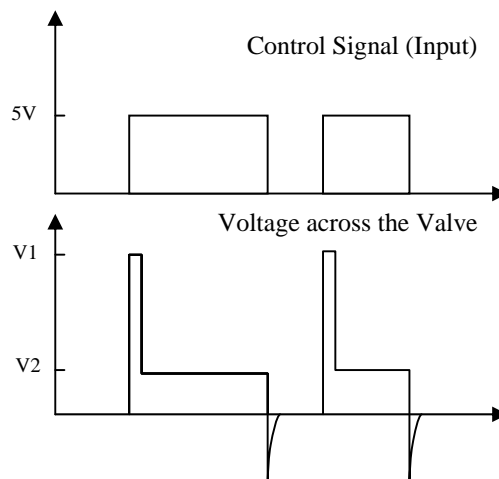


Figure 6-11 Solenoid Valve Over-driver

6.4.2 Displacement Sensor Signal Conditioner

LVDT signal conditioner is used in this application as the signal conditioner for the displacement sensor. The main IC used here is the AD698 provided by Analog Devices. It is a complete, monolithic Linear Variable Differential Transformer (LVDT) signal conditioning subsystem. It is used in conjunction with the displacement sensor to convert mechanical position to a unipolar dc voltage with a high degree of accuracy and repeatability. All circuit functions are included on the chip. With the addition of a few external passive components to set frequency and gain, the AD698 converts the raw displacement sensor output to a scaled dc signal.

6.4.3 Displacement Sensor Multiplexer

As discussed before, for the displacement sensor array, raw signals from the sensor are firstly multiplexed and then sent the signal conditioners. In this 5x5 prototype, five displacement sensors in the same row share one signal conditioner. The schematic circuit is shown in Figure 6-12.

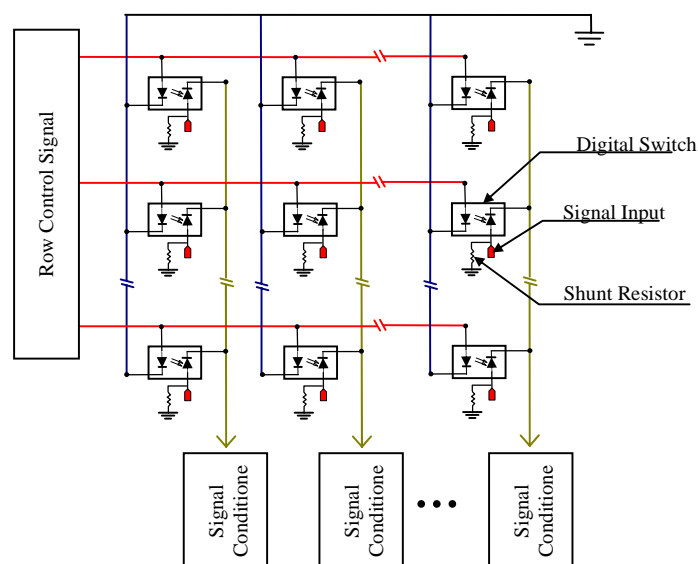


Figure 6-12 Schematic Circuit for Multiplexer

6.4.4 Low-pass Filter for the Pressure Signal

The filter used in this prototype is the MAX280, 5th order, zero DC offset, Butterworth, low pass filter. This chip is available in the PDIP-8 package. It is highly integrated, and only 4 extra components are needed. The calculated values of the components are marked on the schematic circuit as shown in Figure 6-13. An important reason for using this chip is the small size of the die (2.4 x 3 mm). The small size of the die makes it possible to embed a filter nearby each pressure sensor.

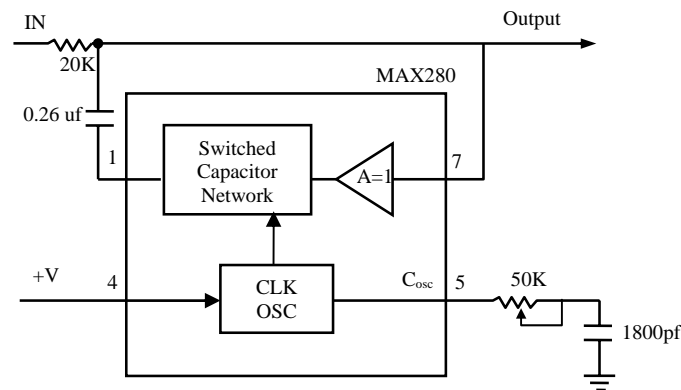


Figure 6-13 Functional Block Diagram for the Low-pass Filter

6.4.5 Pressure Sensor Multiplexer

Pressure sensors used in this research are already amplified and temperature compensated. The problem of the pressure feedback is that it contains the transients generated by both the surface refreshing action and the PWM on-off valve control method. Therefore, 5th order low pass filters are used to smooth the pressure signals. Since the signals after filters are DC signals, and the digital switches are of ultra-high speed, all filtered signals can be multiplexed to a single output channel and acquired by the controller in a small amount of time.

The circuit of the multiplexer is provided as shown in Figure 6-14.

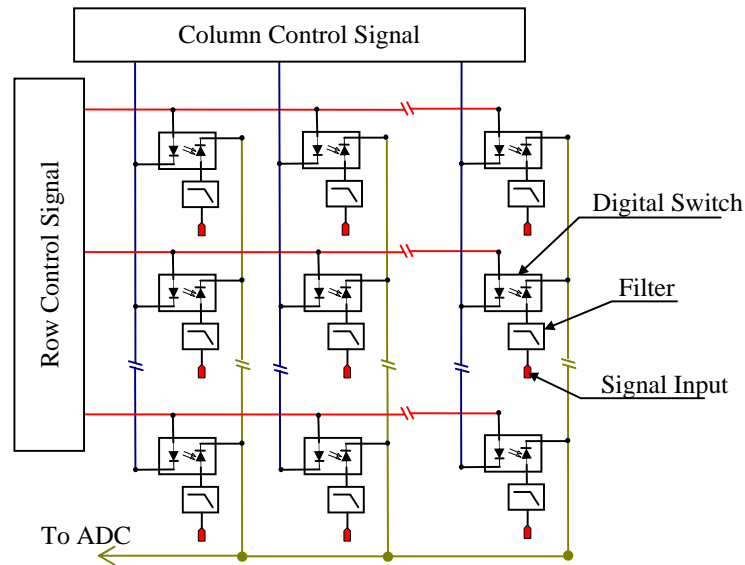


Figure 6-14 Pressure Sensor Array Multiplexing Circuit

6.4.6 Reducing Control Signals for Multiplexers

For an $N \times N$ pressure sensor array, $2N$ switch control signals are needed to multiplex all sensor outputs, since only one A/D channel is provided in this prototype. An $N \times N$ displacement sensor array needs N switch control signals to multiplex all sensor signals, since N signal conditioners and N A/D channels are provided in this prototype. Therefore, it needs $3N$ switch control signals. (i.e. 15 digital output channels, in this application)

To reduce the control resource, a solution is brought forward. As shown in Figure 6-15, using N switch control signals to control the rows of both pressure sensor multiplexer and displacement sensor multiplexer, while using another N switch control signals to control the columns of pressure sensor array. By this method, the total control signals are reduced to $2N$. (i.e. 10 digital output channels)

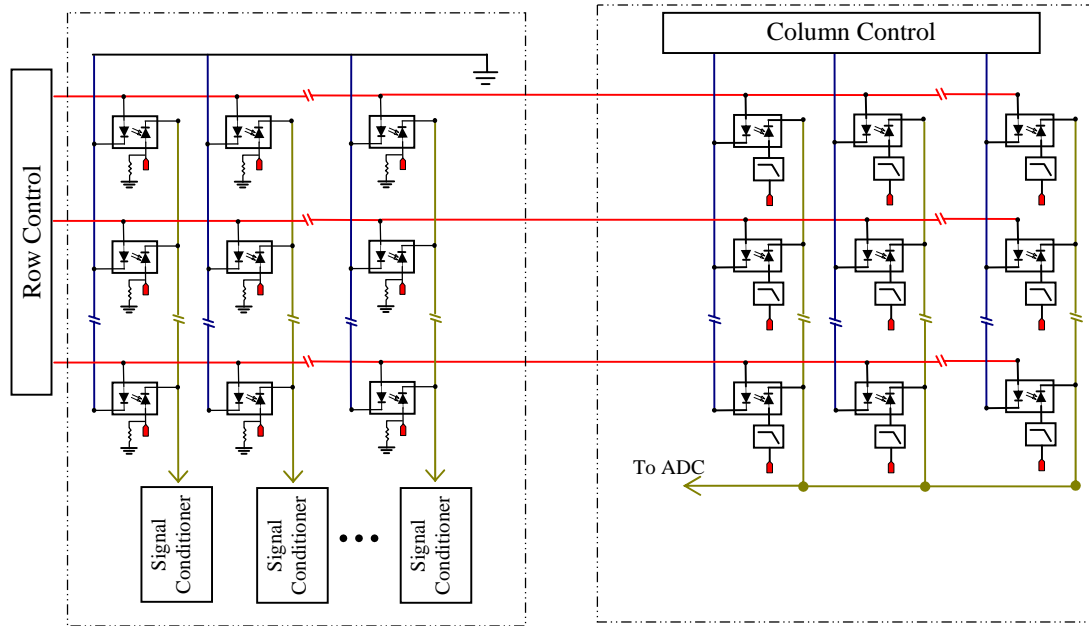


Figure 6-15 Schematic Circuit for Sharing Control Signals

6.5 TEST OBJECTIVES, CONTROL STRUCTURE AND TEST RESULTS

The 5 x 5 cell array Digital Clay prototype is built to test the efficacy of structural design and the control methods presented in this work. Therefore, all the hardware designs and fabrication processes for the 5 x 5 prototype are guided by the design and manufacturing solutions presented in previous chapters. Due to the time limitation, the test objectives and results are still preliminary. Further test on the control algorithm will be carried out in the near future.

The success of the structural design can be proved by the functional success of:

1. Every functional module can be designed and fabricated using the presented manufacturing solution;
2. The prototype can be successfully assembled;
3. Every cell works;

4. The proposed Fluidic Matrix Drive is functional. (i.e. each cell can be addressed and controlled to move independently);

The success of the control can be proved by:

1. The control hardware is successfully designed, assembled and tested. This includes:
 - a. Peripheral electronic modules are functional (i.e. the valve drivers, signal conditioners, filters, etc.)
 - b. The multiplexers are functional;
 - c. Hardware connections between the control hardware and the host PC are functional;
 - d. Displacement sensors and pressure sensors are functional.
2. The proposed control algorithm is functional. This includes:
 - a. Every actuator can be controlled to reach the desired position;
 - b. A set of actuators can work together to provide surface;
 - c. User contacts can be located based on the pressure measurement.

Obviously, some of the objectives are dependant to each other. For instance, every cell can be controlled to reach the desired position implies that the structural design is successful and that part of the electronics is working. Therefore, two experiments are designed and performed: surface generation and speed control on one of the cells. Details of these two experiments are described below.

6.5.1 5x5 Cell Array Prototype

The assembled 5x5 cell array prototype (mechanical part) is shown in figure 6-16. Every functional module is denoted.

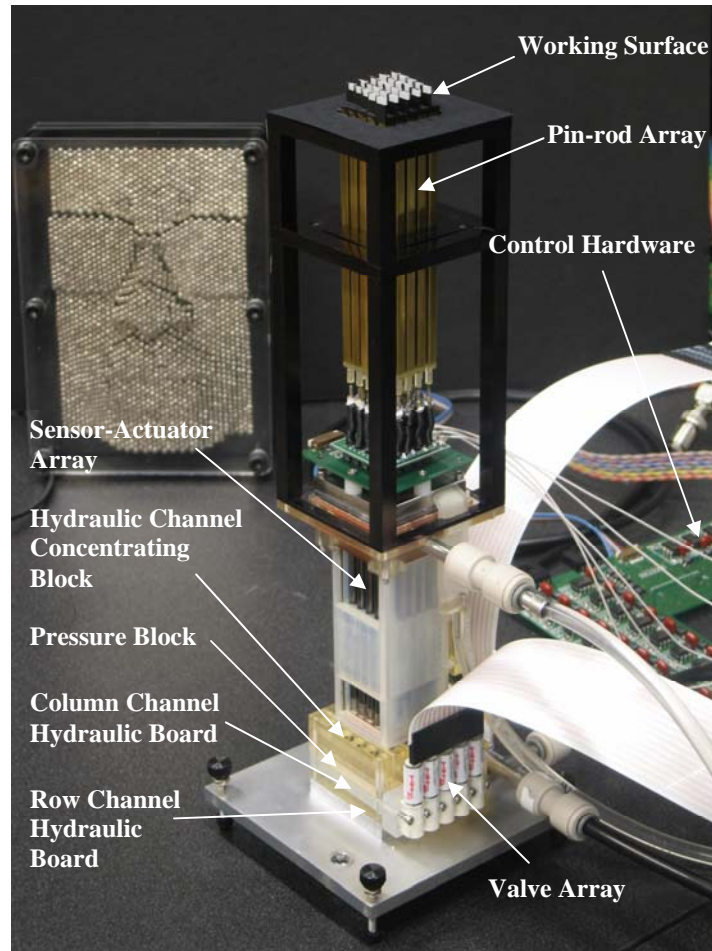


Figure 6-16 5x5 Cell Array Prototype

6.5.2 Surface Generation Testing

The experiment of surface generation is to generate a tilted planar surface by controlling the displacement of every cell based on the displacement feedback. The surface refresh method used here is the one-time refresh method presented in chapter 4.3.3. The cell array is commanded to realize a surface represented by the following matrix and the testing result is shown in figure 6-17.

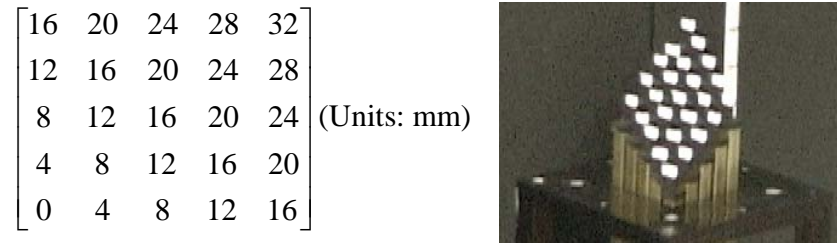


Figure 6-17 Result of the Surface Generation

Machine vision technology is applied to verify the results. To get the tip position of each cell, a retro-reflective material is mounted on each tip (the white piece in figure 6-17). The camera is placed in the front of the prototype. The processed image is shown in figure 6-18.

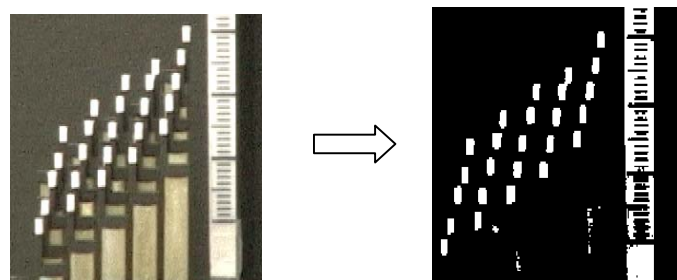


Figure 6-18 Displacement Verification using Machine Vision

Matlab calculates the displacement of each cell and the results is shown as follow.

0	4.3	8.2	12.1	16.5
4.3	8.7	11.7	17.1	19.5
7.8	12.1	16.0	20.9	24.8
11.7	16.5	20.9	23.8	28.7
15.1	20.4	24.3	27.7	31.2

From above results, we can find that the error is less than 1.5 mm, which is not very perceptible by human eye. In addition, the error also comes from the accuracy of the machine vision process. This experiment preliminarily verified the success of the design and construction of the mechanical structure, the displacement sensor, the multiplexer, the valve controller and the one-time surface generation method.

6.5.3 Speed Control on a Single Cell

This experiment verified the feasibility of applying the PWM speed control method on the Fluidic Matrix Drive. In the experiment, one cell is commanded to track the following sinusoidal curve by using the PWM speed control: $y = 4 * \sin(0.244 * t)$.

Machine vision is used to verify the result as shown in figure 6-19.

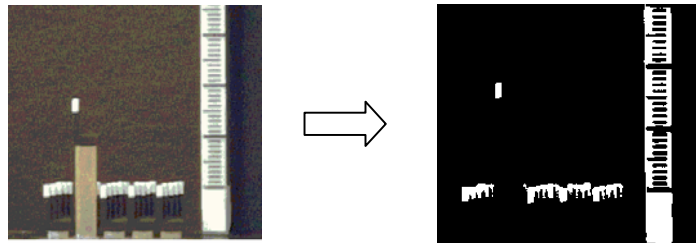


Figure 6-19 Displacement Verification for Speed Control using Machine Vision

The control efficacy is calculated using Matlab. The result is shown in figure 6-20.

(“o” represents the measured data, dashed curve is the reference sine curve)

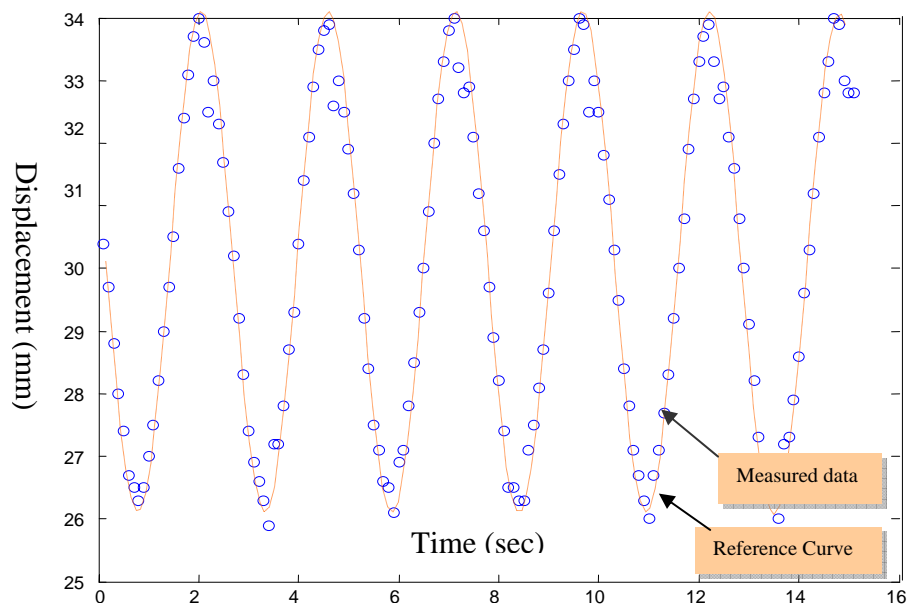


Figure 6-20 Testing Result for Single Cell Speed Control

6.5.4 Pressure Sensor Testing

The test on the pressure sensor is pretty simple, but the result is not very easy to show in the form of a figure or plot. Therefore, following test is designed to test the functionality of the pressure sensor array. As shown in figure 6-21, a weight is put on the working surface (which is controlled to be flat and horizontal) through a triangular hard board. The feedback from the pressure sensor array is shown in a matrix form as following: (Note that the full range of the value is 65535)

$$\begin{bmatrix} -113 & 125 & -124 & 20315 & 350 \\ 22305 & 1324 & 77 & 190 & 214 \\ 321 & 568 & -11 & 502 & -31 \\ 230 & -231 & 102 & -54 & 196 \\ 19870 & -35 & -23 & 233 & -178 \end{bmatrix}$$

In above measurement, the contacting points of the working surface and the hard board have a much larger value than those non-contacted points. This test proved the efficacy of the pressure sensor array when detecting contact force. (Detailed scale from the reading value to the actual contact force needs to be determined in the future)



Figure 6-21 Test of the Pressure Sensor Array

6.6 CONCLUSIONS

In this chapter, details on the 5x5 cell array prototype are discussed. SLA technology has the advantage of fast and is accurate enough for the 5x5 cell array system prototyping.

Therefore it is used to reduce the fabrication time and ease the research and development process. Concrete designs and fabrications to realize the mechanical structure and electronics are presented in this chapter. Objectives and test results for the 5x5 prototype are also discussed and shown. The test results proved the success for the structural design and the preliminary control algorithms. However, problems are also found during the experiments. Two main problems are listed below.

1. When sequencing from one displacement sensor to another, which are sharing the same signal conditioner, the measurement of the current sensor is affected by the previous sensor. The problem is relieved when the time gap between these two sensors are increased. Later investigation shows the reason is because there is a filtering capacitor in the signal conditioning circuit. Tradeoff needs to be determined in the future between the fast response (reducing the capacitance) and the small output signal ripple (because the capacitor is part of the signal filter.).

2. The cross talking interference discussed in chapter 5, is found in the experiment. The experiment results showed a little different from the theoretical analysis.

Above problem will affect the accuracy of the feedback. Therefore, further investigation is necessary.

CHAPTER 7

CONCLUSIONS AND RECOMMENDATIONS

In this chapter, conclusions are drawn first from this research. This is followed by a list of contributions provided by this work and some comments on possible direction for continuing research.

7.1 SUMMARY AND CONCLUSIONS

This work is to research on and find out solutions for realizing a novel human computer interface --- Digital Clay. Starting from single cell system to multi-cell array system, this research presented a set of findings, solutions, designs, testing results, and prototypes. Some of these contributions are not limited to benefit the project Digital Clay, or similar projects, but to a wide range from hydraulics, sensor technologies to control methods.

Digital Clay is discussed in details. The cell is the elementary unit of Digital Clay. In the chapter, complete cell level control and related sensing technology are discussed and good results are shown; displacement sensor design and actuator design are presented. An experimental system using conventional devices is successfully constructed for testing the cell level control concepts. Research on the pressure signal shows that when measure the pressure that affected by the solenoid valve, electrical low-pass filter maybe a good solution to get the desired signal. Research also shows that for Digital Clay to provide haptic effect, displacement control based on the pressure (caused by the user's pressing force) feedback will be better than to regulate the pressure based on the

displacement. Please note that, it seems more straightforward that the control should base on the displacement measurement to regulate pressure just like a spring which provides reaction force according to the displacement. However, since Digital Clay utilizes solenoid valves, pressure regulation is more difficult than displacement control.

To simulate / mimic a point on a material surface, the system must be able to switch between several control states. Moreover, by introducing a special control state --- shaping state, Digital Clay can realize the adding or subtraction of volume like the real clay. Furthermore, by carefully designed intelligent procedure, Digital Clay can understand the user's intention expressed just by the user's gesture.

In chapter 3, experimental results demonstrated and elaborated the success of the control on the single cell Digital Clay, and furthermore, proved the feasibility of the concept of Digital Clay.

To advance to the multi-cell array of Digital Clay, proper components and technologies are also presented in Chapter 3. Displacement sensing is critical to Digital Clay. Therefore, the displacement sensing technologies are investigated. PWM displacement estimation method is discussed first. Testing results confirmed the feasibility and accuracy of the proposed PWM velocity control and displacement estimation method for hydraulic systems using solenoid valves. However, drifting of the parameters of solenoid valve and pressure sensor requires recalibration, which prevents this method to be applied onto the large numbered cell array. Therefore, design on physical displacement sensors is necessary.

Potentiometer is kind of contacting sensor and requires a big space, so it is not considered. The capacitive sensor has simple structures, but they are too sensitive to the

environmental variation. LVDT style sensor are too complicate and of high cost. Finally, a novel non-contacting resistive sensor is introduced and selected as the displacement sensor for Digital Clay. Preliminary test shows that Non-contacting resistive sensor has high accuracy, and requires very small space to be embedded into the actuator. Moreover, this sensor occupies negligible space when being embedded into the actuator. Low cost also makes it very suitable for large size sensor array. Based on the displacement sensor and the actuator structure for Digital Clay, a novel displacement sensor embedded actuator is provided.

In Chapter 4, structure and control concepts for the multi cell array of Digital Clay are presented. At the current stage of the actuation technology, planar pin-rod matrix array concept is the most suitable for construction of the working surface of Digital Clay and is introduced first. To be able to drive a pin-rod matrix array that consists of large number of actuators, the Fluidic Matrix Drive is proposed. Based on the row and column matching principle, Fluidic Matrix Drive can reduce the number of control valves from $2N^2$ to $2N + 1$ for an N by N fluidic actuator array. By using the Fluidic Matrix Drive, not only is the number of the control valves reduced but also the amount of control resource needed is reduced. The Fluidic Matrix Drive is suitable for actuator array that consists of either single acting or double acting actuator.

To control the Fluidic Matrix Drive, three control methods to realize the surface refresh are proposed. One-time refresh method is the most straight forward and simplest method. The drawback is the slow refresh speed and bad visional effect caused by the discontinuity change of the working surface. Gradual refresh method takes more time than one-time refresh method, but provides a visually continuous changing surface. If

well designed, gradual approximation refresh method can provides continuously changing surface as fast as one time refresh method.

Control architecture for Digital Clay using fluidic matrix drive is a little different from the control structure proposed in chapter 3. Cell level controller may need to control a set of cells instead of one cell. Passive display and haptic display are controlled by different processors inside the cell level control system. Concepts on the general control architecture, functions of the User API, the surface level controller, the cell level controller are presented. Relationship and information flows between the important control mechanisms are proposed and described in detail.

In Chapter 5, details on the implementation of the multi-cell array Digital Clay are discussed. To simplify the design, manufacturing and maintenance (which are critical for a large size subsystem array like Digital Clay), mechanical structure of Digital Clay is organized into 5 modular functional blocks. The function of each block is discussed. Solutions for the key element of the Fluidic Matrix Drive --- the control adapter are investigated. The coaxial type solution for the control adapter is chosen for its structural simplicity and its low residual volume. Based on the hardware, the time sequence table is provided to control the Fluidic Matrix Drive. The structure of single acting, constant pressure return actuator array is chosen for Digital Clay. Structural design of the actuator- displacement sensor assembly and the pressure sensor array assembly are discussed in details. The SLA mounting base for pressure sensor array is preferred at the current research stage due to accessibility to the SLA equipment. (Using SLA is prefer for its fast fabrication speed)

The general structure for the electronic system for Digital Clay is discussed. Details on the pressure sensor filtering, pressure sensor multiplexing and position sensor signal conditioning and multiplexing are investigated. Two multiplexer circuits for displacement sensor are theoretically analyzed and the better one is chosen. Simulation shows the feasibility and efficacy of using the chosen solution for multiplexing up to 1000 displacement sensors.

In chapter 6, details on the design and fabrication and control for a 5 x 5 cell array system of Digital Clay are presented. The 5x5 prototype is built following all the concepts, designs and fabrication methods and controlled using the proposed control solution. Though it has only a 5 x 5 array formed by 25 cells, it is designed, built and controlled using the methods applicable for large size array system such as 100 x 100 to 1000x 1000. Therefore, the success of the proposed practical structural design methods and the control methods are proved by the success of the 5x5 cell array prototype.

7.2 CONTRIBUTIONS

The major contributions of this work can be summarized as following:

For the system development, this work provides:

- The cell level control architecture and realization. More specifically, the haptic control for solenoid valve based hydraulic system (Position control, shaping state, user gesture interpretation) is investigated and realized. (chapter 3)
- Three novel surface refresh methods for Fluid Matrix Drive are studied and the first and second refresh methods are test on the 5x5 prototype.(chapter 4)
- The surface level control architecture based on the Fluid Matrix Drive is designed and discussed. (chapter 4)

- The design concept to reduced the structural complexity and simplify the manufacturing process, the vertical modular design for multi-cell system, is provided. (chapter 5)

The contributions on the key components design are listed below:

- The design and development of a novel displacement sensor embedded micro actuator are provided and discussed in detail. (chapter 3)
- A novel concept and realization, the Fluidic Matrix Drive for multi-cell system with huge number of cells, are presented and discussed in details. (chapter 4-5)
- Novel methods for constructing the pressure sensor array assembly is provided and discussed in details. (chapter 5)

The contributions on the measurement technology are:

- Designed and developed a novel PWM displacement estimation technology for hydraulic actuator's displacement estimation without displacement sensor. Detailed processes and good test results are shown. (chapter 3)
- Designed and developed a novel non-contacting displacement sensing technology and related device based on the non-contacting voltage sensing using capacitance. (chapter 3)
- Designed and developed a multiplexing technology for huge amount (up to 1000) AC signals. (chapter 5)
- Designed and developed a method to reduce the control signals for the multiplexers for sensor arrays. (chapter 6)

7.3 RECOMMENDATIONS FOR FUTURE RESEARCH

Though the 5x5 prototype proves the proposed structural design solutions and control methods, there is still a lot of research recommended to expand the 5x5 system to the large size cell array system and to improve the design and control for Digital Clay in the future. The further research can be expected on following areas / topics:

Actuator and sensors

The displacement sensor embedded actuator presented in this work is proved to be effective and low cost (which is critical for manufacturing in large amount). However, the structure of the discrete displacement sensor embedded actuator could be improved. The dangling output wire is the weakness of this kind of sensor. Solutions to using stationary output connection are desired in the future. Moreover, further standard and comprehensive tests on the performances of the proposed sensor are necessary.

As for the sensor-actuator array, suitable methods to assemble large amount of actuators into an array are critical. In the 5x5 prototype, actuators are assembled together by hand and using either rubber gasket or glue to seal. Further research can be performed on finding a solution to assemble the cell array more efficiently and quickly.

For the pressure sensor array, further efforts are needed on the design of the micro miniature pressure sensor or finding the proper supplier. The methods to quickly and massively assemble the pressure sensors into the pressure sensor array are also desired.

Micro valve for the Fluidic Matrix Drive

Currently, conventional micro miniature solenoid valves are used as the control valve for the 5x5 cell array system. However, for the large size cell array in the future, micro valve fabricated using MEMS technology is critical. The micro valve will be investigated and designed by MEMS group. However how to integrate the valve into the cell array system (either using conventional drive method or fluidic matrix drive) is a challenge can be foreseen in the near future.

Especially for the micro valve used in the system using fluidic matrix drive, since the flow passing through one valve may supply hundreds of actuators, the orifice size

need to be big, other wise the speed will be very slow. Redesign the fluidic matrix drive to provide some kind of mechanism using the micro valve as the pilot valve to control a bigger on-off orifice maybe a potential solution.

Refresh method for Fluidic Matrix Drive

As mentioned in chapter 4, three refresh methods are studied to efficiently control the fluidic matrix drive. The one-time refresh method is simple and fast, but the haptic and visual effects are not good. The gradual refresh method provides good haptic and visual effects, but speed is slow when smooth transitions are required. The third method, the gradual approximation refresh method can provide good visual and haptic effects at relatively high speed but the matrix decomposition needs to be solved theoretically before deployment.

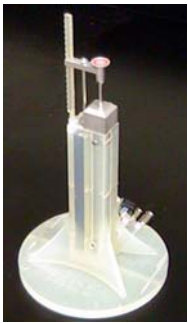
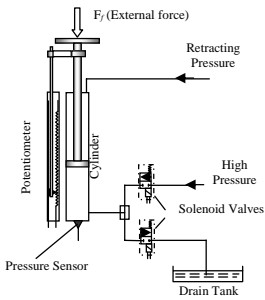
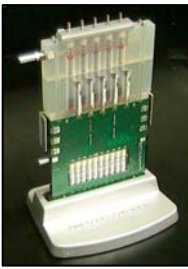
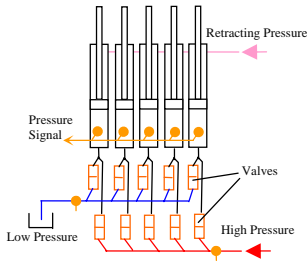
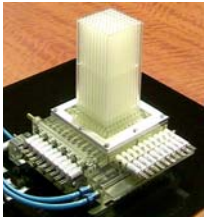
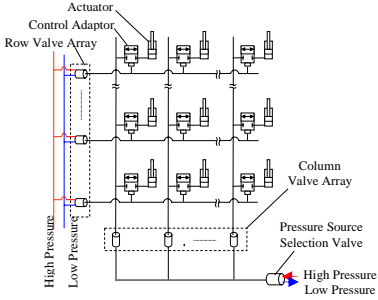
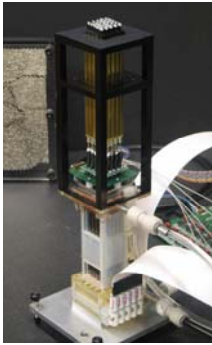
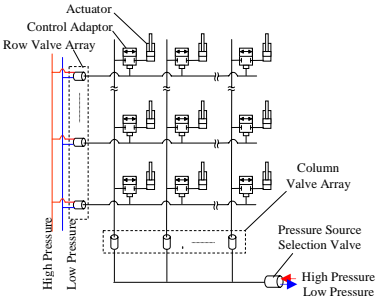
Other general topics

Current control architecture for the cell array system is based on the fluid matrix drive. In the future, due to the success of the micro MEMS components, the cell array system may go back to used the conventional “2 valves per cell” driving scheme. Therefore, control architecture will need to be modified. When dealing with the “2 valves per cell” system control, the research presented for the single cell Digital Clay in chapter 3 can be a good reference.

The manufacturing procedure to low down the cost is also a problem that will be encountered in the future. Digital Clay is comprised of thousands even millions of identical cells. The cost for manufacture the cell array will vary greatly depending on the manufacturing method.

APPENDIX A

DEVELOPED PROTOTYPES

	Picture	Main Hydraulic Circuit	Notes
Single cell System (2002)			For testing: <ul style="list-style-type: none"> The single cell control methods
1x5 Cell Array System (2003)			For testing: <ul style="list-style-type: none"> The horizontally modular system design concept PWM speed and position estimation control
10x10 Cell Array System (2004)			For testing: <ul style="list-style-type: none"> The Fluid Matrix Drive concept and realization
5x5 Cell Array System (2005)			For testing: <ul style="list-style-type: none"> The overall control architecture Cell level and surface level control methods Sensor array and feedback measurement methods Vertically modular design concept Manufacturability and mass productivity

APPENDIX B

PSEUDO PROGRAMS

B1 Pseudo program for the Single Cell System Control (Real-time Linux, C++ program)

```
//===Initiating PCI cards===
int init_PCI(void)
{
    Initial DAQ Card;
    Initial Digital I/O Card;
}

//===Initiating the virtual spring system===
void *initial_thread(void *param)
{
    Command the piston to the equilibrium position;
    Set the control state to be elastic state;
    Wake up position control thread;
    Wake up valve control thread;
}

// === Valve Control ===
void *valve_thread(void *param)
{
    Suspend current thread;

    while(1)
    {
        if (PWM duty > 0) Using the inlet valve;
        else Using the outlet valve;

        Output PWM wave based on the PWM duty;
    }
}

//===Position Control===
void *po_thread(void *param)
{
    Suspend current thread;

    while(1)
    {
        if (plastic state==1)
        {
            if (Pressure > Yielding value) PWM duty= - 15%;
            else PWM duty=0;
        }
        else if (Shaping state ==1)
        {

```

```

        if( Pressure > Upper limit) PWM duty= -30%;
        else if(Pressure < Lower limit) PWM duty=30%;
        else    PWM duty=0;
    }
    else if (Elastic state ==1)
    {
        Calculate desired position based on the pressure feedback;
        Calculate corresponding PWM duty;
    }
    else    PWM duty=0;
}

}

//=== Sampling thread ===
void *sampling_thread(void *param)
{
    while(1)
    {
        Sampling pressure;
        Sampling displacement;
    }
}

//=== logic control ===
void *logic_thread(void *param)
{
    while(1)
    {
        if(Elastic state==1)
        {
            if( Pressure > Yielding Pressure )
            {
                Elastic state =0;
                Yielding state =1;
            }
        }
        else if (Shaping State ==1)
        {
            if( Pressure Change > 30% of Current Pressure )
            {
                Calculate equilibrium position;
                Shaping state =0;
                Elastic state =1;
            }
        }
        else if (Yielding state==1)
        {
            if( Pressure < yielding pressure)
            {
                Calculate new equilibrium position;
                Yielding state =0;
                Elastic state =1;
            }
            else if ( position is constant for a while)
            {
                Yielding state =0;
            }
        }
    }
}

```

```

        Shaping state =1;
    }
}

}

//==== INITIAL_MODULE ====
int init_module(void){

//==== Cleanup_Module ====
void cleanup_module(void){}

```

B2 Pseudo program for the 1x5 array System Control (Real-time Linux, C++ program)

```

//====Initiating PCI cards====
int init_PCI(void)
{
    Initial DAQ Card;
    Initial DIO Card;
}

//====Duty calculation and position estimation thread====
void *Duty_Dsp_thread(void *param)
{
    Suspend current thread;

    while(1)
    {
        for (Cylinder = 1 to 5)
        {
            Duty calculation (based on lookup table);
            Position Estimation (based on lookup table);
        }
        Send PWM duties to PIC microcontroller;
    }
}

//====Manager Thread====
void *manager_thread(void *param)
{
    Home all actuators;
    Wake up duty calculation and position estimation thread

    Command the speeds and positions to form a sloped line;
    Command the speeds and positions to form a V-shaped line;
    Command the speeds and positions to form dynamically changing sine line;
}

//====Sampling thread====
void *sampling_thread(void *param)
{

```

```

        while ( 1 )
        {
            Sample pressure feedbacks;
        }
    return 0;
}

```

```
int init_module(void){}
```

```
void cleanup_module(void){}
```

B3 Pseudo programme for the 5x5 array System Control (Real-time Linux, C++ program)

```

disp_desired[5][5]={
    { 0, 4000, 8000,12000,16000},
    { 4000, 8000,12000,16000,20000},
    { 8000,12000,16000,20000,24000},
    {12000,16000,20000,24000,28000},
    {16000,20000,24000,28000,32000}};

```

```
//===Initiating PCI cards===
```

```

int init_PCI(void)
{
    Initial DAQ Card;
    Initial DIO Card;
}

```

```
// === calibrate position sensors ===
```

```

void *calib_thread(void *param)
{
    Command actuators go to lower limit;
    Record initial displacements;
    Command actuators go to upper limit;
    Record largest displacements;

    Wake up pwm_exec_thread;
    Wake up main_thread;
}

```

```
//=== main thread ===
```

```

void *main_thread(void *param)
{
    Suspend current thread;

    Select high pressure source;
    Enable first row valve array;

    while (row number < 5)
    {
        for (column valve = 1 to 5)
        {
            if (displacement of valve (column, row) > disp_desired(column, row) )
            {

```

```

        Write the shutting down command for that column valve to cln_temp;
    }
}
cln_reg = cln_temp;

if (all the column valves are closed)
{
    Row number ++;
    Reset cln_temp value;
    Enable the new row
}
}
}

//===Sampling thread===
void *sampling_thread(void *param)
{
    while ( 1 )
    {
        for(column= 1 to 5)
        {
            Enable that column (for multiplexer control)
            for(row = 1 to 5)
            {
                Sample position feedbacks;
            }
        }
    }
}

//===valve control===
void *pwm_exec_thread(void *param)
{
    Suspend current thread;

    while ( 1 )
    {
        Open valves based on "cln_reg";
        Wait for the time corresponding to the PWM duty;
        close valves;

        Wait for the remain time; (Note: PWM open time + remain time = PWM base period)
    }
}

int init_module(void){}

void cleanup_module(void){}

```


APPENDIX C

LIST OF KEY MATERIAL/COMPONENTS

Materials

Hypodermic stainless steel tubing/rods

Sizes of these tubes used in the prototypes range from 0.2mm to 6.35mm. They can be found either at www.mcmaster.com or at www.smallparts.com

High precision graphite rod

The high precision graphite rod is used to build the piston of the micro actuators. It can be found at www.graphitestore.com

Micro miniature coaxial cables

Sizes of these cables range from 0.3mm to 0.8 mm (OD). They are very useful when used in limited spaces. They can be found at www.digikey.com and www.hcm.hitachi.com

Silicon thin rubber sheets

They are used for sealing and membrane and can be found at www.mcmaster.com

Conductive copper tapes

They can found at www.3M.com

High precision glass tubes

These tubes are used to construct the micro actuators. They can be found at www.wilmad.com

Components

Micro miniature solenoid valves

These high efficient micro miniature solenoid valves can be found at www.theleeco.com

Ultra low friction cylinders

These cylinders have extremely low friction and can be found at www.airport.com

Micro miniature pressure sensors (IC, PC40 serials)

These are the smallest amplified and signal conditioned pressure sensors. They can be found at www.honeywell.com

LVDT monolithic signal conditioner (IC, AD698)

This is the signal conditioner used in the 5x5 prototype. It can be found at www.digikey.com

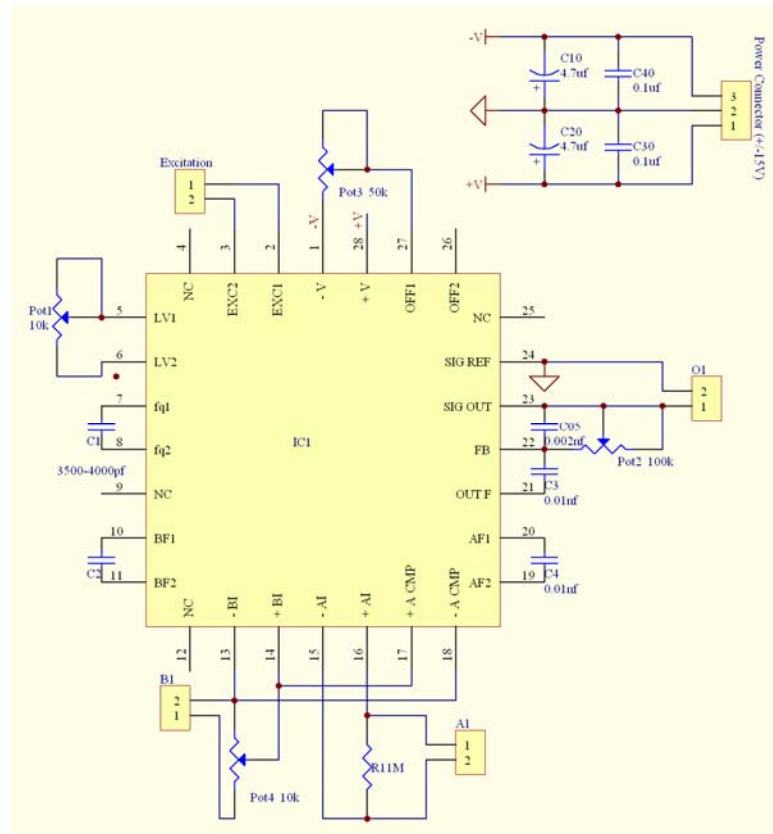
5th order monolithic low pass filter (IC MAX280)

It can be found at www.digikey.com

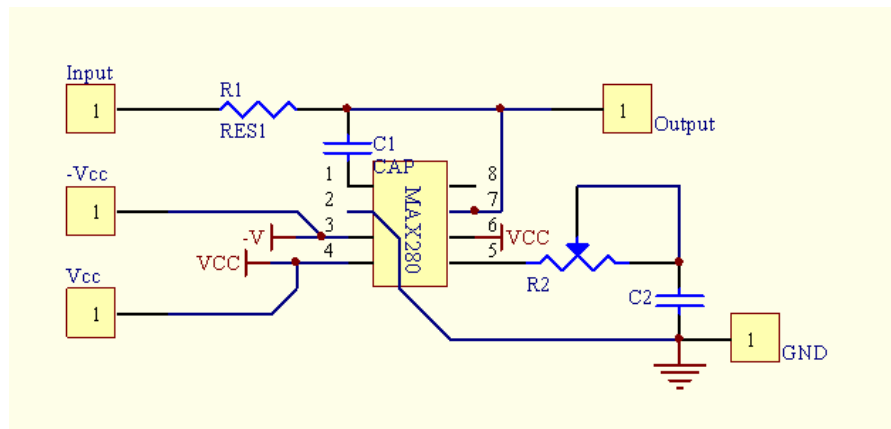
APPENDIX D

SCHEMATIC CIRCUITS FOR BASIC ELECTRONICS

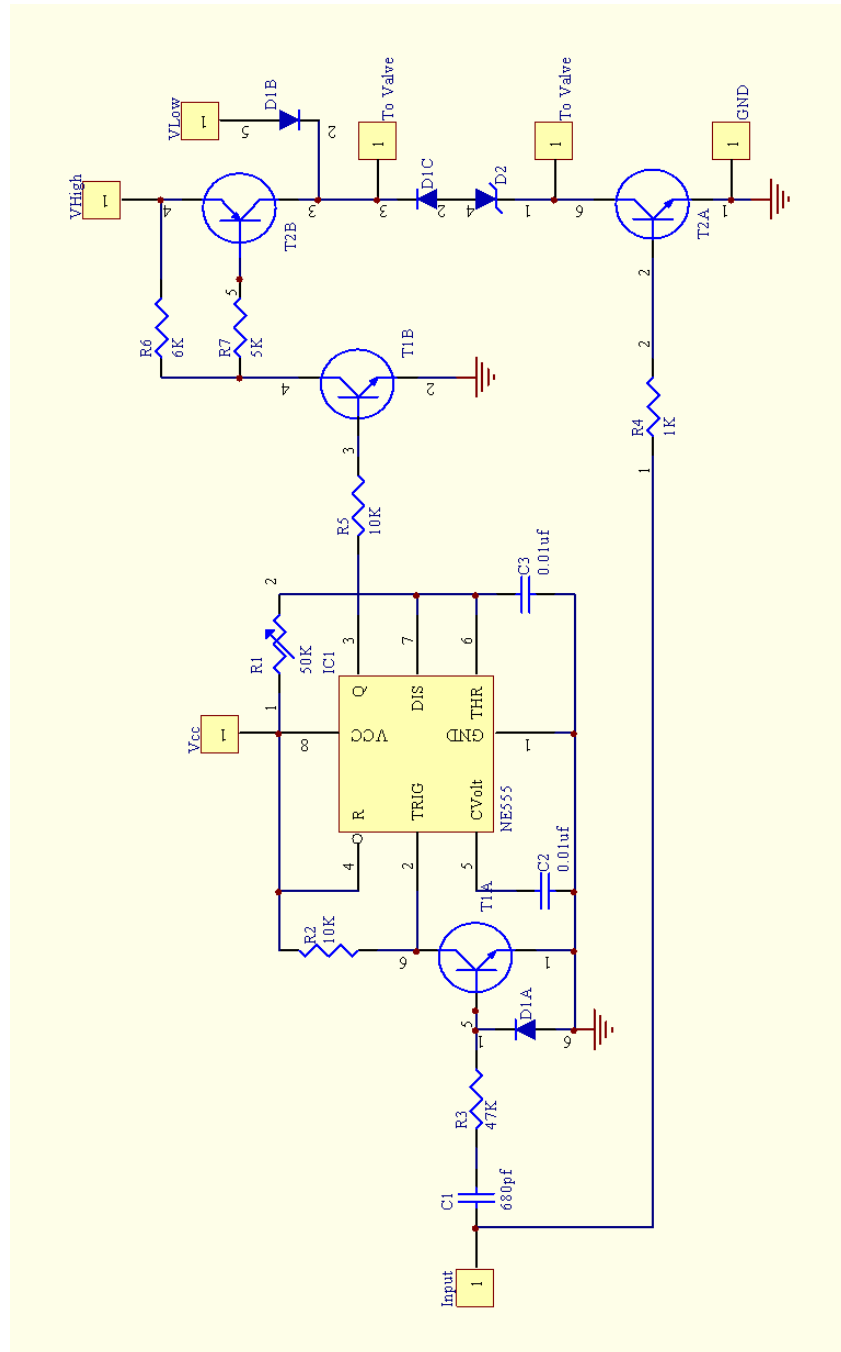
C1 *LVDT Signal Conditioner for Non-contacting Position Sensor*



C2 *5th Order Filter*



C3 Solenoid Valve Over-driver



REFERENCES

- [1] Amato, Ivan, "Helping Doctors Feel Better," Technology Review, April, 2001, pp 65-71
- [2] <http://vr.isdale.com/index.html>
- [3] <http://webvision.med.utah.edu/>
- [4] T. Miller and R.C., Zeleznik. The design of 3D haptic widgets. In Proceedings of the 1999 Symposium on Interactive 3D Graphics, pp. 97-102, 1999
- [5] M.A. Srinivasan and C. Basdogan. Haptics in virtual environments: taxonomy, research status, and challenges. Computers & Graphics, vol. 21, no. 4, pp 393-404, July 1997
- [6] Jacobsen, S.C., Smith, F.M., Iversen, E.K., and Backman, D.K., "High Performance, High Dexterity, Force Reflective Teleoperator," in Proc. 38th Conf. Remote Systems Technology, Washington, D.C., pp. 180-185, November, 1990
- [7] T.M. Massie and J.K. Salisbury. The phantom haptic interface: A device for probing virtual objects. Proc. of ASME Haptic Interfaces for Virtual Environment and Teleoperator Systems, volume 1, pages 295-301, 1994
- [8] K. Salisbury, D. Brock, T. Massie, N. Swarup, and C. Zilles. Haptic rendering: Programming touch interaction with virtual objects. Proc. of 1995 ACM Symposium on Interactive 3D Graphics, pages 123-130, 1995
- [9] R. Balakrishnam, G. Fitzmaurice, g. Kurtenbach, and K. Singh. Exploring interactive curve and surface manipulation using a bend and twist sensitive input strip. In Proceedings of the 1999 ACM Symposium on Interactive 3D Graphics, pages 111-118, 1999
- [10] McDonnell, K.T., Qin, H., Wlodarczyk, R.A. Virtual Clay: A Real-Time Sculpting System with Haptic Toolkits. In Proceedings Visualization 2000, pp. 179-190, Salt Lake City, Oct. 8-13, 2000
- [11] A. Mascarenhas, M.C. Lin and D. Manocha. Six Degree-of-Freedom Haptic Visualization of Force Fields Technical Report, Computer Science Department, University of North Carolina at Chapel Hill, 2000
- [12] R. Avila and L.M. Sobierajski. "A Haptic Interaction Method for Volume Visualization", Proc. visualization 96, San Francisco, CA, pp. 197-204, 485, Oct. 1996

- [13] Lawrence, D.A., Lee, C.D., Pao, L.Y., Novoselov, R.Y. Shock and Vortex Visualization Using A Combined Visual/Haptic Interface. In Proceeding 1997 Symposium on Interactive 3D Graphics, pp. 131-137, Providence, R.I., April 27-30
- [14] Thompson, II, Thomas V., Johnson, D.E., Cohen, E. Direct Haptic Rendering of Sculptured Models. Dept. of Computer Science, University of Utah
- [15] Gregory, A., Mascarenhas, A., Ehmann, S., Lin, M., Manocha, D. Six Degree-of-Freedom Haptic Display of Polygonal Models. In Proceedings Visualization 2000, pp. 139-146, Salt Lake City, UT, Oct. 8-13
- [16] <http://haptic.mech.northwestern.edu/intro/tactile/>
- [17] Fearing, R. S., G. Moy, and E. Tan. Some Basic Issues in Teletaction . In Proceedings of the IEEE Int. Conf. Robotics and Automation, April 1997, pp 3093-3099
- [18] Bliss, J.C. "A Relatively High-Resolution Reading Aid for the Blind," IEEE Trans. On Man-Machine Systems, Vol 10: pp1-9, 1969
- [19] Howe RD, Peine WJ, Kontarinis DA, Son JS. Remote palpation technology. IEEE Engineering in Medicine and Biology, 14(3):318-323, May/June 1995
- [20] Kammermeier, P. M. Buss, and G. Schmidt, "Dynamic display of distributed tactile shape information by a prototypical array," Proceedings of the 2000 IEEE/RSJ International Conference on Intelligent Robotics and Systems, pp 1119-1124
- [21] Cohn, M., M. Lam, and R. Fearing, "Tactile feedback for teleoperation," SPIE Telemanipulator Technology, 1833:240-254, 1992
- [22] Howe RD, Peine WJ, Kontarinis DA, Son JS. Remote palpation technology. IEEE Engineering in Medicine and Biology, 14(3):318-323, May/June 1995
- [23] Howe, R. "Tactile sensing and control of robotic manipulation." Advanced Robotics, v. 8 N. 3, 1994, pp245-261
- [24] Jarek Rossignac, Mark Allen, Wayne J. Book, Ari Glezer, Imme Ebert-Uphoff, Chris Shaw, David Rosen, Stephen Askins, Jing Bai, Paul Bosscher, Joshua Gargus, ByungMoon Kim, Ignacio Llamas, Austina Nguyen, Guang Yuan, Haihong Zhu, "Finger Sculpting with Digital Clay: 3D Shape Input and Output through a Computer-Controlled Real Surface", Shape Modeling International Conference in Korea, Seoul, vol. May, 2003
- [25] Zhu, Haihong and Wayne J. Book, "Practical Structure Design and Control for Digital Clay", 2004 ASME International Mechanical Engineering Congress and Exhibition, vol., p. 1051, 2004

- [26] Haihong Zhu, Wayne Book, "Structure and control for cells of Digital Clay", ASME Journal of Dynamic Systems, Measurement, and Control, 2005 (Submitted)
- [27] Ma, L., Lau, R., Feng, J., Peng, Q. and Way J. (1997), "Surface Deformation Using the Sensor Glove," ACM Symposium on Virtual Reality Software and Technology, pp. 189-196, 1997
- [28] Kunii, Y., Nishino, T. and Hashimoto, K.H. (1997), "Development of 20 DOF Glove Type Haptic Interface Device – Sensor Glove II," IEEE/ASME International Conference on Advanced Intelligent Mechatronics, p. 132, 1997
- [29] Massie, T.H. and Salisbury, J.K. (1994), "The PHANTOM Haptic Interface: A Device for Probing Virtual Objects." Proc. Of the ASME Winter Meeting, Symposium on Haptic Interfaces for Virtual Environment and Teleoperator Systems, Chicago, IL, Nov. 1994
- [30] Haptic Technologies Inc., <http://www.hapttech.com/prod/index.htm>
- [31] T. Yoshikawa, T. Sugie, and M. Tanaka, "Dynamic hybrid position/force control of robot manipulators---controller design and experiment," IEEE J. Robot. Automat., vol. 4, pp. 699--705, Dec. 1988
- [32] H. Iwata, H. Yano, F. Nakaizumi, and R. Kawamura, "Project FEELEX: Adding haptic surface to graphics," in Proceedings of SIGGRAPH2001, 2001
- [33] Nakatani, Kajimoto, Sekiguchi, Kawakami, Tachi, "3D Form Display with Shape Memory Alloy, " in Proc. of International Conference on Artificial Reality and Telexistence 2003. (ICAT 2003)
- [34] Bliss, Katcher, Rogers and Shepard: "Optical-to-Tactile Image Conversion for the Blind," IEEE Transactions on Man-Machine Systems, Vol. MMS-11, No. 1, pp. 58-65, March, 1970
- [35] H. Raffle, M. W. Jachim and J. Tichenor: "Super Cilia Skin: An Interactive Membrane," Conference on Human Factors in Computing Systems, April, 2003
- [36] C. Dyner, B. Kaanta and H. Ishii, "Pins," at the day of 2004/2/4
- [37] Y. Wang, A. Biderman, B. Piper, C. Ratti and H. Ishii: "SandScape", Feb 2004
- [38] Linjama, M., Tammisto, J., Koskinen, K.T. & Vilenius, M. 2000. On/off position control of low-pressure water hydraulic cylinder using low-cost valves. In: Laneville, A. (ed.). Proceedings. Sixth Triennial International Symposium on Fluid Control, Measurement and Visualization, FLUCOME 2000, August 13-17, 2000, Sherbrooke, Canada
- [39] IMAIZUMI, Tatsuhiko; OYAMA, Osamu; YOSHIMITSU, Toshihiro (2000) Study of Pneumatic Servo System Employing Solenoid Valve Instead of Proportional

- Valve by Keeping the Solenoid Valve Plunger to be Floating. In: FULCOME 2000 Conferenc, Sherbrooke, Canada
- [40] Q.Yang, Y.Kawakami, S.Kawai, PWM Position Control of a Pneumatic Cylinder, Journal of the Japan Hydraulics & Pneumatics Society, 27-6, 1995, 803/809
 - [41] Linjama, M., Tammisto, J., Koskinen, K.T. & Vilenius, M. 2000. On/off position control of low-pressure water hydraulic cylinder using low-cost valves. In: Laneville, A. (ed.). Proceedings. Sixth Triennial International Symposium on Fluid Control, Measurement and Visualization, FLUCOME 2000, August 13-17, 2000, Sherbrooke, Canada
 - [42] O.Oyama, M.Harada, Pressure Servo System Using High Response Solenoid Valve: Journal of the Japan Hydraulics & Pneumatics Society, 20-4, 1989, 344/349.
 - [43] Haihong Zhu and Wayne J. Book, "Control Concepts for Digital Clay", Proceedings of the 7th IFAC Symposium on Robot Control (SyRoco 2003), vol. 2, (2003), p. 405
 - [44] Book, Wayne J. and Davin K. Swanson, "Reach out and Touch Someone: Controlling Haptic Manipulators Near and Far", Annual Reviews in Control, vol. 28, (2003), p. 87
 - [45] G.J. Pappas, G. Laeriere, & S.S. Sastry, Hierarchically Consistent Control Systems," IEEE Trans. Automatic COntrol, 45(6) 1144-1160, June, 2000
 - [46] Drouin, M., Abou-Kandil, H., and Mariton, M.,Control of Complex Systems, Plenum Press, New York, 1991
 - [47] D. Gavel and D. Siljak, Decentralized adaptive control: structural conditions for stability, IEEE Trans. Autom. Contr. 34 (1989), no. 4, 413-426
 - [48] J. Baillieul, Feedback Designs for Controlling Device Arrays with Communication Channel andwidth Constraints, in Lecture Notes of the Fourth ARO Workshop on Smart Structures, Penn State Univ., August 16-18, 1999.
 - [49] P. Bosscher and I. Ebert-Uphoff, "Digital Clay: Architecture Designs for Shape-Generating Mechanisms", Proceedings of the 2003 IEEE International Conference on Robotics and Automation, Taipei, Taiwan, September 2003, vol., (2003), p. 834. Published
 - [50] P. Bosscher and I. Ebert-Uphoff, "A Novel Mechanism for Implementing Multiple Collocated Spherical Joints", Proceedings of the 2003 IEEE International Conference on Robotics and Automation, Taipei, Taiwan, September 2003, vol., (2003), p.336. Published",
 - [51] Rosen, D.W., Nguyen, A., and Wang, H, "On the Geometry of Low Degree-of-Freedom Digital Clay Human-Computer Interface Devices", Proceedings ASME

Computers and Information in Engineering Conference, Chicago, Sept. 2-6, 2003, vol. DETC, (2003), p. 48295. Published

- [52] Xiaosong Wu and Mark Allen, “Kinematically-Stabilized Microbubble Actuator Arrays”, Proceedings of IEEE Micro Electro Mechanical Systems, vol., (2005), p.554. Published
- [53] Zhu, Haihong and Wayne J. Book, “Speed Control and Position Estimation of Small Hydraulic Cylinders for Digital Clay Using PWM Method”, Japan-US Conference on Flexible Automation, vol., (2004), p. 1. Published